Efficient wireless networked control

Towards practical event-triggered implementations

Fu, Anqi

DOI
10.4233/uuid:47d557ea-9ff9-4851-883a-4ce5e943a8b7

Publication date
2018

Document Version
Final published version

EFFICIENT WIRELESS NETWORKED CONTROL

TOWARDS PRACTICAL EVENT-TRIGGERED IMPLEMENTATIONS

EFFICIENT WIRELESS NETWORKED CONTROL

TOWARDS PRACTICAL EVENT-TRIGGERED IMPLEMENTATIONS

Proefschrift

ter verkrijging van de graad van doctor
aan de Technische Universiteit Delft,
op gezag van de Rector Magnificus prof. dr. ir. T.H.J.J. van der Hagen
voorzitter van het College voor Promoties,
in het openbaar te verdedigen op maandag 26 februari 2018 om 12:30 uur

door

Anqi FU

Master of Science in Instrumentation Science and Technology,
Beihang University,
geboren te Qinhuangdao, Hebei, China.

This dissertation has been approved by the

promotor:	dr. ir. M. Mazo Jr.
promotor:	prof. dr. R. Babuška

Composition of the doctoral committee:

Rector Magnificus,	chairperson
Dr. ir. M. Mazo Jr.	Delft University of Technology
Prof. dr. R. Babuška	Delft University of Technology
Independent members:	
Prof. dr. ir. B. De Schutter	Delft University of Technology
Prof. dr. ir. M. Cao	University of Groningen
Prof. S. Chakraborty	Technical University of Munich
Prof. D. V. Dimarogonas	KTH Royal Institute of Technology
Dr. ir. M.C.F. Donkers	Eindhoven University of Technology
Reserve member:	
Prof. dr. ir. J. Hellendoorn	Delft University of Technology

This dissertation has been completed in fulfillment of the requirements of the Dutch Institute of Systems and Control (DISC) for graduate study and the TU Delft Graduate School for the Doctoral Education Program.

The research described in this dissertation is partly supported by the China Scholarship Council (CSC) and has received additional funding from the Adaptive Emergent Systems Engineering (AESE) Group of Imperial College London.

Front & Back:	Keywords of the dissertation.
Cover designed by:	Anqi Fu.
Printed by:	Gildeprint.

ISBN 978-94-6186-894-7

An electronic version of this dissertation is available at
`http://repository.tudelft.nl/`.

CONTENTS

PREFACE

This dissertation is a result of four years of research at the Delft Center for Systems and Control (DCSC) of Delft University of Technology. In this acknowledgement, I would like to give my thanks to those who helped and supported me to accomplish this dissertation.

First of all, I would like to express my sincere gratitude to my promotor Dr. Manuel Mazo Jr. for his great supervision during these four years. I really appreciate his trust, support, and patience. He encouraged me to explore different exciting research directions, look into interesting topics, and research with new ideas. Whenever I had any ideas or results, he could always give me supervision and suggestions. No matter how busy he was, he was always ready to discuss with me and looked into even the smallest details. From him, I really had learnt a lot. I would also like to thank my promotor Prof. Robert Babuška, for his kindness to me and for the interesting discussions over the years.

Next I must thank my group members in DCSC, Anton, Ivan, Cees, Arman, Carlos, and Daniel. We met every Monday discussing current work and interesting ideas. My special thanks to Anton for his mathematical support on my research; to Cees for his help on refining my English and helping me with the Dutch; to Arman for explaining me his work carefully and with patience. It was very nice to work with you all.

Third I am grateful to my collaborators in the WaterBox project for their contributions to my research: Prof. Julie McCann and Dr. Sokratis Kartakis. Julie invited me to visit Imperial College London, and opened me a window to the computer science society. Sokratis helped me a lot during my stay in London. It was a pleasure to work with them. Besides, I would like to thank all the people working in the Adaptive Emergent Systems Engineering (AESE) Group of Imperial College London for all those nice talks and teas.

Then I would like to acknowledge all my colleagues in DCSC. I would like to give my thanks to Kitty, Kiran, Heleen, Marieke, and Mascha for their kind help, they were always ready to help me; to Will for his kind support on my technical problems; to Simone, Riccardo, and Jens for those unforgettable discussions and cooperations; to Laura, Cristiano, and Zhou for the nice trip we had together in the US; to Chengpu and Shuai Yuan for the nice trip we had together in Macedonia; to Zhe, Yihui, Yiming, Yu, Huizhen, Hai, Le, Shuai Liu, Renshi, Jia, Fan, Zhao, Yue, Juan, Jun, and Shu for those nice BBQs and hotpots. I would also like to thank everyone in the department for the small talks, coffees, beers, social events, and numerous foosballs. This list of people includes but is not limited to Tamas, Ton, Max, Michel, Jan-Willem, Javier, Peyman, Raf, Sander, Gleb, Oleq, Paolo, Cornelis, Tope, Farid, Hildo, Laurens, Elisabeth, Tim, Reinier, Amir, Yasin, Ana, Subramanya, Tomas, Pieter, Vahab, Baptiste, Kim, Hans, Wouter, Yashar, Kees, Alessandro, Noortje, Mohammad, Esmaeil, Ilya, Patricio, Dieky, Edwin, Sachin, Sadegh, Bart, Marco, Majid, and Gabriel. My stay at DCSC with all of you will remain always a nice memory.

Next I would like to extend my gratitude to my friends who accompanied and supported me during these four years. I would like to thank Dr. Lei Tong, for all the experiences we had exchanged about PhD life and the cocktails; Dr. Yiwei Wang, for the memories we had together. A special thanks to Fei for her help and support. I am thankful to Yueting, Peiyao, Long, Yixiao, Sixin, Daijie, Jie, Xian, Yu, Zhijie, Jingtang, Yang, Qujiang, Lian, Xinyuan, Xi, Yili, Yangyu, Rong, Zhimin, Minghe, Zhi, Pengling, Chuang, Yalin, Xu, Chenjie, Lei Xie, Mingjuan, Tian, Jing, Chong, Xueli, Fan, Changgong, Zi, Ziqiao, Huarong, LiLi, Wenhua, Jianbin, Shanshan, Xiang, Jian, and all the other friends who travelled, played basketball, enjoyed dinner, played cards, and most importantly, drank beer with me. A special acknowledgment goes to Anke for her help.

I would like to give my special thanks to all my committee members: Prof. Bart De Schutter, Prof. Ming Cao, Prof. Samarjit Chakraborty, Prof. Dimos Dimarogonas, and Dr. Tijs Donkers. I would also like to thank Prof. Hans Hellendoorn for his time.

A special mention goes to to my country. I want to thank Prof. Zhong Wu, Prof. Pingkang Li, and Mrs Xiuxia Du for the supervision, help and support.

Last but most importantly, I would like to thank my family. It was the love and encourage from my father and mother that helped me to overcome those hard times and persevered in my choices. I love you all.

Anqi Fu
Delft, October 2017

SUMMARY

Wireless networked control systems, as the name indicates, employ wireless networks to interconnect their components, e.g. sensors, computing units, and actuators, in their implementation. Removing wires from control system implementations, the components can be more easily installed in spatial positions that are hard to access, and facilitate their deployment within large physical scales. This enables the expansion of control applications to new domains or objectives previously not attainable. However, as a trade-off, in a wireless networked control system, the transmission bandwidth is much smaller compared to a wired one. Besides, to achieve flexibility and mobility, some nodes may have energy supplies from batteries, which have limited capacity and are usually costly to replace. The limitations in bandwidth and energy supplies is a major problem when designing wireless networked control systems. The purpose of this thesis is to study how to guarantee pre-designed stability and performance under limitations of bandwidth and energy supplies, with the goal to enrich the control approaches for resource-aware industrial applications.

In wireless networked control systems, feedback controllers are usually employed. These controllers compute control signals by measuring system outputs. Designing properly the control laws implemented at the controllers, one can stabilize the system. Since the sensors and controllers are digitized, the execution time of this feedback process is discretized. The execution time can be dependent on the system's clock or the system's state. The controllers are called time-triggered controllers if the execution time is dependent on the system's clock. In general, these execution instants are selected equally distributed, which one calls periodic control. If the execution times are dependent on the system's state, the controllers are called event-triggered controllers. Usually event-triggered controllers are activated only when the pre-designed stability or performance level is about to be violated. Before execution of a feedback action, the corresponding sensor nodes, computing units, and actuator nodes are required to wake up and access the transmission channels, to guarantee that the feedback controller works properly. Therefore, arrangement on working time is required to avoid conflicts.

This thesis presents two methods to improve the efficiency of controller implementations: applying event-triggered control to the feedback loop, and enabling scheduling the actions of the implementation.

A version of decentralized periodic event-triggered control is presented first. This control strategy has asynchronous communications and is equipped with dynamic quantizers. Asynchronous communications here means that the updates of the inputs are performed independently from each other. Applying a decentralized event-triggered mechanism, local events only depend on local information, and thus the transmissions can be reduced. Periodic sampling reduces the working time of the sensors and the listening time of the nodes. Dynamic quantization allows to reduce the packet length of each transmission. As a result, both bandwidth occupation and energy consump-

tion can be improved, while pre-designed stability and performance levels can still be guaranteed. For comparison purposes, another version of decentralized periodic event-triggered control is also presented. Different from asynchronous decentralized periodic event-triggered control, this control strategy has synchronous communications, i.e. after an event, all inputs are updated simultaneously.

Next the thesis presents the construction of a communication's traffic model for a periodic event-triggered control implementation. This communication's traffic model is derived from the system dynamics. By partitioning the state-space into finite number of regions, and computing lower and upper bounds of the inter-event intervals, a finite abstraction is constructed. This abstraction formalizes the traffic model. This model captures the communication traffic generated by the periodic event-triggered control implementation. This model can then be used to automatically schedule the actions of the implementation, e.g. wake up time of each sensor and transmission time from each node. As a result, bandwidth occupation and energy consumption can be saved.

Finally, a comparison of various triggering mechanisms in a real cyber-physical system, the WaterBox, is presented. The WaterBox is a scaled version of a smart water distribution system, having all its components connected via a WiFi network. We identify a model for the system, design a switched controller and triggering mechanisms. The triggering mechanisms implemented are: traditional periodic time-triggered control, centralized periodic event-triggered control, decentralized periodic event-triggered control with synchronous and asynchronous transmissions. The corresponding TDMA protocols for each triggering mechanism are also designed. More than four hundred experiments are analysed and summarized through comparisons on the bandwidth occupation and energy consumption of different triggering mechanisms.

The contributions of this thesis demonstrate the potential of advanced control technologies, event-triggered control in particular, to solve actual problems e.g. improve efficiency in smart water distribution systems.

SAMENVATTING

Draadloze netwerk regelsystemen, zoals de naam suggereert, gebruiken draadloze netwerken ter verbinding van diens componenten, zoals sensoren, verwerkingseenheden (processoren) en actuatoren. Door bedrading te verwijderen uit de implementatie van regelsystemen is het mogelijk om componenten gemakkelijker te installeren op plaatsen die moeilijker te bereiken zijn en kunnen ze makkelijker worden ingezet binnen grote fysieke schalen. Dit faciliteert de expansie van regelapplicaties naar nieuwe domeinen en toepassingen die voorheen niet mogelijk waren. Echter, een draadloze netwerk regelsysteem heeft een kleinere transmissiebandbreedte vergeleken met een bedraad systeem. Daarnaast, om flexibiliteit en mobiliteit mogelijk te maken, hebben sommige nodes mogelijk een energievoorziening van batterijen nodig. Deze batterijen hebben een gelimiteerde capaciteit hebben en zijn vaak duur om te vervangen. De limitaties in bandbreedte en energievoorzieningen zijn significante problemen bij het ontwerpen van draadloze netwerk regelsystemen. Het doel van deze dissertatie is het bestuderen hoe garanties op voor-ontworpen stabiliteit en prestaties kunnen worden gegeven onder gelimiteerde bandbreedte en energievoorzieningen, met als doel de regelmethodes voor resource-bewuste industriële toepassingen te verrijken.

In draadloze netwerk regelsystemen worden doorgaans feedback controllers (terugkoppeling regelaars) gebruikt. Deze controllers berekenen regelsignalen aan de hand van de uitgangsignalen van het systeem. Door middel van correct ontwerp van de regelwet in deze controllers kan men de systemen stabiliseren. Doordat de sensoren en controllers gedigitaliseerd zijn, is de executietijd van dit feedbackproces gediscretiseerd. De executietijd kan afhankelijk zijn van de systeemklok of de systeemtoestand. Een controller wordt tijd-getriggerd controllers genoemd indien de executietijd afhangt van de systeemklok. In het algemeen zijn deze executie-instanties gelijk verdeeld geselecteerd, wat men periodische control noemt. Indien de executietijd afhankelijk is van de systeemtoestand, noemt men deze controllers event-getriggerde (gebeurtenis getriggerde) controllers. Doorgaans hebben event-getriggerde controllers alleen executies indien de voor-ontworpen stabiliteit of prestatieniveau op het punt staat geschonden te worden. Voor de executie van een feedbackactie zal de corresponderende sensor nodes, de verwerkingseenheden en actuator nodes gewekt moeten worden en toegang krijgen tot de transmissiekanalen om te garanderen dat de feedback controller correct werkt. Als gevolg is er een planning op de werkingstijd nodig om conflicten te voorkomen.

Deze dissertatie presenteert twee methoden ter verbetering van de efficiëntie van controller implementaties: het toepassen van event-getriggerde control op de feedbackloop en het plannen van acties van de implementatie.

Een versie van decentraliseerde periodische event-getriggerde control is allereerst voorgesteld. Deze control strategie heeft asynchronische communicatie en is uitgerust met dynamische kwantiseringseenheden. In deze context betekent asynchronische communicatie dat updates van de invoer onafhankelijk van elkaar worden uitgevoerd. Bij

de toepassing van een gedecentraliseerde event-getriggerde mechanisme hangen lokale gebeurtenissen alleen af van lokale informatie, waardoor de transmissies gereduceerd kunnen worden. Periodische sampling (steekproeven) reduceert de werkingstijd van sensoren en de luistertijd van de nodes. Dynamische kwantisering maakt het mogelijk dat pakketlengte van iedere transmissie verkleint kan worden. Als gevolg kan zowel de bandbreedtebezetting en het energieverbruik worden verbeterd, terwijl voor-ontworpen stabiliteit en prestatieniveau nog steeds gegarandeerd kunnen worden. Ter vergelijking wordt een andere versie van gedecentraliseerde periodische event-getriggerde control gepresenteerd. Verschillend aan asynchronische gedecentraliseerde periodische event-getriggerde control heeft deze regelstrategie synchrone communicatie, d.w.z. na een gebeurtenis wordt alle invoer simultaan bijgewerkt.

Daarop volgend beschrijft deze dissertatie de constructie van een communicatieverkeermodel voor een periodische event-getriggerde control implementatie. Dit communicatieverkeermodel is afgeleid van de systeemdynamica. Door de statespace (toestandsruimte) te partitioneren in eindige regio's en de onder en boven grens van de inter-event (tussen gebeurtenis) intervallen te berekenen, kan een eindige abstractie geconstrueerd worden. Deze abstractie vormt het verkeermodel. Dit model beschrijft het communicatieverkeer gegenereerd door de periodische event-getriggerde control implementatie. Als gevolg kan dit model gebruikt worden om automatisch de acties van de implementatie plannen, bijvoorbeeld de ontwakingstijd van iedere sensor en de transmissietijd van iedere node. Als gevolg kan er bespaard worden op de bandbreedtebezetting en het energieverbruik.

Tot slot wordt er een vergelijking gepresenteerd tussen verschillende triggermechanismes in een echt cyberfysieksysteem, de WaterBox. De WaterBox is een geschaalde versie van een smart (slim) waterdistributiesysteem, waarbij alle componenten verbonden zijn via een wifinetwerk. We identificeren een model voor het systeem, en ontwerpen een schakelende controller en triggermechanismes. De geïmplementeerde triggermechanismes zijn: traditionele periodische tijd-getriggerde control, gecentraliseerde periodische event-getriggerde control, gedecentraliseerde periodische event-getriggerde control met synchrone en asynchrone transmissies. Daarnaast worden ook de bijbehorende TDMA-protocollen voor iedere triggermechanisme worden ontworpen. Meer dan vierhonderd experimenten zijn geanalyseerd en samengevat middels vergelijkingen van bandbreedtebezetting en energieverbruik voor verschillende triggermechanismes.

The bijdragen van deze dissertatie demonstreren de potentie van geavanceerde regeltechnologieën, met name van event-getriggerde control, ter oplossing voor daadwerkelijke problemen, zoals bijvoorbeeld het verbeteren van de efficiëntie in intelligente waterdistributiesystemen.

1

INTRODUCTION

This chapter motivates and introduces the challenges addressed in this work, followed by a review of some existing solutions. Then the contributions of this thesis are presented. The chapter finishes with an outline of the thesis.

1.1. MOTIVATION AND CHALLENGES

In a Wireless Networked Control System (WNCS), there are two major components: a continuous-time physical plant and a wireless networked digital controller. Controllers collect output measurements of the physical system from the sensors, and after some computations produce control signals to be applied to the actuators of the physical system. In WNCS, sensors, computing units, and actuators communicate via a wireless network. Thanks to the development of sensing, information, and communication technologies, these systems are flexible to design, establish, and update, resulting in reduced life-time costs and suitability to a wider range of physical systems. Due to all these benefits, WNCSs have been attracting increasing research attention.

According to [49], several practical constrains must be considered in the design of the closed loops of Networked Control Systems (NCSs):

- the presence of shared communication media and corresponding protocols;
- variable sampling and transmission intervals;
- variable transmission delays;
- packet dropouts;
- quantization errors in the signals transmitted over the network.

All these constraints are a consequence of the bandwidth of a network being limited: one cannot transmit an infinitely large packet (i.e. with infinite precision) via the network; or transmit a packet in an arbitrarily small time (i.e. with zero delay). When

employing wireless networks in control systems, these problems exacerbate since the bandwidth of a wireless network is usually smaller.

Additionally, some other problems may arise when employing wireless networks. Among them, one major problem is the requirement of batteries' maintenance. With the equipment of a wireless transmission module, each node is not required to be connected via wires. This often means that batteries are employed to supply the energy, to provide the nodes with increased mobility and flexibility. Without the constrains imposed by routing wires, the nodes can be established to the most preferred places. However, because of the special spatial positions, these batteries can also be difficult or costly to replace. Therefore, it is desired to reduce the energy consumption of the nodes to enlarge the system's working time and shrink maintenance plan.

This work considers a WNCS and develops approaches to improve the resource consumption efficiency for such implementations, in terms of bandwidth constraints and energy constraints. Besides, this work also validates the proposed approaches in a real physical plant. In short, this work tries to answer the following question:

Problem 1.1.1. *How to increase the resource consumption efficiency of a WNCS?*

1.2. EXISTING WORK

There are several possible approaches to reduce resources' consumption in WNCSs.

EVENT-TRIGGERED CONTROL TO REDUCE THE NUMBER OF TRANSMISSIONS.
Normally the control tasks, i.e. compute and apply control signals by measuring the systems' outputs, are executed base on system clocks, which is named as Time-Triggered Control (TTC). Periodic control is the most typical TTC approach. In this thesis, when TTC appears, we mean traditional periodic control. This strategy may waste resources since it does not regard the system requirements. In an Event-Triggered Control (ETC) implementation, on the other hand, the control tasks are executed aperiodically: only when necessary. This often allows to reduce the usage of resources. There are many results already available studying ETC, see [8], [31], [32], [48], [70], [72], [95], [110], [111], and references therein. In [8], Åström and Bernhardsson present the comparison between periodical sampling (Riemann sampling) and event-based sampling (Lebesgue sampling). The event-based sampling here means the signals are sampled only when measurements cross certain limits. Their work shows that, for some simple systems, event-based sampling has better performance. Tabuada presents an ETC strategy in [95]. In this work, the event condition is a relation between the system current state and the sample-and-hold error, i.e. the error between the current state of the system and the sampled state in the controller. The event mechanism is a centralized one since the event condition requires the whole vector of the state and sample-and-hold error. By analysing the Lyapunov function, pre-designed convergence performances can be guaranteed. In [72], Mazo and Tabuada extend the work of [95] and present a Synchronous Decentralized Event-Triggered Control (SDETC) approach. In that work, the centralized event condition is decentralized to the sensor nodes by means of an adaptation parameter. This adaptation parameter is computed such that when applied to the local event condition, the next event time from each sensor node will be as close to each other

Table 1.1: CC2420 and CC2530 parameters. *P* stands for output power.

Operation	CC2420	CC2530	Unit
Idle	0.426	0.2	mA
Listening to channel	18.8	24.3	mA
Receive	18.8	24.3	mA
Transmit	17.4 (P=0 dBm)	28.7 (P=1 dBm)	mA

as possible. Whenever there is an event locally, all the sensor nodes update the current measurements in the controller synchronously. Further, Mazo and Cao present an Asynchronous Decentralized Event-Triggered Control (ADETC) in [70]. This triggering mechanism not only decentralizes the event condition to each of the sensor nodes, but also introduces an asynchronous sampling update mechanism. That is, it only requires the measurement from the node which triggered a local event to update the controller after such an event happens. This decentralization mechanism is realized by introducing an extra dynamical threshold. However, all these three Event-Triggered Mechanisms (ETMs) require the sensors to continuously monitor the plant output in order to validate the event conditions. This continuous monitoring requires large amounts of energy supplies. Besides, such monitoring is also difficult to realize in real physical systems.

For the centralized mechanisms [95], if the sensors are not co-located with the ETMs, which is a part of the ETC that determines event time sequences, continuous transmission of the local measurements is required. When one looks at the synchronous decentralized ETC [72], the sensors are required to continuously listen to the channel for transmission requirements; for the asynchronous one [70], the sensors are required to wake up and listen to the channel periodically for some threshold update signals. All these effects result in unnecessary energy consumption. In wireless networks, listening/receiving consumes as much or even more energy than transmitting. Table 1.1 shows a comparison of the required current between two different radio devices CC2420 [99] and CC2530 [100] under different operations. Therefore, to reduce the wireless bandwidth occupation and energy consumption, it is desirable to reduce the listening time of the sensors.

REDUCING THE SENSORS' AND ETMS' WORKING TIME.

To reduce the sensor and ETM working time, a possible approach is to replace continuous monitoring of the output by periodic checking of these triggering conditions. However, this introduces additional delays to the system. There are two ways to compensate the delays caused by the discretization: either design a more conservative event condition which will result in more events, e.g. the work shown in [71]; or modify the Lyapunov function, e.g. the work shown in [48]. In [48], a Periodic Event-Triggered Control (PETC) is presented. PETC combines ETC and the periodic sampling method. By modifying the Lyapunov function, the event condition can be made less conservative while the predesigned stability and performance can still be guaranteed. [48] presents a centralized PETC and a decentralized PETC, the difference being that the former one requires the whole vector of the plant output and sample-and-hold error for the event condition validation; while the latter one only requires local information for the local event condition

validation. In the latter one, the transmission is also asynchronous. The centralized PETC will be introduced in detail in Chapter 2, since it will be demonstrated in the WaterBox presented in Chapter 6. However, in [48] none of the proposed mechanisms consider quantization of the sampled signals, whose inclusion is the first contribution of this thesis.

REDUCING THE PACKET LENGTH TO REDUCE EACH TRANSMISSION TIME.
Another way to reduce the bandwidth occupation and energy consumption is to reduce the packet length of each transmission, thus reducing the transmission and reception times. The total number of bits of each transmission is dependent on the quantizers employed. There are mainly two types of quantizers: static and dynamic ones. In a static quantizer, the quantization mapping is time invariant. Examples can be found in the quantizers presented in [25], [34], [42]. In a dynamic quantizer, the quantization mapping is time variant and sometimes dependent on the system's current state, e.g. the quantizer presented in [66], [67], [85]. In [42], Fu and Xie present a type of logarithmic quantizer in which the quantization error is dependent on the plant output: the quantization error is larger if the plant output is further away from the origin. However the quantization mapping from plant output to the quantized output is still invariant. Different from this static quantizer, in [66] a dynamic quantizer is presented. In this quantizer, the quantization mapping has its own dynamics: the quantization error follows the system's state in a zooming fashion. Whenever the state sets closer to the equilibrium point, the quantizer zooms in, thus the quantization error decreases. In [67], Liberzon and Nešić extend the work of [66] and design a dynamic quantizer for output feedback systems. The dynamic quantizer contained in the ADETC from [71] follows essentially the same idea from [66].

SCHEDULING APPROACHES.
In WNCSs, each node is required to listen to the channel in order to receive data, and access medium during data transmission. Furthermore, the sensors are required to wake up and measure system's output in advance before a transmission to either ETMs if ETC is applied, or to controllers directly otherwise (TTC). It is desirable to apply scheduling approaches to WNCSs, since these approaches can help to avoid channel access conflicts and reduce listening times, which results in reductions on energy consumption. To enable such scheduling approaches, a model for the communication's traffic generated by an implementation is required. Some pieces of work on modelling the traffic of an implementation can be found in, e.g. [37], [38], [62], [64], [113], and the references therein. In [62], Kolarijani and Mazo present a construction approach for communication's traffic model for an implementation applying the ETC from [95]. In their approach, they first divide the state-space into finite cones. By using a line search algorithm and over-approximation techniques (see e.g. [23], [24], [33], [43], [50], [88], [94]), the system dynamics between any two events are analysed. Applying the S-procedure (see e.g. [15]), Linear Matrix Inequalities (LMIs) are constructed to capture event behaviours starting from each state region. Transitions among different conic regions are derived by reachability analysis, see e.g. [6], [7], [21], and [22]. With the constructed traffic model, the scheduling of the implementation actions can be made aiming at reducing bandwidth occupation and saving more energy. Kolarijani and Mazo extend their work and present

a way to construct an approximate power quotient system for the traffic model of ETC systems with disturbances in [64]. However the disturbance is assumed to be vanishing as the state converges, which limits the application of the approach. Constructing a communication's traffic model for PETC implementations without this assumption is the second contribution of this thesis.

COMMUNICATION PROTOCOLS.

To apply ETMs to real WNCSs, the communication protocols should be considered. A properly designed protocol can reduce the packet collisions and the waiting time of the nodes, thus the energy consumption can also be reduced and the communication can be minimized. There is some work that concentrates on the communication protocols in NCSs, e.g. [11], [12], [19], [30], [71], [77], [80], [81], [105]. However, a protocol that can fully exploit the ETC properties and minimize the communications is important but still missing according to [74]. For wireless networks with only one communication channel, Carrier-Sense Multiple Access (CSMA) [17] and Time-Division Multiple Access (TDMA) [73] are two commonly used Media Access Control (MAC) protocols. In CSMA, every node can access the channel at any time. However, the transmission can only happen when the node senses the channel is idle, either by Carrier-Sense Multiple Access with Collision Avoidance (CSMA/CA) or Carrier-Sense Multiple Access with Collision Detection (CSMA/CD). If there is a collision, the node will wait for a random time to try to communicate again. In TDMA, the access time of the channel is divided into slots. Each node can only access the channel on its own slots. There are many other protocols proposed for control applications, e.g. ALOHA [1], Round-Robin (RR) protocol, Try-Once-Discard (TOD) protocol, and Maximum-Error First (MEF) protocol; the latter 3 can be found in [10], [76], [107]. However, these protocols are either based on CSMA or TDMA, or require the whole vector of the last sampling error, making it not resource efficient in WNCSs. In CSMA, because of the collisions and random waiting times, there is no upper bound for the transmission delay caused by the protocol. In a closed-loop feedback system, however, the transmission delay should have a strict bound for the controller design in order to provide strict guarantees of stability and performance. Therefore, CSMA is in general not suitable for real-time control systems. On the other hand, the transmission delay caused by the protocol is bounded from above in TDMA. Therefore, TDMA is usually more suitable for WNCSs. In [5] and [71], customized TDMA-based MAC layers for ETC implementations are proposed. The proposed wireless MAC protocols are based on IEEE 802.15.4 [52]. However, both of these pieces of work do not study the energy consumed by the sensors. Customizing TDMA protocols for some ETC implementations with study on energy consumption is another contribution of this thesis.

WIRED NETWORKED CONTROL SYSTEMS APPLYING ETC

ETC has already been applied to a number of experimental control systems, including wired and wireless networked ones.

In the literature applying ETC to wired NCSs, the networks are usually based on IEEE 802.3 [54]. In [65], Lehmann and Lunze apply ETC to a chemical pilot plant VERA for thermo fluid processes. The network employed in their work is an Ethernet, a version

of IEEE 802.3. In [87], Sigurani et al. apply ETC to a continuous flow process with two reactors. The network therein is an Ethernet employing UDP/IP.

WIRELESS NETWORKED CONTROL SYSTEMS APPLYING ETC

In the literature applying ETC to WNCSs, mostly networks based on either IEEE 802.11 [53] or IEEE 802.15.4 [52] are employed. For those systems applying IEEE 802.11, one can find examples in [14], [20], and [109]. In [14], Borgers presents experimental results based on a Toyota Prius vehicle platoon. In this system, a WiFi (IEEE 802.11a) wireless network is employed. In [20] and [109], WiFi (IEEE 802.11b) based ETC for DC motors is presented. For those systems applying IEEE 802.15.4, one can find examples in [2], [5], and [79]. Altaf et al. present their work applying ETC to a 3D tower crane in [2]. The network is based on IEEE 802.15.4, and the protocol is CSMA/CA. Araújo et al. present their work of applying ETC to a double tank system in [5]. The network they employed is again an IEEE 802.15.4 based customized wireless network. In [79], Peng et al. apply ETC to an inverted pendulum. The network is constructed based on IEEE 802.15.4.

However, the testbeds are still not as varied compared to the physical implementations applying TTC. There still lack experimental results comparing energy consumption across several ETCs. The experimental comparison will also be one of the contributions of this thesis.

1.3. ORIGINAL CONTRIBUTIONS

The main contributions of this thesis are summarized here:

- We propose two new versions of ETC, namely Asynchronous Decentralized Periodic Event-Triggered Control (ADPETC) and Synchronous Decentralized Periodic Event-Triggered Control (SDPETC). ADPETC incorporates a zooming quantizer, a decentralized event-triggered strategy with asynchronous communications, and periodic sampling, and can be applied to both state-feedback and output-feedback systems. For systems employing dynamic controllers, the update of the plant input can also be included in the ETM. Additionally, the necessary packet length of each transmission can be established thanks to the dynamic quantizer. Further analysis shows that this ADPETC can greatly reduce the number of transmissions compared to TTC, sensor listening time compared to centralized ETC, and the length of each transmitted packet, while guaranteeing pre-designed stability and performance. SDPETC incorporates a decentralized event-triggered strategy with synchronous communications and periodic sampling. It can reduce the sensing time and controller listening time compared to continuously monitored ETC, thus reducing the energy consumption.

- We propose a constructive approach, with which a finite abstraction can be made to model the communication's traffic generated by PETC implementations from [48]. By computing the upper and lower bounds of the inter-event intervals and reachable states starting from each state region of the state-space, the communication behaviours of PETC systems can be captured. This result can be used to automatically design schedulers [63] for PETC implementations to further reduce the

bandwidth occupation and energy consumption. In this approach, disturbances affecting that system are only required to be both $\mathscr{L}_2$ and $\mathscr{L}_\infty$.

- We extend the WaterBox from [56] by introducing a controller and a wireless networked feedback channel. We identify the hardware, linearise the model, design corresponding TDMA based MAC protocols for the chosen triggering mechanisms, namely: TTC, centralized PETC, SDPETC, and ADPETC; design a hybrid controller for the identified model; complete hundreds of experiments; analyse and compare the bandwidth occupation and energy consumption among the chosen triggering mechanisms.

1.4. THESIS OUTLINE

To answer Problem 1.1.1, in this thesis two research lines are followed. The first one focus on the development of new ETC strategies (Chapter 3 and 4), and then demonstrating and comparing the newly developed strategies with some existed strategies (Chapter 6). The second one constructs communication's traffic models of existing event-triggered controller implementations (Chapter 5). These traffic models allow to employ advanced scheduling methods with which the waiting time of the nodes can be reduced. Therefore the nodes can wake up only when necessary and in this manner save energy. A brief introduction of each chapter follows.

- **Chapter 2** presents necessary definitions and results from hybrid system and system theory. These preliminaries will be used in the following chapters. TTC and centralized PETC are also reviewed for use in later chapters.
- **Chapter 3** introduces ADPETC. We present the decentralized event-triggering strategy, asynchronous output sampling, update mechanism, and threshold update mechanism. We analyse the system stability and performance conditions, maximum packet size of each transmission, and provide a numerical demonstration.
- **Chapter 4** introduces SDPETC. We present the decentralized event-triggering strategy, synchronous state sampling and update mechanism, and adaption parameter algorithm. We analyse the system stability, and provide a numerical demonstration.
- **Chapter 5** introduces the abstraction of PETC systems. We present the detailed construction of a power quotient system for the traffic model of the original system, including state partition, output map computation, and transition relation analysis. A numerical result is given, showing the feasibility of the presented approach.
- **Chapter 6** presents the experiments on the WaterBox. We first present a customized TDMA medium access mechanism for the triggering mechanisms implemented, namely: TTC, centralized PETC, SDPETC, and ADPETC. Then the thesis shows the system identification, controller design, and parameters design of the triggering conditions for each of these mechanisms. This chapter is concluded with the analysis of the results of more than 400 experiments.

- **Chapter 7** summarizes the results of this thesis and gives an outline for future work.

2

PRELIMINARIES

In this chapter, we present some definitions of notions of stability, hybrid system, and system theory employed in the remaining of the thesis. We present some existing results about TTC and centralized PETC that are used in later chapters.

2.1. STABILITY NOTIONS

We first present some general mathematical definitions. Starting with 4 classes of functions. In particular, we introduce $\mathcal{K}$, $\mathcal{K}_\infty$, and $\mathcal{KL}$ functions since they are specialized comparison functions employed to define the stability of systems.

Definition 2.1.1. *($\mathcal{K}$ function) [61]*
A function $\alpha: \mathbb{R}^+ \to \mathbb{R}^+$ belongs to class $\mathcal{K}$ ($\alpha \in \mathcal{K}$) if: α is a continuous function, $\alpha(0) = 0$ and $s_1 > s_2 \Rightarrow \alpha(s_1) > \alpha(s_2)$.

Definition 2.1.2. *($\mathcal{K}_\infty$ function) [61]*
A function $\alpha: \mathbb{R}^+ \to \mathbb{R}^+$ belongs to class $\mathcal{K}_\infty$ ($\alpha \in \mathcal{K}_\infty$) if: $\alpha \in \mathcal{K}$ and $\lim_{s\to\infty} \alpha(s) = \infty$.

Definition 2.1.3. *($\mathcal{L}$ function) [61]*
A function $\alpha: \mathbb{R}^+ \to \mathbb{R}^+$ belongs to class $\mathcal{L}$ ($\alpha \in \mathcal{L}$) if: α is a continuous function, $s_1 \geq s_2 \Rightarrow \alpha(s_1) \leq \alpha(s_2)$ and $\lim_{s\to\infty} \alpha(s) = 0$.

Definition 2.1.4. *($\mathcal{KL}$ function) [61]*
A function $\alpha: \mathbb{R}^+ \to \mathbb{R}^+$ belongs to class $\mathcal{KL}$ ($\alpha \in \mathcal{KL}$) if: $\forall\, t : \beta(\cdot, t) \in \mathcal{K}$ and $\forall\, s : \beta(s, \cdot) \in \mathcal{L}$.

Definition 2.1.5. *($\mathcal{L}_2$-norm) [103]*
For a signal $w: \mathbb{R}^+ \to \mathbb{R}^n$, the $\mathcal{L}_2$-norm is $\|w\|_{\mathcal{L}_2} = \sqrt{\int_0^\infty |w(t)|^2 dt}$.

Definition 2.1.6. *($\mathcal{L}_\infty$-norm) [103]*
For a signal $w: \mathbb{R}^+ \to \mathbb{R}^n$, the $\mathcal{L}_\infty$-norm is $\|w\|_{\mathcal{L}_\infty} = \sup_{t\geq 0} \|w(t)\|$.

Now we give some stability definitions, since stability analysis is one of the main objects of this thesis.

Definition 2.1.7. *(Asymptotical Stability) [90]*
A system $\dot{\xi}(t) = f(\xi(t))$, $t \in \mathbb{R}_0^+$, $\xi(t) \in \mathbb{R}^n$ is said to be Uniformly Global Asymptotical Stable (UGAS) if there exists $\beta \in \mathcal{KL}$ such that for any $t_0 \geq 0$ the following holds:

$$\forall \xi(t_0) \in \mathbb{R}^n, |\xi(t)| \leq \beta(|\xi(t_0)|, t - t_0), \forall\, t \geq t_0. \tag{2.1}$$

Definition 2.1.8. *(Exponential Stability) [90]*
A system $\dot{\xi}(t) = f(\xi(t))$, $t \in \mathbb{R}_0^+$, $\xi(t) \in \mathbb{R}^n$ is said to be Uniformly Global Exponential Stable (UGES) if there exists $a, c \in \mathbb{R}^+$ such that for any $t_0 \geq 0$ the following holds:

$$|\xi(t, \xi(0))| \leq c|\xi(0)|e^{-at}, \forall\, t \geq t_0. \tag{2.2}$$

We employ also the Lyapunov exponential stability theorem (see e.g. [90]) stating that:

Theorem 2.1.9. *(Lyapunov exponential stability) [90]*
Consider a system $\dot{\xi}(t) = f(\xi(t))$, $t \in \mathbb{R}_0^+$, $\xi(t) \in \mathbb{R}^n$. If there exist a function $V : \mathbb{R}^n \to \mathbb{R}_0^+$ and a constant $\lambda > 0$ such that $V(x) > 0$, $x \neq 0$, $V(0) = 0$ and $\dot{V}(\xi(t)) \leq -\lambda V(\xi(t))$ for all ξ, then the system is UGES. λ is called the decay rate.

However these stability notions do not consider inputs. Here we introduce the Input-to-State Stablility (ISS) property as follows. ISS is a notion of robustness to external inputs.

Definition 2.1.10. *(Input-to-State Stability) [90]*
A control system $\dot{\xi} = f(\xi, v)$ is said to be (uniformly globally) ISS with respect to v if there exist $\beta \in \mathcal{KL}$, $\gamma \in \mathcal{K}_\infty$ such that for any $t_0 \in \mathbb{R}_0^+$ the following holds:

$$\begin{aligned} &\forall \xi(t_0) \in \mathbb{R}^n, \|v\|_\infty < \infty \Rightarrow \\ &|\xi(t)| \leq \beta(|\xi(t_0)|, t - t_0) + \gamma(\|v\|_\infty), \forall\, t \geq t_0. \end{aligned} \tag{2.3}$$

The ISS property of a system can also be established by means of ISS-Lyapunov functions.

Definition 2.1.11. *(ISS Lyapunov function) [90]*
A continuously differentiable function $V : \mathbb{R}^n \to \mathbb{R}_0^+$ is said to be an ISS Lyapunov function for the closed-loop system $\dot{\xi} = f(\xi, v)$ if there exist class $\mathcal{K}_\infty$ functions $\underline{\alpha}$, $\overline{\alpha}$, α_V, and α_v such that for all $\xi \in \mathbb{R}^n$ and $v \in \mathbb{R}^m$ the following is satisfied:

$$\begin{aligned} &\underline{\alpha}(|\xi(t)|) \leq V(\xi(t)) \leq \overline{\alpha}(|\xi(t)|) \\ &\nabla V \cdot f(\xi, v) \leq -\alpha_V \circ V(\xi(t)) + \alpha_v(|v(t)|). \end{aligned} \tag{2.4}$$

Theorem 2.1.12. *(Sufficient conditions for ISS) [90]*
A system is ISS if and only if a smooth ISS-Lyapunov function exists.

2.2. NOTIONS FOR HYBRID SYSTEMS

So far, the presented stability notions are restricted to continuous-time systems. In many cases, the control system's dynamics contain both flows and jumps. These systems are called hybrid systems. When studying hybrid systems, stability and other properties should be carefully adjusted. Next we present some definitions and results for Hybrid systems.

Definition 2.2.1. *(Hybrid system) [44]*
A system $\mathcal{H} := (C_H, F_H, D_H, G_H)$ is a hybrid system, if it can be represented in the following form:

$$\begin{cases} x \in C_H, & \dot{x} \in F_H(x) \\ x \in D_H, & x^+ \in G_H(x), \end{cases}$$

in which C_H is the flow set, F_H is the flow map, D_H is the jump set, G_H is the jump map. x^+ represents the value of the state after an instantaneous change.

Hybrid systems have both continuous-time and discrete-time dynamics, therefore, it is convenient to parameterize the solutions to hybrid systems by both t, the elapsed time, and j, the elapsed jumps.

Definition 2.2.2. *(Hybrid time domain) [44]*
Consider a hybrid system $\mathcal{H} := (C_H, F_H, D_H, G_H)$. A subset E_H of $\mathbb{R}_0^+ \times \mathbb{N}$ is a hybrid time domain, if it is the union of infinitely many intervals of the form $[t_j, t_{j+1}] \times \{j\}$, where $0 = t_0 \le t_1 \le t_2 \le \cdots$, or of finitely many such intervals, with the last one possible of the form $[t_j, t_{j+1}] \times \{j\}$, $[t_j, t_{j+1}[\times \{j\}$, or $[t_j, \infty] \times \{j\}$.

Definition 2.2.3. *(Hybrid arc) [44]*
Consider a hybrid system $\mathcal{H} := (C_H, F_H, D_H, G_H)$. A hybrid arc is a function $\phi : dom\, \phi \to \mathbb{R}^n$, where dom ϕ is a hybrid time domain and, for each fixed j, $t \to \phi(t, j)$ is a locally absolutely continuous function on the interval $I_j = \{t : (t, j) \in dom\, \phi\}$.

Definition 2.2.4. *(Hybrid system solution) [44]*
The hybrid arc ϕ is a solution to the hybrid system $\mathcal{H} = (C_H, F_H, D_H, G_H)$, if $\phi(0,0) \in C_H \cup D_H$, and:

- *flow condition. For each $j \in \mathbb{N}$ such that I_j has non-empty interior,*

$$\dot{x}(t, j) \in F_H(x(t, j)) \text{ for a lmost all } t \in I_j,$$
$$x(t, j) \in C_H \text{ for all } t \in [\min I_j, \sup I_j].$$

- *jump condition. For each $(t, j) \in dom\, x$ such that $(t, j+1) \in dom\, x$,*

$$x(t, j+1) \in G_H(x(t, j)),$$
$$x(t, j) \in D_H.$$

A system's state may converge to a set instead of a point. Therefore, to describe the convergence of the state, we introduce the notation of distance of a vector to a set: for a vector x and a closed set $\mathcal{A}$, the distance of this vector to the set is

$$|x|_{\mathcal{A}} = \min \{|x - y| : y \in \mathcal{A}\}.$$

Definition 2.2.5. *(Pre-asymptotical stability) [45]*
Consider a hybrid system $\mathcal{H}$ on $\mathbb{R}^n$. Let $\mathcal{A} \subset \mathbb{R}^n$ be closed. The set $\mathcal{A}$ is said to be

- *uniformly globally stable for $\mathcal{H}$ if there exists a class-$\mathcal{K}_\infty$ function α such that any solution ϕ to $\mathcal{H}$ satisfies $|\phi(t,j)|_{\mathcal{A}} \leq \alpha(|\phi(0,0)|_{\mathcal{A}})$ for all $(t,j) \in dom\,\phi$;*
- *uniformly globally pre-attractive for $\mathcal{H}$ if for each $\varepsilon > 0$ and $r > 0$ there exists $T > 0$ such that, for any solution ϕ to $\mathcal{H}$ with $|\phi(0,0)|_{\mathcal{A}} \leq r$, $(t,j) \in dom\,\phi$ and $t + j \geq T$ imply $|\phi(t,j)|_{\mathcal{A}} \leq \varepsilon$;*
- *Uniformly Global pre-Asymptotical Stable (UGpAS) for $\mathcal{H}$ if it is both uniformly globally stable and uniformly globally pre-attractive.*

The definition of Lyapunov function candidate for hybrid systems and corresponding sufficient Lyapunov function conditions for pre-asymptotical stability are presented here:

Definition 2.2.6. *(Lyapunov function candidate) [44]*
Given the hybrid system $\mathcal{H} = (C_H, F_H, D_H, G_H)$, and the compact set $\mathcal{A} \subset \mathbb{R}^n$, the function V: dom $V \to \mathbb{R}$ is a Lyapunov function candidate for $(\mathcal{H}, \mathcal{A})$ if the following conditions hold:

- *V is continuous and non-negative on $(C_H \cup D_H) \setminus \mathcal{A} \subset dom\,V$;*
- *V is continuously differentiable on an open set $\mathcal{O}$ satisfying $C_H \setminus \mathcal{A} \subset \mathcal{O} \subset dom\,V$;* $\lim_{\{x \to \mathcal{A}, x \in dom\,V \cap (C_H \cup D_H)\}} V(x) = 0$,

where $x \to \mathcal{A}$ denotes $\lim_{t\to\infty} x(t) \in \mathcal{A}$.

Theorem 2.2.7. *(Sufficient Lyapunov conditions) [44]*
Consider the hybrid system $\mathcal{H} = (C_H, F_H, D_H, G_H)$ and the compact set $\mathcal{A} \subset \mathbb{R}^n$ satisfying $G_H(\mathcal{A} \cap D_H) \subset \mathcal{A}$. If there exists a Lyapunov function candidate V for $(\mathcal{H}, \mathcal{A})$ such that

$$\langle \nabla V(x), f \rangle \leq 0,\ \forall x \in C_H \setminus \mathcal{A}, f \in F_H(x)$$
$$V(g) - V(x) \leq 0,\ \forall x \in D_H \setminus \mathcal{A}, g \in G_H(x) \setminus \mathcal{A}.$$

then $\mathcal{A}$ is pre-asymptotically stable and the basin of pre-attraction contains every forward invariant, compact set.

Besides the stability of a system, we are also interested in the performance, in particular the $\mathcal{L}_2$ performance.

Definition 2.2.8. *($\mathcal{L}_2$-gain) [49]*
The system $\dot{\xi}(t) = f(\xi(t), w(t))$, $z(t) = g(\xi(t), w(t))$ is said to have an $\mathcal{L}_2$-gain from w to z smaller than or equal to γ, if there is a $\mathcal{K}_\infty$ function $\delta : \mathbb{R}^{n_\xi} \to \mathbb{R}^+$ such that for any $w \in \mathcal{L}_2$, any initial state $\xi(0) = \xi_0 \in \mathbb{R}^{n_\xi}$, the corresponding solution to the system satisfies $\|z\|_{\mathcal{L}_2} \leq \delta(\xi_0) + \gamma \|w\|_{\mathcal{L}_2}$.

The signal z is a particular controlled output variable, which can be either nonlinearly dependent on ξ and w as shown in [49] or linearly dependent on ξ and w as shown in [32]. The $\mathcal{L}_2$-gain of a system captures the influence of the disturbance input w on the output z.

2.3. SYSTEMS THEORY

Now we present some definitions and results from the field of systems theory, which will be used in Chapter 5. We use the mathematical notion of system, which is a synonym for mathematical model of a dynamical phenomenon, since it is a versatile notion including relationships which shows how different systems can be related.

Definition 2.3.1. *(System) [96]*
A system is a sextuple $(X, X_0, U, \longrightarrow, Y, H)$ *consisting of:*

- *a set of states* X*;*
- *a set of initial states* $X_0 \subseteq X$*;*
- *a set of inputs* U*;*
- *a transition relation* $\longrightarrow \subseteq X \times U \times X$*;*
- *a set of outputs* Y*;*
- *an output map* $H : X \to Y$*.*

The term finite-state (infinite-state) system indicates X is a finite (an infinite) set. Further, if X is countable, then the system is said to be countable. For a system, if the cardinality of U is smaller than or equal to one, then this system is said to be autonomous.

Definition 2.3.2. *(Metric) [35]*
Consider a set T*,* $d : T \times T \to \mathbb{R} \cup \{+\infty\}$ *is a metric (or a distance function) if the following three conditions are satisfied* $\forall\, x, y, z \in T$*:*

- $d(x, y) = d(y, x)$*;*
- $d(x, y) = 0 \leftrightarrow x = y$*;*
- $d(x, y) \leq d(x, z) + d(y, z)$*.*

The ordered pair (T, d) is said to be a metric space.

Definition 2.3.3. *(Metric system) [96]*
A system $\mathscr{S} = (X, X_0, U, \longrightarrow, Y, H)$ *is said to be a metric system if the set of outputs* Y *is equipped with a metric* $d : Y \times Y \to \mathbb{R}_0^+$*.*

If Z is a set, then a relation in Z is a subset $Q \subset Z \times Z$, and two points $x_1, x_2 \in Z$ are Q-related if $(x_1, x_2) \in Q$.

Definition 2.3.4. *(Equivalence relation) [16]*
If Z *is a set, a relation* Q *is an equivalence relation in* Z*, if*

- *for each* $x \in Z$*,* $(x, x) \in Q$ *(reflexivity);*
- *if* $(x_1, x_2) \in Q$*, then* $(x_2, x_1) \in Q$ *(symmetry);*
- *if* $(x_1, x_2) \in Q$ *and* $(x_2, x_3) \in Q$*, then* $(x_1, x_3) \in Q$ *(transitivity).*

When Q is an equivalence relation on a set Z, define $[z]$ the equivalence class of $z \in Z$, define Z/Q the set of all equivalence classes [96].

In many Cyber-Physical Systems (CPSs), the system behaviours can be described by automata. Usually these automata may be very large, making it difficult to study and analyse. Instead of analysing directly such system, one can alternatively construct a model with desired behaviours, and verify the relationship between the system and constructed model.

For the construction, we present the notion of quotient system first, which is the background of the type of system we construct in Chapter 5.

Definition 2.3.5. *(Quotient system) [96]*
Let $\mathscr{S} = (X, X_0, U, \longrightarrow, Y, H)$ be a system and Q be an equivalence relation on X such that $(x, x') \in Q$ implies $H(x) = H(x')$. The quotient of $\mathscr{S}$ by Q, denoted by $\mathscr{S}_{/Q}$, is the system $\left(X_{/Q}, X_{/Q,0}, U_{/Q}, \xrightarrow[/Q]{}, Y_{/Q}, H_{/Q}\right)$ consisting of:

- $X_{/Q} = X/Q$;
- $X_{/Q,0} = \left\{x_{/Q} \in X_{/Q} \middle| x_{/Q} \cap X_0 \neq \emptyset\right\}$;
- $U_{/Q} = U$;
- $\left(x_{/Q}, u, x'_{/Q}\right) \in \xrightarrow[/Q]{}$ *if* $\exists (x, u, x') \in \longrightarrow$ *in* $\mathscr{S}$ *with* $x \in x_{/Q}$ *and* $x' \in x'_{/Q}$;
- $Y_{/Q} = Y$;
- $H_{/Q}\left(x_{/Q}\right) = H(x)$ *for some* $x \in x_{/Q}$.

Applying the notion of power set, we introduce an alternative notion of quotient system, called power quotient system:

Definition 2.3.6. *(Power quotient system) [62]*
Let $\mathscr{S} = (X, X_0, U, \longrightarrow, Y, H)$ be a system and R be an equivalence relation on X. The power quotient of $\mathscr{S}$ by R, denoted by $\mathscr{S}_{/R}$, is the system $\left(X_{/R}, X_{/R,0}, U_{/R}, \xrightarrow[/R]{}, Y_{/R}, H_{/R}\right)$ consisting of:

- $X_{/R} = X/R$;
- $X_{/R,0} = \{x_{/R} \in X_{/R} | x_{/R} \cap X_0 \neq \emptyset\}$;
- $U_{/R} = U$;
- $\left(x_{/R}, u, x'_{/R}\right) \in \xrightarrow[/R]{}$ *if* $\exists (x, u, x') \in \longrightarrow$ *in* $\mathscr{S}$ *with* $x \in x_{/R}$ *and* $x' \in x'_{/R}$;
- $Y_{/R} \subset 2^Y$;
- $H_{/R}(x_{/R}) = \bigcap_{x \in x_{/R}} H(x)$.

Now we first present the notion of Hausdorff distance, to measure the distance of two subsets in a metric space, and then present a relationship between systems employing such a distance.

Definition 2.3.7. *(Hausdorff distance) [35]*
Assume X and Y are two non-empty subsets of a metric space (T,d). The Hausdorff distance $d_H(X,Y)$ is given by:

$$\max\left\{\sup_{x\in X}\inf_{y\in Y} d(x,y), \sup_{y\in Y}\inf_{x\in X} d(x,y)\right\}. \tag{2.5}$$

Definition 2.3.8. *(Approximate simulation relation) [96]*
Consider two metric systems $\mathcal{S}_a = (X_a, X_{a0}, U_a, \underset{a}{\longrightarrow}, Y_a, H_a)$ and $\mathcal{S}_b = (X_b, X_{b0}, U_b, \underset{b}{\longrightarrow}, Y_b, H_b)$ with $Y_a = Y_b$, and let $\epsilon \in \mathbb{R}_0^+$. A relation $R \subseteq X_a \times X_b$ is an ϵ-approximate simulation relation from $\mathcal{S}_a$ to $\mathcal{S}_b$ if the following three conditions are satisfied:

- $\forall x_{a0} \in X_{a0}, \exists x_{b0} \in X_{b0}$ *such that* $(x_{a0}, x_{b0}) \in R$;
- $\forall (x_a, x_b) \in R$ *we have* $d(H_a(x_a), H_b(x_b)) \leq \epsilon$;
- $\forall (x_a, x_b) \in R$ *such that* $(x_a, u_a, x_a') \in \underset{a}{\longrightarrow}$ *in* $\mathcal{S}_a$ *implies* $\exists (x_b, u_b, x_b') \in \underset{b}{\longrightarrow}$ *in* $\mathcal{S}_b$ *satisfying* $(x_a', x_b') \in R$.

We denote the existence of an ϵ-approximate simulation relation from $\mathcal{S}_a$ to $\mathcal{S}_b$ by $\mathcal{S}_a \preceq^{\epsilon}_{\mathscr{S}} \mathcal{S}_b$, and say that $\mathcal{S}_b$ ϵ-approximately simulates $\mathcal{S}_a$ or $\mathcal{S}_a$ is ϵ-approximately simulated by $\mathcal{S}_b$. Whenever $\epsilon = 0$, the inequality $d(H_a(x_a), H_b(x_b)) \leq \epsilon$ implies $H_a(x_a) = H_b(x_b)$ and the resulting relation is called a (exact) simulation relation.

A ϵ-approximate simulation condition for a metric system and its power quotient system is presented in the following lemma.

Lemma 2.3.9. *[62]*
Let $\mathcal{S} = (X, X_0, U, \longrightarrow, Y, H)$ be a metric system, R be an equivalence relation on X, and let the metric system $\mathcal{S}_{/R} = (X_{/R}, X_{/R0}, U_{/R}, \underset{/R}{\longrightarrow}, Y_{/R}, H_{/R})$ be the power quotient system of $\mathcal{S}$ by R. For any

$$\epsilon \geq \max_{\substack{x \in x_{/R} \\ x_{/R} \in X_{/R}}} d(H(x), H_{/R}(x_{/R})), \tag{2.6}$$

with d the Hausdorff distance over the set 2^Y, $\mathcal{S}_{/R}$ ϵ-approximately simulates $\mathcal{S}$, i.e. $\mathcal{S} \preceq^{\epsilon}_{\mathscr{S}} \mathcal{S}_{/R}$.

Minkowski addition is presented now for reachability analysis in Chapter 5.

Definition 2.3.10. *(Minkowski addition) [83]*
The Minkowski addition of two sets of vectors $\mathscr{A}$ and $\mathscr{B}$ in Euclidean space is formed by adding each vector in $\mathscr{A}$ to each vector in $\mathscr{B}$:

$$\mathscr{A} \oplus \mathscr{B} = \{\boldsymbol{a} + \boldsymbol{b} | \, \boldsymbol{a} \in \mathscr{A}, \boldsymbol{b} \in \mathscr{B}\},$$

where $\oplus$ denotes the Minkowski addition.

Also note that, in this thesis, we some time denote symmetric matrices of the form $\begin{bmatrix} A & B \\ B^{\mathrm{T}} & C \end{bmatrix}$ as $\begin{bmatrix} A & B \\ \star & C \end{bmatrix}$ for the sake of brevity.

2.4. CONTROLLER IMPLEMENTATIONS

In this section, we review some controller implementations which will be used in Chapter 6 for comparison purposes.

2.4.1. TIME-TRIGGERED CONTROL

In this mechanism, the plant output is sampled and updated with a fixed frequency, regardless of the system requirements. Consider a Linear Time-Invariant (LTI) plant:

$$\dot{\xi}(t) = A\xi(t) + B\nu(t), \tag{2.7}$$

where $\xi(t) \in \mathbb{R}^n$ and $\nu(t) \in \mathbb{R}^m$ are the state vector and input vector at time t respectively. Consider also a controller given by:

$$\nu(t) = K\xi(t), \tag{2.8}$$

such that $A+BK$ is Hurwitz. Apply a sample-and-hold mechanism to the controller (2.8) to obtain:

$$\nu(t) = K\hat{\xi}(t), \tag{2.9}$$

where

$$\hat{\xi}(t) := \xi(t_k), t \in [t_k, t_{k+1}[, \tag{2.10}$$

and $\{t_k\}_{k\in\mathbb{N}}$ is the sequence of the state update times. Let the sample-and-hold effect be modelled as a measurement error:

$$\varepsilon(t) := \hat{\xi}(t) - \xi(t). \tag{2.11}$$

We consider TTC as a controller implementation in which the samples are obtained periodically, i.e. there exists an h such that $h = t_{k+1} - t_k$, $\forall k \in \mathbb{N}$. This h is called the sampling period. The sequence of sample and update times t_k is thus determined by:

$$\{t_k | t_k = kh, k \in \mathbb{N}, h > 0\}. \tag{2.12}$$

Define

$$\bar{A} := \begin{bmatrix} A & BK \\ 0 & 0 \end{bmatrix}, J_1 := \begin{bmatrix} I & 0 \\ I & 0 \end{bmatrix}, J_2 := \begin{bmatrix} I & 0 \\ 0 & I \end{bmatrix},$$

where $I \in \mathbb{R}^{n\times n}$ is an identity matrix.

The following corollary is derived from Corollary III.3 in [48]

Corollary 2.4.1. *Consider the system (2.7), (2.9), (2.10), (2.11), and (2.12), given a scalar $\rho > 0$, if there exist a matrix $P \succ 0$ and a scalar $\mu \geq 0$, such that*

$$\begin{bmatrix} e^{-2\rho h}P - \mu Q & J_1^{\mathrm{T}} e^{\bar{A}^{\mathrm{T}} h} P \\ \star & P \end{bmatrix} \succ 0, \tag{2.13}$$

holds, then the system is UGES with decay rate ρ.

2.4.2. CENTRALIZED PERIODIC EVENT-TRIGGERED CONTROL

In Chapter 1, we have briefly introduced the PETC from [48], including centralized and decentralized versions. Now we review the centralized version in detail. This strategy will be demonstrated in Chapter 6.

Consider the system (2.7), (2.9), (2.11), and a sampling sequence defined by (2.12). At each sampling time t_k, the plant output is updated as:

$$\hat{\xi}(t_k) = \begin{cases} \xi(t_k), & \text{when } \xi_d^{\mathrm{T}}(t_k) Q \xi_d(t_k) > 0 \\ \hat{\xi}(t_{k-1}), & \text{when } \xi_d^{\mathrm{T}}(t_k) Q \xi_d(t_k) \leq 0, \end{cases} \tag{2.14}$$

where $\xi_d(t) = \begin{bmatrix} \xi^{\mathrm{T}}(t) & \hat{\xi}^{\mathrm{T}}(t) \end{bmatrix}^{\mathrm{T}}$, Q satisfies $Q := \begin{bmatrix} (1-\sigma)I & -I \\ -I & I \end{bmatrix}$, and $\sigma > 0$ is a pre-designed parameter.

Corollary 2.4.2. *[48]*
Consider the system (2.7), (2.9), (2.11), (2.12), and (2.14), given a scalar $\rho > 0$, if there exist a matrix $P \succ 0$ and scalars $\mu_i \geq 0$, $i \in \{1,2\}$, such that

$$\begin{bmatrix} e^{-2\rho h} P + (-1)^i \mu_i Q & J_i^{\mathrm{T}} e^{\bar{A}^{\mathrm{T}} h} P \\ \star & P \end{bmatrix} \succ 0, \; i \in \{1,2\}, \tag{2.15}$$

holds, then the system is UGES with decay rate ρ.

3

DECENTRALIZED PERIODIC EVENT-TRIGGERED CONTROL WITH QUANTIZATION AND ASYNCHRONOUS COMMUNICATION

ADETC is an implementation of controllers characterized by decentralized event generation, asynchronous sampling updates, and dynamic quantization. Combining those elements in ADETC results in a parsimonious transmission of information which makes it suitable for wireless networked implementations. We extend the previous work on ADETC by introducing periodic sampling, denoting our proposal ADPETC, and study the stability and $\mathscr{L}_2$-gain of ADPETC for implementations affected by disturbances. In ADPETC, at each sampling time, quantized measurements from those sensors that triggered a local event are transmitted to a dynamic controller that computes control actions; the quantized control actions are then transmitted to the corresponding actuators only if certain events are also triggered for the corresponding actuator. The developed theory is demonstrated and illustrated via a numerical example.

Sections 3.2-3.6 and appendix of this chapter are extracted from [39].

3.1. INTRODUCTION

As we have discussed in Chapter 1, when designing a WNCS, a major challenge is to guarantee a pre-designed stability and performance under limited bandwidth and energy supplies. One possible solution is to apply ETC strategies. Although ADETC from [70] can reduce the communication, as a trade-off, the sensor nodes are required to work continuously to monitor the plant outputs and to validate the local event conditions; thus large amounts of energy are consumed. In this chapter, we extend the work of [70] and present ADPETC, to reduce both bandwidth occupation and energy consumption, and guarantee stability and performance levels.

The presented ETM is inspired mainly by the works of [48], [67], and [70]. More specifically, this ADPETC integrates dynamic quantization from [67], ADETC from [70], and periodic sampling from [48]. In this event-triggered strategy, all nodes of the implementation, i.e. the sensors, controller, and actuators, share a global threshold. This global threshold is computed and broadcasted by the controller periodically at each sampling time following a pre-designed threshold update mechanism. The design of this threshold update mechanism is one of the key missions in this chapter. This threshold update mechanism considers all the available information currently in the controller. With this global threshold, each of the sensors and actuators compute their local threshold. During the sampling time, each of the sensors wakes up, measures the corresponding element of the plant output, and checks if the sampling error, i.e the error between the current measurement and the last updated measurement, exceeds the local threshold. If so, then this sensor verifies that there is an event happening locally. All those sensors that have events transmit the current measurements to the controller with the packets indicating the sign of the error and how many times the error exceeds the local threshold. Therefore, transmissions happen asynchronously, i.e. independently of each other. The controller approximates the output of the plant with these packets of information together with the previous updated output and the shared threshold. Then the controller computes the controller output. The controller output is also sampled and updated following the same triggering manner. In this way, both the wireless channel bandwidth occupation and energy consumption can be reduced.

Compared with [67] and [70], the quantization error and global threshold in our approach are dependent on the available information in the controller, instead of the estimation of the plant state. Compared with [48], in which the algorithm for designing the decentralized event condition parameters is complex (since it requires to solve a set of LMIs), our approach only requires to solve one single LMI. Meanwhile, the work [48] do not consider quantization. Our preliminary version in [41] requires to solve a set of Bilinear Matrix Inequalities (BMIs) to design the event condition parameters. Compared with this preliminary work, the work presented in this chapter can result in less conservative event conditions, which leads to less triggered events.

The organization of the remainder of the chapter is as follows. The introduction of the presented ADPETC and formal problem definition are presented in Section 3.2. Section 3.3 presents the threshold update mechanism, system stability and performance analysis. The maximum packet size of each transmission is analysed in Section 3.4. Finally, the presented theory is illustrated by a numerical example in Section 3.5 and this chapter is concluded in Section 3.6.

3.2. PROBLEM DEFINITION

Let us consider an LTI plant given by:

$$\begin{cases} \dot{\xi}_p(t) = A_p\xi_p(t) + B_p\hat{v}(t) + Ew(t) \\ y(t) = C_p\xi_p(t), \end{cases} \tag{3.1}$$

where $\xi_p(t) \in \mathbb{R}^{n_p}$ and $y(t) \in \mathbb{R}^{n_y}$ denote the state vector and output vector of the plant respectively, $\hat{v}(t) \in \mathbb{R}^{n_v}$ denotes the input applied to the plant, $w(t) \in \mathbb{R}^{n_w}$ denotes an unknown disturbance. The plant is controlled by a discrete-time controller given by:

$$\begin{cases} \xi_c(t_{k+1}) = A_c\xi_c(t_k) + B_c\hat{y}(t_k) \\ v(t_k) = C_c\xi_c(t_k) + D_c\hat{y}(t_k), \end{cases} \tag{3.2}$$

where $\xi_c(t_k) \in \mathbb{R}^{n_c}$, $v(t_k) \in \mathbb{R}^{n_v}$, and $\hat{y}(t_k) \in \mathbb{R}^{n_y}$ denote the state vector, output vector of the controller, and input applied to the controller respectively. Define $h > 0$ the sampling interval. A periodic sampling sequence is given by:

$$\mathcal{T} := \{t_k | t_k := kh, k \in \mathbb{N}\}.$$

Define $\tau(t)$ be the elapsed time since the last sampling time, i.e.

$$\tau(t) := t - t_k,\ t \in [t_k, t_{k+1}[.$$

Define two vectors for the implementation input and output:

$$u(t) := \begin{bmatrix} y^{\mathrm{T}}(t) & v^{\mathrm{T}}(t) \end{bmatrix}^{\mathrm{T}} \in \mathbb{R}^{n_u},$$
$$\hat{u}(t_k) := \begin{bmatrix} \hat{y}^{\mathrm{T}}(t_k) & \hat{v}^{\mathrm{T}}(t_k) \end{bmatrix}^{\mathrm{T}} \in \mathbb{R}^{n_u},$$

with $n_u := n_y + n_v$. $u^i(t_k)$ $\hat{u}^i(t_k)$ are the i-th elements of the vector $u(t_k)$, $\hat{u}(t_k)$ respectively. At each sampling time $t_k \in \mathcal{T}$, the input applied to the implementation $\hat{u}(t_k)$ is determined by:

$$\hat{u}^i(t_k) := \begin{cases} \tilde{q}(u^i(t_k)), & \text{if a local event is triggered at } t_k \\ \hat{u}^i(t_{k-1}), & \text{otherwise,} \end{cases} \tag{3.3}$$

where $\tilde{q}(s)$ denotes the quantized signal of s. Therefore, at each sampling time, only those inputs with events are required to transmit measurements or actuation signals through the network. Between the samplings, a zero-order hold mechanism is applied, i.e. $\hat{u}(t) = \hat{u}(t_k)$, $\forall\, t \in [t_k, t_{k+1}[$.

We also introduce a performance variable $z \in \mathbb{R}^{n_z}$ given by:

$$z(t) = g(\xi(t), w(t)), \tag{3.4}$$

where

$$\xi(t) := \begin{bmatrix} \xi_p^{\mathrm{T}}(t) & \xi_c^{\mathrm{T}}(t) & \hat{y}^{\mathrm{T}}(t) & \hat{v}^{\mathrm{T}}(t) \end{bmatrix}^{\mathrm{T}} \in \mathbb{R}^{n_\xi}$$
$$n_\xi := n_p + n_c + n_y + n_v,$$

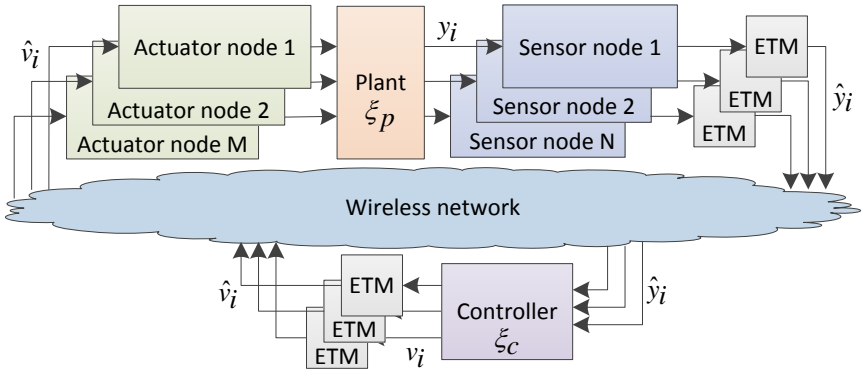

Figure 3.1: Wireless networked systems architecture, indicating the ETMs.

$g(s)$ is a function that depends on the specific design requirements.

The architecture of the implementation is shown in Figure 3.1. In this implementation, the controller, sensors, and actuators are assumed to be physically distributed, and none of the nodes are co-located.

In the local event conditions in (3.3), an event occurs when the following inequality holds:

$$|\hat{u}^i(t_{k-1}) - u^i(t_k)| \geq \sqrt{\eta_i(t_k)},\ i \in \{1, \cdots, n_u\}, \tag{3.5}$$

in which $\eta_i(t_k)$ is a local threshold, computed as:

$$\eta_i(t) := \theta_i^2 \eta^2(t), \tag{3.6}$$

where θ_i is a designed distributed parameter satisfying $|\theta| = 1$ and $\eta : \mathbb{R}_0^+ \to \mathbb{R}^+$, determines the global threshold, which will be discussed in Section 3.3. When an event takes place at a sampling time t_k, $\hat{u}(t_k)$ is updated by:

$$\begin{aligned} \hat{u}^i(t_k) &= \tilde{q}(u^i(t_k)) \\ &= q_\eta(u^i(t_k), \hat{u}^i(t_{k-1})) \\ &:= \hat{u}^i(t_{k-1}) - \text{sign}(\hat{u}^i(t_{k-1}) - u^i(t_k))\, m^i(t_k) \sqrt{\eta_i(t_k)}, \end{aligned} \tag{3.7}$$

where

$$m^i(t_k) := \left\lfloor \frac{|\hat{u}^i(t_{k-1}) - u^i(t_k)|}{\sqrt{\eta_i(t_k)}} \right\rfloor.$$

The error after this update is:

$$\begin{aligned} e_u^i(t_k) &:= \hat{u}^i(t_k) - u^i(t_k) \\ &= -\text{sign}(\hat{u}^i(t_{k-1}) - u^i(t_k)) \left(m^i(t_k) - \frac{|\hat{u}^i(t_{k-1}) - u^i(t_k)|}{\sqrt{\eta_i(t_k)}} \right) \sqrt{\eta_i(t_k)}. \end{aligned} \tag{3.8}$$

One can easily observe that, $|e_u^i(t_k)| < \sqrt{\eta_i(t_k)}$. That is, when there is an event locally, after the update by (3.7), (3.5) does not hold anymore. Later in Proposition 3.4.1, we show

that, $\forall i \in \{1,\cdots,n_u\}, k \in \mathbb{N}, m^i(t_k) \leq \bar{m}_x < \infty$. Thus, in practice one only needs to send $\text{sign}(\hat{u}^i(t_{k-1}) - u^i(t_k))$ and $m^i(t_k)$ for each input update. Therefore, only $\log_2(m^i(t_k))+1$ bits are required for each transmission from a single sensor or to a single actuator.

Define

$$\Gamma_{\mathscr{J}} := \text{diag}\left(\Gamma^y_{\mathscr{J}}, \Gamma^v_{\mathscr{J}}\right) = \text{diag}\left(\gamma^1_{\mathscr{J}} \cdots, \gamma^{n_u}_{\mathscr{J}}\right),$$

where $\mathscr{J}$ is an index set: $\mathscr{J} \subseteq \bar{\mathscr{J}} = \{1,\cdots,n_u\}$ for $u(t)$, indicating the occurrence of events. Define $\mathscr{J}_c := \bar{\mathscr{J}} \setminus \mathscr{J}$. For $l \in \{1,\cdots,n_u\}$, if $l \in \mathscr{J}$, $\gamma^l_{\mathscr{J}} = 1$; if $l \in \mathscr{J}_c$, $\gamma^l_{\mathscr{J}} = 0$. Furthermore, we use the notation $\Gamma_j = \Gamma_{\{j\}}$. Define

$$C := \begin{bmatrix} C_p & 0 \\ 0 & C_c \end{bmatrix}, D := \begin{bmatrix} 0 & 0 \\ D_c & 0 \end{bmatrix}.$$

The local event-triggered condition (3.5) can now be reformulated as a set membership:

$$i \in \mathscr{J} \text{ iff } \xi^{\mathrm{T}}(t_k) Q_i \xi(t_k) \geq \eta_i(t_k), \tag{3.9}$$

where

$$Q_i = \begin{bmatrix} C^{\mathrm{T}}\Gamma_i C & C^{\mathrm{T}}\Gamma_i D - C^{\mathrm{T}}\Gamma_i \\ D^{\mathrm{T}}\Gamma_i C - \Gamma_i C & (D-I)^{\mathrm{T}}\Gamma_i (D-I) \end{bmatrix}.$$

The ADPETC implementation determined by (3.1), (3.2), (3.3), (3.4), and (3.9) can be re-written as an impulsive system model by:

$$\begin{aligned} \begin{bmatrix} \dot{\xi}(t) \\ \dot{\tau}(t) \end{bmatrix} &= \begin{bmatrix} \bar{A}\xi(t) + \bar{B}w(t) \\ 1 \end{bmatrix}, \text{ when } \tau(t) \in [0, h[, \\ \begin{bmatrix} \xi(t_k^+) \\ \tau(t_k^+) \end{bmatrix} &= \begin{bmatrix} J_{\mathscr{J}}\xi(t_k) + \Delta_{\mathscr{J}}(t_k)\eta(t_k) \\ 0 \end{bmatrix}, \text{ when } \tau(t) = h, \\ z(t) &= g(\xi(t), w(t)), \end{aligned} \tag{3.10}$$

where $\bar{B} = \begin{bmatrix} E^{\mathrm{T}} & 0 & 0 & 0 \end{bmatrix}^{\mathrm{T}}$ and

$$\bar{A} = \begin{bmatrix} A_p & 0 & 0 & B_p \\ 0 & 0 & 0 & 0 \\ 0 & 0 & 0 & 0 \\ 0 & 0 & 0 & 0 \end{bmatrix}, \Delta_{\mathscr{J}}(t_k) = \begin{bmatrix} 0 \\ B_c\Gamma^y_{\mathscr{J}}\epsilon_y(t_k)\Theta_y \\ \Gamma^y_{\mathscr{J}}\epsilon_y(t_k)\Theta_y \\ \Gamma^v_{\mathscr{J}}\epsilon_v(t_k)\Theta_v \end{bmatrix},$$

$$J_{\mathscr{J}} = \begin{bmatrix} I & 0 & 0 & 0 \\ B_c\Gamma^y_{\mathscr{J}}C_p & A_c & B_c(I-\Gamma^y_{\mathscr{J}}) & 0 \\ \Gamma^y_{\mathscr{J}}C_p & 0 & (I-\Gamma^y_{\mathscr{J}}) & 0 \\ 0 & \Gamma^v_{\mathscr{J}}C_c & \Gamma^v_{\mathscr{J}}D_c & (I-\Gamma^v_{\mathscr{J}}) \end{bmatrix},$$

with I an identity matrix of corresponding dimension,

$$\epsilon_y(t_k) := \operatorname{diag}\left(\frac{e_u^1(t_k)}{\sqrt{\eta_1(t_k)}},\cdots,\frac{e_u^{n_y}(t_k)}{\sqrt{\eta_{n_y}(t_k)}}\right),$$
$$\epsilon_v(t_k) := \operatorname{diag}\left(\frac{e_u^{n_y+1}(t_k)}{\sqrt{\eta_{n_y+1}(t_k)}},\cdots,\frac{e_u^{n_y+n_v}(t_k)}{\sqrt{\eta_{n_y+n_v}(t_k)}}\right),$$
$$\Theta_y := \begin{bmatrix}\theta_1 & \cdots & \theta_{n_y}\end{bmatrix}^{\mathrm{T}},$$
$$\Theta_v := \begin{bmatrix}\theta_{n_y+1} & \cdots & \theta_{n_y+n_v}\end{bmatrix}^{\mathrm{T}}.$$

The term $\Delta_{\mathscr{J}}(t_k)\eta(t_k)$ represents the quantization error after input updates and $\frac{e_u^i(t_k)}{\sqrt{\eta_i(t_k)}} \in]-1,1[$ due to (3.7), (3.8).

Lemma 9 in [70] indicates that, for a system applying the ADETC mechanism to be UGAS when $w=0$, $\eta(t)$ should be a monotonically decreasing function with $\lim_{t\to\infty}\eta(t)=0$. However, this mechanism does not consider systems with disturbances. According to [67], when $w\neq 0$, if $\eta(t)$ is arbitrarily small, the mechanism is not robust against disturbances. Meanwhile, in [70], the $\eta(t)$ update is determined by an upper bound estimate of the current state of the plant. This estimate is not always obtainable in an output-feedback system, making it inapplicable in such systems. We overcome the first problem by imposing a lower bound on $\eta(t_k)$, defined as $\eta_{\min}>0$, i.e. $\eta(t_k)\geq\eta_{\min}, \forall\, t_k\in\mathscr{T}$. For the second problem, we use $\xi_c(t_k)$, $\hat{y}(t_k)$, and $\hat{v}(t_k)$ to determine the current threshold instead of $\xi_p(t_k)$, since this information is available to the controller.

Remark 3.2.1. *By imposing a lower bound $\eta_{\min}$ on η, $\lim_{t\to\infty}\eta(t)\neq 0$, and thus $\xi(t)$ can only converge to a set even when $w=0$. Therefore, no $\mathscr{L}_2$-gain can be obtained for a linear performance function, proportional to the state of the system as in [48], since in that case $\xi\notin\mathscr{L}_2$ implies $z\notin\mathscr{L}_2$. We circumvent this problem picking a performance function that is zero on a compact set around the origin.*

Denote a set $\mathscr{X}$ as $(x,r)\in\mathscr{X}\subseteq\mathbb{R}^{n_\xi}\times[0,h]$, such that $x=\xi(t)$, $r=\tau(t)$ for some $t\in\mathbb{R}_0^+$, where ξ is a solution to system (3.10). $\mathscr{A}\subseteq\mathscr{X}$ is a compact set around the origin. Redefine the variable $z(t)$ in (3.10) by:

$$z_{\mathscr{A}}(t) := \begin{cases}\bar{C}\xi(t)+\bar{D}w(t), & \forall(\xi(t),\tau(t))\in\mathscr{X}\setminus\mathscr{A}\\ 0, & \forall(\xi(t),\tau(t))\in\mathscr{A},\end{cases} \tag{3.11}$$

in which, $\bar{C}$ and $\bar{D}$ are some matrices of appropriate dimensions.

Now we present the main problem we solve in this chapter.

Problem 3.2.2. *Design an update mechanism for η and an $\eta_{\min}$ such that $\mathscr{A}$ is UGpAS for (3.10), (3.11) when $w=0$, and the $\mathscr{L}_2$-gain from w to $z_{\mathscr{A}}$ is smaller than or equal to γ.*

3.3. STABILITY AND $\mathscr{L}_2$-GAIN ANALYSIS

Denote $\tilde{z}(t)$ a reference function of $z_{\mathscr{A}}(t)$, given by:

$$\tilde{z}(t) := \bar{C}\xi(t) + \bar{D}w(t),\ \forall(\xi(t),\tau(t)) \in \mathscr{X}. \tag{3.12}$$

Now let us consider a Lyapunov function candidate for the impulsive system (3.10), (3.12) of the form:

$$V(x,r) = x^{\mathrm{T}}P(r)x, \tag{3.13}$$

where $x \in \mathbb{R}^{n_\xi}$, $r \in [0,h]$, with $P : [0,h] \to \mathbb{R}^{n_\xi \times n_\xi}$ satisfying the Riccati differential equation:

$$\frac{d}{dr}P = -\bar{A}^{\mathrm{T}}P - P\bar{A} - 2\rho P - \gamma^{-2}\bar{C}^{\mathrm{T}}\bar{C} - G^{\mathrm{T}}MG, \tag{3.14}$$

in which $M := (I - \gamma^{-2}\bar{D}^{\mathrm{T}}\bar{D})^{-1}$; $G := \bar{B}^{\mathrm{T}}P + \gamma^{-2}\bar{D}^{\mathrm{T}}\bar{C}$, with $\bar{A}$, $\bar{B}$, $\bar{C}$, and $\bar{D}$ defined in (3.10) and (3.12), and ρ and γ are pre-design parameters. We often use the shorthand notation $V(t)$ to denote $V(\xi(t),\tau(t))$. Construct the Hamiltonian matrix:

$$H := \begin{bmatrix} H_{11} & H_{12} \\ H_{21} & H_{22} \end{bmatrix},\ F(r) := e^{-Hr} = \begin{bmatrix} F_{11}(r) & F_{12}(r) \\ F_{21}(r) & F_{22}(r) \end{bmatrix},$$

where

$$\begin{cases} H_{11} := \bar{A} + \rho I + \gamma^{-2}\bar{B}M\bar{D}^{\mathrm{T}}\bar{C} \\ H_{12} := \bar{B}M\bar{B}^{\mathrm{T}} \\ H_{21} := -\bar{C}^{\mathrm{T}}(\gamma^2 I - \bar{D}\bar{D}^{\mathrm{T}})^{-1}\bar{C} \\ H_{22} := -(\bar{A} + \rho I + \gamma^{-2}\bar{B}M\bar{D}^{\mathrm{T}}\bar{C})^{\mathrm{T}}. \end{cases}$$

Assumption 3.3.1. *$F_{11}(r)$ is invertible $\forall r \in [0,h]$.*

Since $F_{11}(0) = I$ and $F_{11}(r)$ is continuous, Assumption 3.3.1 can always be satisfied for sufficiently small h. According to Lemma A.1 in [48], if Assumption 3.3.1 holds, then $-F_{11}^{-1}(h)F_{12}(h)$ is positive semi-definite. Define the matrix $\bar{S}$ satisfying

$$\bar{S}\bar{S}^{\mathrm{T}} := -F_{11}^{-1}(h)F_{12}(h).$$

We present next the designed threshold update mechanism. At each sampling time t_k^+, right after a jump of system (3.10), the controller executes the threshold update mechanism:

$$\eta(t_k^+) = \mu^{-n_\mu(t_k^+)}\eta_{\min}, \tag{3.15}$$

in which

$$n_\mu(t_k^+) := \max\left\{0, \left\lceil -\log_\mu\left(\frac{|\xi'(t_k^+)|}{\varrho\eta_{\min}}\right) - 1 \right\rceil\right\},$$

$\eta_{\min}$ is a pre-designed minimum threshold; $\varrho > 0$ is a finite design parameter; and the scalar $\mu :\in]0,1[$ is also a pre-designed parameter. The vector of variables available at the controller at sampling time t_k^+, denoted by

$$\xi'(t_k^+) := \left[\xi_c^{\mathrm{T}}(t_k^+) \quad \hat{y}^{\mathrm{T}}(t_k^+) \quad \hat{v}^{\mathrm{T}}(t_k^+)\right]^{\mathrm{T}}.$$

Lemma 3.3.2. *Consider the system (3.10), (3.12), after the execution of the threshold update mechanism (3.15), if* $\eta(t_k^+) \neq \eta_{\min}$*, then:*

$$\varrho\eta(t_k^+) < |\xi'(t_k^+)| \leq \mu^{-1}\varrho\eta(t_k^+). \tag{3.16}$$

Now we analyse the jump part of the impulsive system.

Lemma 3.3.3. *Consider the system (3.10), (3.12), (3.13), (3.14), and (3.15), and that Assumption 3.3.1 holds. If* $\gamma^2 > \lambda_{\max}(\bar{D}^{\mathrm{T}}\bar{D})$, $\exists P(h) \succ 0$ *satisfying* $I - \bar{S}^{\mathrm{T}}P(h)\bar{S} \succ 0$*, and scalars* $\varrho > 0, \epsilon > 0$ *such that the LMI:*

$$\begin{bmatrix} \epsilon I & \tilde{F}_1 & \tilde{F}_2 & -\epsilon J_{\bar{\mathscr{J}}} \\ \tilde{F}_1^{\mathrm{T}} & \tilde{F}_3 & 0 & 0 \\ \tilde{F}_2^{\mathrm{T}} & 0 & \tilde{F}_2 & 0 \\ -\epsilon J_{\bar{\mathscr{J}}}^{\mathrm{T}} & 0 & 0 & P(h) + \epsilon J_{\bar{\mathscr{J}}}^{\mathrm{T}} J_{\bar{\mathscr{J}}} - \epsilon\frac{|\bar{\Delta}_{\bar{\mathscr{J}}}|^2}{\varrho^2} I \end{bmatrix} \succeq 0 \tag{3.17}$$

holds, where

$$\begin{aligned} \tilde{F}_1 &:= F_{11}^{-\mathrm{T}}(h)P(h)\bar{S} \\ \tilde{F}_2 &:= F_{11}^{-\mathrm{T}}(h)P(h)F_{11}^{-1}(h) + F_{21}(h)F_{11}^{-1}(h) \\ \tilde{F}_3 &:= I - \bar{S}^{\mathrm{T}}P(h)\bar{S} \\ \bar{\Delta}_{\mathscr{J}} &:= \Delta_{\mathscr{J}}(t_k)_{|\epsilon_y(t_k)=I, \epsilon_v(t_k)=I}, \end{aligned}$$

then $\forall\, t_k \in \mathcal{T}$ *such that* $|\xi(t_k)| > \varrho\eta(t_k)$*, the following also holds:* $V(\xi(t_k^+), 0) \leq V(\xi(t_k), h)$.

Note that ϱ enters the LMI in a nonlinear fashion, therefore we cannot compute ϱ directly. Instead, we apply a line search algorithm to find feasible parameters h and ϱ. Define

$$\begin{aligned} C_H &= \{(x,r) | (x,r) \in \mathscr{X}, r \in [0, h[\} \\ D_H &= \{(x,r) | (x,r) \in \mathscr{X}, r = h\}, \end{aligned}$$

and the set $\underline{\mathscr{A}}$ as:

$$\underline{\mathscr{A}} := \left\{(x,r) \,\middle|\, (x,r) \in \mathscr{X}, V(x,r) \leq \bar{\lambda}\bar{\varrho}^2\eta_{\min}^2\right\}, \tag{3.18}$$

where

$$\begin{aligned} \bar{\lambda} &:= \max\{\lambda_{\max}(P(r)), \forall\, r \in [0,h]\} \\ \bar{\varrho} &:= \max\{|J_{\mathscr{J}}|\varrho + |\bar{\Delta}_{\mathscr{J}}|, \forall\, \mathscr{J} \subseteq \bar{\mathscr{J}}\}. \end{aligned}$$

Selecting $\eta_{\min}$ sufficiently small, one can make sure that $\underline{\mathscr{A}} \subseteq \mathscr{A}$. Define a new Lyapunov function candidate for system (3.10), (3.12), and (3.15), as:

$$W(x,r) := \max\left\{V(x,r) - \bar{\lambda}\bar{\varrho}^2\eta_{\min}^2, 0\right\}. \tag{3.19}$$

Note that (3.19) defines a proper Lyapunov function candidate. We also use the shorthand notation $W(t)$ to denote $W(\xi(t), \tau(t))$.

Finally, let:

$$z_{\underline{\mathscr{A}}}(t) := \begin{cases} \bar{C}\xi(t) + \bar{D}w(t), & \forall (\xi(t), \tau(t)) \in \mathscr{X} \setminus \underline{\mathscr{A}} \\ 0, & \forall (\xi(t), \tau(t)) \in \underline{\mathscr{A}}. \end{cases} \tag{3.20}$$

It is obvious that if $\underline{\mathscr{A}} \subseteq \mathscr{A}$, $|z_{\underline{\mathscr{A}}}(t)| \geq |z_{\mathscr{A}}(t)| \geq 0$.

Theorem 3.3.4. *Consider the system (3.10), (3.11), (3.13), (3.14), (3.15), (3.18), and (3.19). If $\rho > 0, \gamma^2 > \lambda_{\max}(\bar{D}^{\mathrm{T}}\bar{D})$, the hypotheses of Lemma 3.3.3 hold, and $\eta_{\min}$ is selected s.t. $\underline{\mathscr{A}} \subseteq \mathscr{A}$, then $\mathscr{A}$ is UGpAS for the impulsive system (3.10) when $w = 0$; and the $\mathscr{L}_2$-gain from w to $z_{\mathscr{A}}$ is smaller than or equal to γ, i.e. $\|z_{\mathscr{A}}\|_{\mathscr{L}_2} \leq \delta(\xi(0)) + \gamma\|w\|_{\mathscr{L}_2}$, where $\delta : \mathbb{R}^{n_\xi} \to \mathbb{R}^+$ is a $\mathscr{K}_\infty$ function.*

3.4. PRACTICAL CONSIDERATIONS

In our proposed implementation, the data a sensor sends is actually $m^i(t_k)$ and the sign of the error, see (3.7). Therefore, computing an upper bound $\bar{m}_x \geq m^i(t_k)$, $\forall\, t_k \in \mathscr{T}$ is desirable to properly design the supporting communication protocol.

Proposition 3.4.1. *Consider the system (3.10), (3.11), (3.13), (3.14), (3.15), and (3.19). If w is bounded (i.e. $w \in \mathscr{L}_2 \cap \mathscr{L}_\infty$), and the hypotheses of Theorem 3.3.4 hold, then:*

$$\bar{m}_x = \max\{\bar{m}_x^i | i \in \{1, \cdots, n_u\}\} \tag{3.21}$$

where

$$\bar{m}_x^i = \frac{(1 + |[C\,D]|)}{\theta_i}\sqrt{\frac{W(0)}{\eta_{\min}^2\underline{\lambda}} + \frac{\|w\|_{\mathscr{L}_\infty}^2}{2\rho\eta_{\min}^2\underline{\lambda}} + \frac{\bar{\lambda}\bar{\varrho}^2}{\underline{\lambda}}} \geq m^i(t_k),\ \forall\, t_k \in \mathscr{T},$$
$$\underline{\lambda} = \min\{\lambda_{\min}(P(r)), \forall\, r \in [0, h]\}.$$

Similarly, an upper bound of $n_\mu(t)$, denoted by $\bar{m}_\mu$ can be obtained:

Proposition 3.4.2. *Consider the system (3.10), (3.11), (3.13), (3.14), (3.15), and (3.19). If w is bounded and the hypotheses of Theorem 3.3.4 hold, then $\bar{m}_\mu$ is given as*

$$\bar{m}_\mu = \max\left\{0, -\log_\mu\left(\frac{(1 + |[C\,D]|)}{\varrho}\sqrt{\frac{W(0)}{\eta_{\min}^2\underline{\lambda}} + \frac{\|w\|_{\mathscr{L}_\infty}^2}{2\rho\eta_{\min}^2\underline{\lambda}} + \frac{\bar{\lambda}\bar{\varrho}^2}{\underline{\lambda}}}\right)\right\}. \tag{3.22}$$

Remark 3.4.3. *For a packet from node i, the packet length is computed by $\lceil \log_2 m^i(t_k) \rceil + 1$, with the additional bit used to indicate the sign of the error.*

3.5. NUMERICAL EXAMPLE

In this section, we consider the batch reactor system from [106]:

$$A_p = \begin{bmatrix} 1.380 & -0.208 & 6.715 & -5.676 \\ -0.581 & -4.290 & 0 & 0.675 \\ 1.067 & 4.273 & -6.654 & 5.893 \\ 0.048 & 4.273 & 1.343 & -2.104 \end{bmatrix},$$
$$B_p = \begin{bmatrix} 0 & 0 \\ 5.679 & 0 \\ 1.136 & -3.146 \\ 1.136 & 0 \end{bmatrix}, C_p = \begin{bmatrix} 1 & 0 & 1 & -1 \\ 0 & 1 & 0 & 0 \end{bmatrix}.$$

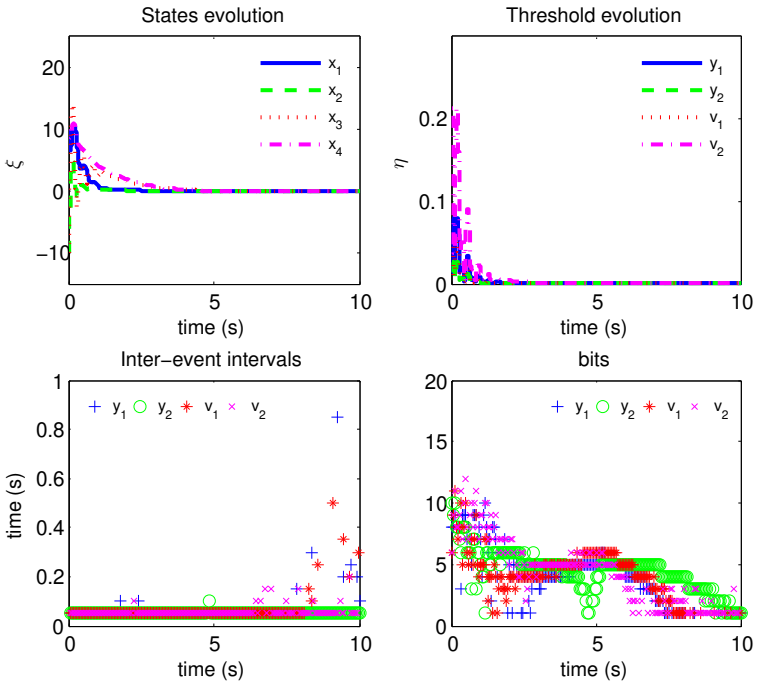

Figure 3.2: Simulation result when $w = 0$: system state, threshold, inter-event intervals, and bits of each event.

Given $h = 0.05s$, the controller is obtained as:

$$\left[\begin{array}{c|c} A_c & B_c \\ \hline C_c & D_c \end{array}\right] = \left[\begin{array}{cc|cc} 1 & 0 & 0 & 0.05 \\ 0 & 1 & 0.05 & 0 \\ \hline -2 & 0 & 0 & -2 \\ 0 & 8 & 5 & 0 \end{array}\right].$$

With $\rho = 0.01$, $\gamma = 0.9$, and

$$z = \begin{bmatrix} 1 & 0 & 0 & 0 & 0 & 0 & 0 & 0 & 0 & 0 \end{bmatrix} \xi,$$

$$\mathscr{A} = \{(x,r) | (x,r) \in \mathscr{X}, |x^{\mathrm{T}} P(r) x| \leq 3.11\},$$

Assumption 3.3.1 is satisfied. Solving (3.17), one can obtain $\varrho = 200.2$. Other parameters are given by $\mu = 0.75$, $\eta_{\min} = 0.0001$, $\theta_1 = 0.3397$, $\theta_2 = 0.1132$, $\theta_3 = 0.2265$, and $\theta_4 = 0.9058$. $\xi_p(0) = \begin{bmatrix} 10 & -10 & -10 & 10 \end{bmatrix}^{\mathrm{T}}$, $\xi_c(0) = \mathbf{0}$, $\hat{y}(0) = C_p \xi_p(0)$, and $\hat{v}(0) = D_c C_p \xi_p(0)$. Let $\eta_{\min} = 0.0001$, resulting in the set $\underline{\mathscr{A}} = \mathscr{A}$.

Fig 3.2 shows the simulation results of the system without disturbances. The system state converges to the set $\mathscr{A}$, however one can see that the estimate of $\mathscr{A}$ is very conservative compared with the simulation result ($|x^{\mathrm{T}} P(r) x| = 2.36 \times 10^{-6}$ at 10s). The sensor transmissions are reduced by 11.07% compared to a time-triggered mechanism with the

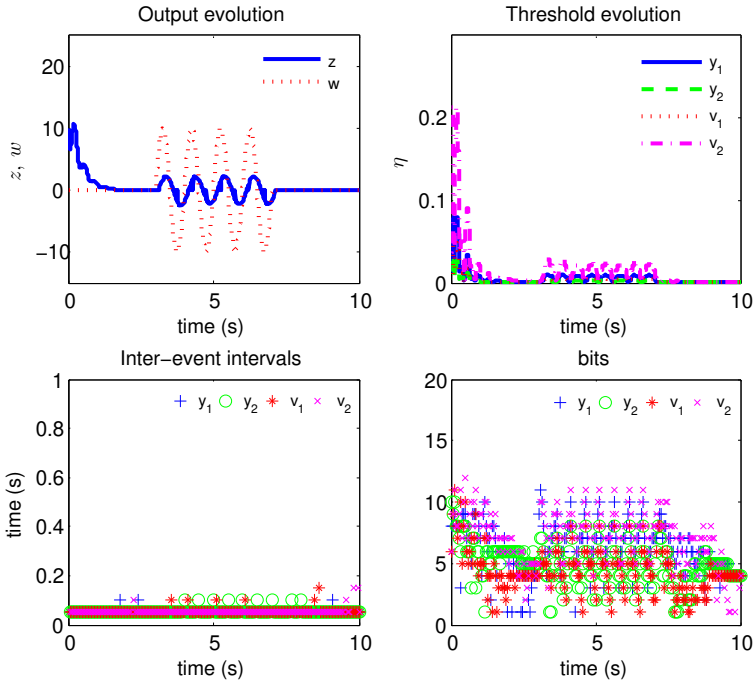

Figure 3.3: Simulation result when $w(t) = 10\sin(2\pi t)$, $t = [3,7]$: evolution of z and w, threshold, inter-event intervals, and bits of each event.

same sampling interval h. The maximum inter-event interval is 0.85 seconds. The following bounds are obtained from our analysis: $\bar{m}_x = 2.3997 \times 10^8$ (29 bits), and $\bar{m}_\mu = 42$. The maximum observed $m^i(t_k)$ is 1303 (12 bits), i.e. 1.8417×10^5 times smaller than the computed $\bar{m}_x$. Most of the time (95.38%), $m^i(t_k)$ is smaller than or equal to 128 (8 bits); 46.15% of the $m^i(t_k)$ can be transmitted with solely 4 bits.

Fig 3.3 shows the simulation results in the presence of a finite sine wave disturbance. It can be seen that the performance variable z follows w with a bounded norm ratio. The sensor transmissions are reduced by 3.61% compared to a time-triggered mechanism with the same sampling interval h. The maximum inter-event interval is 0.15 seconds. 89.81% of $m^i(t_k)$ are smaller than or equal to 128 (8 bits); 31.23% of $m^i(t_k)$ can be transmitted with 4 bits; and the maximum $m^i(t_k)$ is still 1303 (12 bits). Note that the saving of transmission increases as the time without disturbances increases.

Further simulation results show that, the sensor transmissions are reduced by 63.81% after running for 50s without additional disturbances. Further simulation also shows that, as the initial state goes closer to the original point, the reduction within 10 seconds increases when there is no disturbance. When there is disturbances, the reduction does not change much.

Fig 3.4 shows the simulation results of the total transmitting time required during

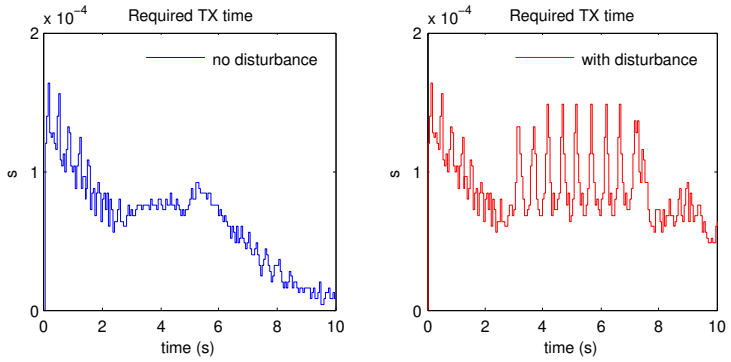

Figure 3.4: Required transmitting time with rate 250 kbit/s, both without and with disturbance.

each sampling time h, under ZigBee (over-the-air data rate 250 kbit/s). One can observe that the required transmission time reduces as the state converges to $\mathscr{A}$. The maximum required transmission time is $1.64 \times 10^{-4} s$, about 304.88 times smaller than the sampling time h.

3.6. CONCLUSIONS

We have proposed ADPETC implementations as an extension to the work of [48] and [70]. This triggering strategy combines decentralized event generation, asynchronous sampling update, and zoom in/out quantization. This approach lets the implementation exchange very few bits every time that an event triggers a transmission, reduces the required amount of transmission compared with time-triggered mechanisms, and reduces the necessary sensing compared with continuously monitored ETMs. The maximum amount of bits that may be needed to update samplings and thresholds after an event is triggered are provided. Such a bound enables the design of actual implementations for wireless systems.

APPENDIX

The following two lemmas are intermediate results from the proof of Theorem III.2 in [48], which will be used in the proofs of Lemma 3.3.3 and Theorem 3.3.4.

Lemma 3.A.1. Consider the system (3.10), (3.12), (3.13), (3.14), and that Assumption 3.3.1 holds. If $\gamma^2 > \lambda_{\max}(\bar{D}^{\mathrm{T}}\bar{D})$ and $\exists P(h) > 0$ satisfying $I - \bar{S}^{\mathrm{T}}P(h)\bar{S} \succ 0$, then for $\tau(t) \in [0, h]$, $P(\tau(t)) \succ 0$; and $P(0)$ can be expressed as

$$P(0) = F_{21}(h)F_{11}^{-1}(h) + F_{11}^{-\mathrm{T}}(h)(P(h) + P(h)\bar{S}(I - \bar{S}^{\mathrm{T}}P(h)\bar{S})^{-1}\bar{S}^{\mathrm{T}}P(h))F_{11}^{-1}(h). \tag{3.23}$$

Lemma 3.A.2. Consider the system (3.10), (3.12), (3.13), and (3.14). If $\gamma^2 > \lambda_{\max}(\bar{D}^{\mathrm{T}}\bar{D})$, $\rho > 0$, then for all $x \in \mathbb{R}^{n_\xi}$ and $\tau(t) \in [0, h]$, the following inequation holds:

$$\frac{d}{dt}V(t) \leq -2\rho V(t) - \gamma^{-2}\tilde{z}^{\mathrm{T}}(t)\tilde{z}(t) + w^{\mathrm{T}}(t)w(t). \tag{3.24}$$

Proof of Lemma 3.3.2 For any $s = \left\lceil -\log_\mu(\frac{|\xi'(t_k^+)|}{\varrho\eta_{\min}}) - 1 \right\rceil$, s satisfies:

$$-\log_\mu\left(\frac{|\xi'(t_k^+)|}{\varrho\eta_{\min}}\right) - 1 \leq s < -\log_\mu\left(\frac{|\xi'(t_k^+)|}{\varrho\eta_{\min}}\right).$$

Noting that $\mu \in]0,1[$, therefore it is easy to obtain that:

$$\mu^{\log_\mu\left(\frac{|\xi'(t_k^+)|}{\varrho\eta_{\min}}\right)+1} \leq \mu^{-s} < \mu^{\log_\mu\left(\frac{|\xi'(t_k^+)|}{\varrho\eta_{\min}}\right)},$$

which, as $\varrho\eta_{\min} > 0$, can be finally simplified as:

$$\mu|\xi'(t_k^+)| \leq \varrho\mu^{-s}\eta_{\min} < |\xi'(t_k^+)|. \tag{3.25}$$

From (3.15), after the execution of the threshold update mechanism, $\eta(t_k^+)$ can be computed as:

$$\eta(t_k^+) = \max\{\eta_{\min}, \mu^{-s}\eta_{\min}\}.$$

If $\eta(t_k^+) \neq \eta_{\min}$, then $\eta(t_k^+) = \mu^{-s}\eta_{\min}$, and thus from (3.25), we have that:

$$\mu|\xi'(t_k^+)| \leq \varrho\eta(t_k^+) < |\xi'(t_k^+)|,$$

which can be re-written as (3.16). This ends the proof. □

Proof of Lemma 3.3.3 For the jump part of the impulsive system (3.10), we have that the relation between the states before and after each jump is given by:

$$\begin{aligned}|\xi(t_k^+) - J_{\bar{\mathscr{J}}}\xi(t_k)| &= |J_{\mathscr{J}}\xi(t_k) + \Delta_{\mathscr{J}}(t_k)\eta(t_k) - J_{\bar{\mathscr{J}}}\xi(t_k)| \\ &= |\tilde{H}_1\xi(t_k) + \Delta_{\mathscr{J}}(t_k)\eta(t_k)|,\end{aligned}$$

where

$$\tilde{H}_1 := \begin{bmatrix} 0 & 0 & 0 & 0 \\ -B_c\Gamma^y_{\mathscr{J}_c}C_p & 0 & B_c\Gamma^y_{\mathscr{J}_c} & 0 \\ -\Gamma^y_{\mathscr{J}_c}C_p & 0 & \Gamma^y_{\mathscr{J}_c} & 0 \\ 0 & -\Gamma^v_{\mathscr{J}_c}C_c & -\Gamma^v_{\mathscr{J}_c}D_c & \Gamma^v_{\mathscr{J}_c} \end{bmatrix},$$

since $\Gamma^y_{\mathscr{J}_c} + \Gamma^y_{\mathscr{J}} = I = \Gamma^y_{\bar{\mathscr{J}}}$ and $\Gamma^v_{\mathscr{J}_c} + \Gamma^v_{\mathscr{J}} = I = \Gamma^v_{\bar{\mathscr{J}}}$. By the definition of the error (3.8) and the event-triggered mechanism (3.9), one has:

$$\begin{aligned}\Gamma^y_{\mathscr{J}_c}\hat{y}(t_k) - \Gamma^y_{\mathscr{J}_c}y(t_k) &= \Gamma^y_{\mathscr{J}_c}\epsilon_y(t_k)\Theta_y\eta(t_k) \\ \Gamma^v_{\mathscr{J}_c}\hat{v}(t_k) - \Gamma^v_{\mathscr{J}_c}v(t_k) &= \Gamma^v_{\mathscr{J}_c}\epsilon_v(t_k)\Theta_v\eta(t_k),\end{aligned}$$

Therefore, it holds that:

$$\begin{aligned}\tilde{H}_1\xi(t_k) + \Delta_{\mathscr{J}}(t_k)\eta(t_k) &= \Delta_{\mathscr{J}_c}(t_k)\eta(t_k) + \Delta_{\mathscr{J}}(t_k)\eta(t_k) \\ &= \Delta_{\bar{\mathscr{J}}}(t_k)\eta(t_k).\end{aligned}$$

Thus we obtain:

$$|\xi(t_k^+) - J_{\bar{\mathscr{J}}}\xi(t_k)| = |\Delta_{\bar{\mathscr{J}}}(t_k)\eta(t_k)| \leq |\bar{\Delta}_{\bar{\mathscr{J}}}|\eta(t_k).$$

Together with the hypothesis that $|\xi(t_k)| > \varrho\eta(t_k)$, one has:

$$|(\xi(t_k^+) - J_{\bar{\mathscr{J}}}\xi(t_k))|^2 < \frac{|\bar{\Delta}_{\bar{\mathscr{J}}}|^2}{\varrho^2}|\xi(t_k)|^2, \tag{3.26}$$

which can be re-written as:

$$\begin{bmatrix}\xi(t_k^+)\\ \xi(t_k)\end{bmatrix}^{\mathrm{T}}\begin{bmatrix} I & -J_{\bar{\mathscr{J}}} \\ -J_{\bar{\mathscr{J}}}^{\mathrm{T}} & J_{\bar{\mathscr{J}}}^{\mathrm{T}}J_{\bar{\mathscr{J}}} - \frac{|\bar{\Delta}_{\bar{\mathscr{J}}}|^2}{\varrho^2}I\end{bmatrix}\begin{bmatrix}\xi(t_k^+)\\ \xi(t_k)\end{bmatrix} < 0. \tag{3.27}$$

3

From the hypotheses, particularly (3.17) together with the result from Lemma 3.A.1, and Schur complement, we have that (3.17) implies:

$$\epsilon\begin{bmatrix} I & -J_{\bar{\mathscr{J}}} \\ -J_{\bar{\mathscr{J}}}^{\mathrm{T}} & J_{\bar{\mathscr{J}}}^{\mathrm{T}}J_{\bar{\mathscr{J}}} - \frac{|\bar{\Delta}_{\bar{\mathscr{J}}}|^2}{\varrho^2}I\end{bmatrix} + \begin{bmatrix}-P(0) & 0\\ 0 & P(h)\end{bmatrix} \geq 0. \tag{3.28}$$

Since $\epsilon > 0$, by applying the S-procedure (see e.g. [15]) from (3.27) and (3.28), one can conclude that:

$$\begin{bmatrix}\xi(t_k^+)\\ \xi(t_k)\end{bmatrix}^{\mathrm{T}}\begin{bmatrix}-P(0) & 0\\ 0 & P(h)\end{bmatrix}\begin{bmatrix}\xi(t_k^+)\\ \xi(t_k)\end{bmatrix} \geq 0. \tag{3.29}$$

This ends the proof. □

Proof of Theorem 3.3.4 We first show that $\mathscr{A}$ is UGpAS for the impulsive system (3.10) when $w = 0$. A new Lyapunov function candidate W, given by (3.19), is introduced. Define $\mathscr{B} := \{(x,r)|(x,r) \in \mathscr{X}, |x| \leq \varrho\eta_{\min}\}$. If $\eta(t_k) = \eta_{\min}$, $|\xi(t_k)| > \varrho\eta_{\min}$ implies $|\xi(t_k)| > \varrho\eta(t_k)$; if $\eta(t_k) > \eta_{\min}$, according to Lemma 3.3.2, $\varrho\eta(t_k) < |\xi'(t_k)| \leq |\xi(t_k)|$. Therefore, $\forall(\xi(t_k),\tau(t)) \in D_H \setminus \mathscr{B}$, $|\xi(t_k)| > \varrho\eta(t_k)$, and thus from Lemma 3.3.3, $\forall(\xi(t_k),\tau(t)) \in D_H \setminus \mathscr{B}$, it holds that:

$$V(\xi(t_k^+),0) \leq V(\xi(t_k),h). \tag{3.30}$$

According to Lemma 3.3.2, if $|\xi'(t_k)| \leq \varrho\eta(t_k)$ then $\eta(t_k) = \eta_{\min}$, i.e. $\forall(\xi(t_k),\tau(t)) \in D_H \cap \mathscr{B}$, $\eta(t_k) = \eta_{\min}$. Furthermore, $(\xi(t_k),\tau(t)) \in D_H \cap \mathscr{B}$ implies $\xi(t_k^+) = J_{\mathscr{J}}\xi(t_k) + \Delta_{\mathscr{J}}\eta_{\min}$, and thus, $|\xi(t_k^+)| \leq |J_{\mathscr{J}}||\xi(t_k)| + |\Delta_{\mathscr{J}}|\eta_{\min} \leq (|J_{\mathscr{J}}|\varrho + |\bar{\Delta}_{\mathscr{J}}|)\eta_{\min} \leq \bar{\varrho}\eta_{\min}$. That is

$$\forall(\xi(t_k),\tau(t)) \in D_H \cap \mathscr{B}, (\xi(t_k^+),0) \in \underline{\mathscr{A}}.$$

Note that, since $|J_{\mathscr{J}}| > 1$, $\forall(x,r) \in \mathscr{B}$, $x^{\mathrm{T}}P(r)x \leq \bar{\lambda}|x|^2 \leq \bar{\lambda}\varrho^2\eta_{\min}^2 < \bar{\lambda}\bar{\varrho}^2\eta_{\min}^2$, i.e. $\mathscr{B} \subset \underline{\mathscr{A}}$. Thus one can conclude that $\forall(\xi(t),\tau(t)) \in \underline{\mathscr{A}} \cap D_H$, $(\xi(t_k^+),0) \in \underline{\mathscr{A}}$. If all the hypotheses in Lemma 3.A.2 hold, together with (3.19), one has $\forall(\xi(t),\tau(t)) \in C_H \setminus \underline{\mathscr{A}}$:

$$\begin{aligned}\frac{d}{dt}W(\xi(t),\tau(t)) &= \frac{d}{dt}V(\xi(t),\tau(t))\\ &\leq -2\rho V(\xi(t),\tau(t)) - \gamma^{-2}\tilde{z}^{\mathrm{T}}(t)\tilde{z}(t) + w^{\mathrm{T}}(t)w(t)\\ &< -2\rho W(\xi(t),\tau(t)) - \gamma^{-2}\tilde{z}^{\mathrm{T}}(t)\tilde{z}(t) + w^{\mathrm{T}}(t)w(t).\end{aligned} \tag{3.31}$$

By (3.19) and (3.30), one has $\forall(\xi(t_k),\tau(t)) \in D_H \setminus \underline{\mathscr{A}}$:

$$\begin{aligned}W(\xi(t_k^+),0) &= \max\{V(\xi(t_k^+),0) - \bar{\lambda}\bar{\varrho}^2\eta_{\min}^2, 0\}\\ &\leq V(\xi(t_k),h) - \bar{\lambda}\bar{\varrho}^2\eta_{\min}^2\\ &= W(\xi(t_k),h).\end{aligned} \tag{3.32}$$

Combine (3.31), (3.32) and $\underline{\mathscr{A}} \subseteq \mathscr{A}$ to see that, when $w = 0$ all the conditions in Theorem 2.2.7 are satisfied. Thus, $\mathscr{A}$ is UGpAS for the impulsive system (3.10).

Now we study the $\mathscr{L}_2$-gain. Define a set of times:

$$\mathscr{T}_s = \left\{(t_i^s, j_i^s) | i \in \mathbb{N}\right\}, \tag{3.33}$$

where (t_0^s, j_0^s) is the initial time, s.t. $\forall t \in [t_{2i+1}^s, t_{2i+2}^s]$, $i \in \mathbb{N}$, $(\xi(t), \tau(t)) \in \underline{\mathscr{A}}$, and the rest of the time $(\xi(t), \tau(t)) \in \mathscr{X} \setminus \underline{\mathscr{A}}$. If $|\mathscr{T}_s|$ is infinite, i.e. $(\xi(t), \tau(t))$ visits $\underline{\mathscr{A}}$ infinitely often, one has:

$$\begin{aligned}\int_0^\infty z_{\underline{\mathscr{A}}}^{\mathrm{T}}(t) z_{\underline{\mathscr{A}}}(t) dt &= \sum_{i=0}^{\infty} \int_{t_i^s}^{t_{i+1}^s} z_{\underline{\mathscr{A}}}^{\mathrm{T}}(t) z_{\underline{\mathscr{A}}}(t) dt \\ &= \sum_{i=0}^{\infty} \int_{t_{2i}^s}^{t_{2i+1}^s} z_{\underline{\mathscr{A}}}^{\mathrm{T}}(t) z_{\underline{\mathscr{A}}}(t) dt + \sum_{i=0}^{\infty} \int_{t_{2i+1}^s}^{t_{2i+2}^s} z_{\underline{\mathscr{A}}}^{\mathrm{T}}(t) z_{\underline{\mathscr{A}}}(t) dt.\end{aligned} \tag{3.34}$$

By (3.31), $\forall (\xi(t), \tau(t)) \in C_H \setminus \underline{\mathscr{A}}$, it holds that:

$$\frac{d}{dt} W(\xi(t), \tau(t)) < -\gamma^{-2} z_{\underline{\mathscr{A}}}^{\mathrm{T}}(t) z_{\underline{\mathscr{A}}}(t) + w^{\mathrm{T}}(t) w(t). \tag{3.35}$$

One can replace the integration of $\frac{d}{dt} W(t)$, $z_{\underline{\mathscr{A}}}^{\mathrm{T}}(t) z_{\underline{\mathscr{A}}}(t)$, and $w^{\mathrm{T}}(t) w(t)$ on the open interval $]t_{2i}^s, t_{2i+1}^s[$ by the integration on the closure of that interval, see [4]. Applying the Comparison Lemma (e.g. Lemma 2.5 in [61]) to (3.32) and (3.35), one has:

$$\begin{aligned}W(t_{2i+1}^s) - W(t_{2i}^s) &= \int_{t_{2i}^s}^{t_{2i+1}^s} \frac{d}{dt} W(t) dt \\ &< \int_{t_{2i}^s}^{t_{2i+1}^s} \left(-\gamma^{-2} z_{\underline{\mathscr{A}}}^{\mathrm{T}}(t) z_{\underline{\mathscr{A}}}(t) + w^{\mathrm{T}}(t) w(t)\right) dt.\end{aligned} \tag{3.36}$$

Since $\forall i \in \mathbb{N}, i \neq 0$, $W(t_i^s) = 0$, therefore $\forall i \in \mathbb{N}$:

$$\sum_{i=0}^{\infty} \int_{t_{2i}^s}^{t_{2i+1}^s} z_{\underline{\mathscr{A}}}^{\mathrm{T}}(t) z_{\underline{\mathscr{A}}}(t) dt < \gamma^2 \sum_{i=0}^{\infty} \int_{t_{2i}^s}^{t_{2i+1}^s} w^{\mathrm{T}}(t) w(t) dt + \gamma^2 W(t_0^s). \tag{3.37}$$

When $(\xi(t), \tau(t)) \in \underline{\mathscr{A}}$, we have $z_{\underline{\mathscr{A}}}(t) = 0$ from (3.11), thus:

$$\sum_{i=0}^{\infty} \int_{t_{2i+1}^s}^{t_{2i+2}^s} z_{\underline{\mathscr{A}}}^{\mathrm{T}}(t) z_{\underline{\mathscr{A}}}(t) dt = 0 \leq \gamma^2 \sum_{i=0}^{\infty} \int_{t_{2i+1}^s}^{t_{2i+2}^s} w^{\mathrm{T}}(t) w(t) dt. \tag{3.38}$$

Put (3.37) and (3.38) into (3.34) to obtain:

$$\|z_{\mathscr{A}}\|_{\mathscr{L}_2}^2 \leq \|z_{\underline{\mathscr{A}}}\|_{\mathscr{L}_2}^2 < \gamma^2 W(t_0^s) + \gamma^2 \|w\|_{\mathscr{L}_2}^2 \leq \left(\delta(\xi(0)) + \gamma \|w\|_{\mathscr{L}_2}\right)^2. \tag{3.39}$$

If $\exists T$ s.t. $\forall t > T$, $(\xi(t), \tau(t)) \in \mathscr{X} \setminus \underline{\mathscr{A}}$, then $|\mathscr{T}_s| = 2I_s$ for some finite $I_s \in \mathbb{N}$. Since $\forall t \in \mathbb{R}_0^+$, $W(t) \geq 0$, and $W(t_{2I_s}^s) = 0$: $-\int_{t_{2I_s}^s}^{\infty} \frac{d}{dt} W(t) dt \leq 0$, and thus

$$\int_{t_{2I_s}^s}^{\infty} z_{\underline{\mathscr{A}}}^{\mathrm{T}}(t) z_{\underline{\mathscr{A}}}(t) dt \leq \gamma^2 \int_{t_{2I_s}^s}^{\infty} w^{\mathrm{T}}(t) w(t) dt.$$

Therefore, it holds that:

$$\begin{aligned}\|z_{\mathscr{A}}\|_{\mathscr{L}_2}^2 &\leq \|z_{\underline{\mathscr{A}}}\|_{\mathscr{L}_2}^2 \\ &= \left(\sum_{i=0}^{I_s-1}\int_{t_{2i}^s}^{t_{2i+1}^s} z_{\underline{\mathscr{A}}}^{\mathrm{T}}(t)z_{\underline{\mathscr{A}}}(t)dt + \int_{t_{2I_s}^s}^{\infty} z_{\underline{\mathscr{A}}}^{\mathrm{T}}(t)z_{\underline{\mathscr{A}}}(t)dt\right) + \sum_{i=0}^{I_s-1}\int_{t_{2i+1}^s}^{t_{2i+2}^s} z_{\underline{\mathscr{A}}}^{\mathrm{T}}(t)z_{\underline{\mathscr{A}}}(t)dt \\ &< \left(\delta(\xi(0)) + \gamma\|w\|_{\mathscr{L}_2}\right)^2.\end{aligned}$$

If $\exists T$ s.t. $\forall t > T$, $(\xi(t),\tau(t)) \in \underline{\mathscr{A}}$, then $|\mathscr{T}_s| = 2I_s + 1$ for some finite $I_s \in \mathbb{N}$, and thus $\int_{t_{2I_s+1}^s}^{\infty} z_{\underline{\mathscr{A}}}^{\mathrm{T}}(t)z_{\underline{\mathscr{A}}}(t)dt = 0$. Therefore, it holds that:

$$\begin{aligned}\|z_{\mathscr{A}}\|_{\mathscr{L}_2}^2 &\leq \|z_{\underline{\mathscr{A}}}\|_{\mathscr{L}_2}^2 \\ &= \left(\sum_{i=0}^{I_s-1}\int_{t_{2i+1}^s}^{t_{2i+2}^s} z_{\underline{\mathscr{A}}}^{\mathrm{T}}(t)z_{\underline{\mathscr{A}}}(t)dt + \int_{t_{2I_s+1}^s}^{\infty} z_{\underline{\mathscr{A}}}^{\mathrm{T}}(t)z_{\underline{\mathscr{A}}}(t)dt\right) + \sum_{i=0}^{I_s}\int_{t_{2i}^s}^{t_{2i+1}^s} z_{\underline{\mathscr{A}}}^{\mathrm{T}}(t)z_{\underline{\mathscr{A}}}(t)dt \\ &< \left(\delta(\xi(0)) + \gamma\|w\|_{\mathscr{L}_2}\right)^2.\end{aligned}$$

Which ends the proof. □

Proof of Proposition 3.4.1 Following the proof of Theorem 3.3.4, by (3.31) one has:

$$\forall(\xi(t),\tau(t)) \in C_H \setminus \underline{\mathscr{A}},\ \frac{d}{dt}W(\xi(t),\tau(t)) < -2\rho W(\xi(t),\tau(t)) + w^{\mathrm{T}}(t)w(t). \tag{3.40}$$

Using the Comparison Lemma to (3.32) and (3.40) on the interval $[t_{2i}^s, T]$, where $T \in [t_{2i}^s, t_{2i+1}^s]$ to obtain:

$$\begin{aligned}W(T) &< e^{-2\rho(T-t_{2i}^s)}W(t_{2i}^s) + \frac{\|w\|_{\mathscr{L}_\infty}^2}{2\rho}\left(1 - e^{-2\rho(T-t_{2i}^s)}\right) \\ &\leq W(t_{2i}^s) + \frac{\|w\|_{\mathscr{L}_\infty}^2}{2\rho} \\ &\leq W(t_0^s) + \frac{\|w\|_{\mathscr{L}_\infty}^2}{2\rho},\end{aligned} \tag{3.41}$$

since $T \geq t_{2i}^s$ indicates $e^{-2\rho(T-t_{2i}^s)} \in]0,1]$. When $(\xi(t),\tau(t)) \in \underline{\mathscr{A}}$, $W(t)$ is bounded by $W(t) = 0 \leq \frac{\|w\|_{\mathscr{L}_\infty}^2}{2\rho}$. Thus to obtain:

$$W(t) \leq W(0) + \frac{1}{2\rho}\|w\|_{\mathscr{L}_\infty}^2,\ \forall(\xi(t),\tau(t)) \in \mathscr{X}. \tag{3.42}$$

From the definition of $W(x,r)$ in (3.19), it holds that:

$$\max\{V(t) - \bar{\lambda}\bar{\varrho}^2\eta_{\min}^2, 0\} = W(t) \leq W(0) + \frac{1}{2\rho}\|w\|_{\mathscr{L}_\infty}^2,$$

together with the fact that $V(t) \geq \underline{\lambda}|\xi(t)|^2$, one obtains:

$$\forall t \in \mathbb{R}_0^+,\ |\xi(t)|^2 \leq \frac{W(0) + \frac{1}{2\rho}\|w\|_{\mathscr{L}_\infty}^2 + \bar{\lambda}\bar{\varrho}^2\eta_{\min}^2}{\underline{\lambda}}. \tag{3.43}$$

According to the definition of $m^i(t_k)$ we obtain:

$$\begin{aligned} m^i(t_k) &= \left\lfloor \frac{|\hat{u}^i(t_{k-1}) - u^i(t_k)|}{\sqrt{\eta_i(t_k)}} \right\rfloor \\ &\leq \frac{|\hat{u}^i(t_{k-1})| + |u^i(t_k)|}{\sqrt{\eta_i(t_k)}} \\ &\leq \frac{|\xi(t_{k-1})| + |[C\,D]||\xi(t_k)|}{\sqrt{\eta_i(t_k)}}. \end{aligned} \tag{3.44}$$

By introducing (3.43) into (3.44), one can conclude the bound of $m^i(t_k)$ as (3.21). This ends the proof. □

Proof of Proposition 3.4.2 By the definition of $n_\mu(t_k)$ in (3.15), one has

$$n_\mu(t_k) \leq \max\left\{0, -\log_\mu\left(\frac{|\xi'(t_k)|}{\varrho\eta_{\min}}\right)\right\} \leq \max\left\{0, -\log_\mu\left(\frac{|\xi(t)|}{\varrho\eta_{\min}}\right)\right\}.$$

Following along the same lines of the proof of Proposition 3.4.1, the bound of $n_\mu(t_k)$ is obtained as (3.22). □

4

DECENTRALIZED PERIODIC EVENT-TRIGGERED CONTROL WITH SYNCHRONOUS COMMUNICATION

SDETC is a type of ETC that decentralise the event-triggered condition to each sensor node. As a result the validation of event conditions does not require the whole vector of the state. However, this SDETC strategy still requires sensors to continuously monitor the output of the plant. In this chapter, we apply periodic sampling to SDETC, and introduce a decentralized PETC with synchronous communication strategy. SDPETC can largely reduce the energy consumed in the sensor nodes and reduce the bandwidth occupation.

4.1. INTRODUCTION

In Chapter 3, we have presented a type of ADPETC which can reduce both bandwidth occupation and energy consumption. Besides the background work of ADPETC, i.e. ADETC, there is an alternative decentralized ETC scheme, named SDETC from [72]. According to our early work in [71], with almost the same stability and performance, SDETC has more transmissions and a higher energy consumption compared to ADETC. However we are still curious about the stability, performance, bandwidth occupation, and energy consumption of SDETC in a real physical implementation which is presented in Chapter 6. Therefore, we propose a version of SDETC that applies periodic sampling, called as SDPETC in this chapter.

The proposed SDPETC is an extension of the work on SDETC [72] by applying periodic sampling to the control approach, i.e. the sampling of the output and corresponding event validation are executed periodically. In SDPETC, a distribution adaptation parameter is introduced. This parameter is computed based on the system's current state, system dynamics, and an estimated next event time. Whenever there is an event, the

Sections 4.2 and 4.3 of this chapter are extracted from [59].

parameter will be re-computed after the controller receives the updated samples. Then this adaptation parameter will be transmitted to all the sensor nodes. The sensor nodes wake up periodically, measure the system output, and validate if there are any events. The event condition is determined based on a pre-designed performance parameter together with the local adaptation parameter. If any of the sensor nodes triggers an event, all the sensor nodes transmit their newly measured state to the controller synchronously. The controller then computes and transmits the control input and the adaptation parameter.

Compared with the work of [72], the main difference in our presented strategy is that we introduce periodic sampling. With this discretized sampling, the sensors are not required to continuously monitor the system's state, thus the energy consumption can be reduced. In the work of [48], the author presents a centralized PETC and a decentralized PETC. Compare with the centralized PETC, in our work the sensors are not required to transmit the measurements to the ETM periodically, since the event-triggered condition is distributed to each sensor node. Thus the number of transmissions can be reduced. Compared with the decentralized PETC [48], in which a bundle of LMIs are required to solve to determine the ETM's parameters, our work only requires to solve 3 LMIs.

The organization of the remainder of the chapter is as follows. The problem is defined in Section 4.2. Section 4.3 presents the main result of this chapter. Following Section 4.3 is a numerical example in Section 4.4. This chapter is concluded in Section 4.5.

4.2. PROBLEM DEFINITION

Consider an LTI plant and controller

$$\dot{\xi}(t) = A\xi(t) + Bv(t), \tag{4.1}$$

$$v(t) = K\xi(t), \tag{4.2}$$

where $\xi(t) \in \mathbb{R}^n$ is the state vector and $v(t) \in \mathbb{R}^m$ is the input vector at time t. Assume $A+BK$ is Hurwitz and the system is completely observable where each sensor can access only one of the system states. A sample-and-hold mechanism is applied to the controller (4.2):

$$v(t) = K\hat{\xi}(t), \tag{4.3}$$

where

$$\hat{\xi}(t) := \xi(t_b), t \in [t_b, t_{b+1}[. \tag{4.4}$$

and $\{t_b\}_{b\in\mathbb{N}}$ are the update times of the state. Representing the sample-and-hold effect as a measurement error to have:

$$\varepsilon(t) := \hat{\xi}(t) - \xi(t). \tag{4.5}$$

A periodic sampling sequence of the state is given by:

$$\mathcal{T} := \{t_k | t_k := kh, k \in \mathbb{N}, h > 0\}. \tag{4.6}$$

where h is a designed sampling period. Define $\tau(t)$ as the elapsed time since the last sampling time, i.e.

$$\tau(t) := t - t_k,\ t \in [t_k, t_{k+1}[.$$

At each sampling time, the state is updated by the following mechanism:

$$\forall t_k \in \mathcal{T}, \hat{\xi}(t_k) = \begin{cases} \xi(t_k), & \text{if there is an event} \\ \hat{\xi}(t_{k-1}), & \text{if there is no event.} \end{cases} \tag{4.7}$$

Now we apply the SDETC presented in [72] and present the SDPETC. For (4.7), a state update mechanism with a decentralized event-triggering condition is given by:

$$\hat{\xi}(t_k) = \begin{cases} \xi(t_k), & \text{when } \exists i : \varepsilon_i^2(t_k) - \sigma \xi_i^2(t_k) > \theta_i \\ \hat{\xi}(t_{k-1}), & \text{when } \forall i : \varepsilon_i^2(t_k) - \sigma \xi_i^2(t_k) \leq \theta_i, \end{cases} \tag{4.8}$$

where $\varepsilon_i(t_k)$ and $\xi_i(t_k)$ denote the i-th entries of $\varepsilon(t_k)$ and $\xi(t_k)$ respectively, σ is a pre-designed scalar, $\{\theta_i\}_{i\leq n}$ are the adaptation parameters. According to (4.8), one can define the event time sequence as:

$$\{t_b\}_{b\in\mathbb{N}} := \left\{ t_k \,\middle|\, t_k \in \mathcal{T}, \exists i, \varepsilon_i^2(t_k) - \sigma \xi_i^2(t_k) > \theta_i \right\}.$$

The set of parameters $\{\theta_i\}_{i\leq n}$ is the adaptation parameters. According to [72], they can be computed by solving the following equations at each event time t_b, $b \in \mathbb{N}$:

$$\begin{cases} \hat{G}_i(t_b + t_e) = \hat{\varepsilon}_i^2(t_b + t_e) - \sigma \hat{\xi}_i^2(t_b + t_e) - \theta_i(b) \\ \hat{G}_i(t_b + t_e) = \hat{G}_j(t_b + t_e), \ \forall i, j \in \{1, 2, \cdots, n\} \\ \sum_{i=1}^{n} \theta_i(b) = 0, \end{cases} \tag{4.9}$$

where for $t \in [t_b, t_{b+1}[$:

$$\begin{cases} \hat{\xi}_i(t) = \xi_i(t_b) + \dot{\xi}_i(t_b)(t - t_b) + \frac{1}{2}\ddot{\xi}_i(t_b)(t - t_b)^2 + \ldots + \frac{1}{q!}\xi_i^{(q)}(t_b)(t - t_b)^q \\ \hat{\varepsilon}_i(t) = 0 - \dot{\xi}_i(t_b)(t - t_b) - \frac{1}{2}\ddot{\xi}_i(t_b)(t - t_b)^2 - \ldots - \frac{1}{q!}\xi_i^{(q)}(t_b)(t - t_b)^q. \end{cases}$$

As long as $\sum_{i=1}^{n} \theta_i = 0$ is satisfied, the stability of the system can be guaranteed regardless of the value and update rules employed of θ. Define $G_i(t) = \varepsilon_i^2(t) - \sigma \xi_i^2(t) - \theta_i(b)$ as the decision gap, and $\hat{G}_i(t)$ is an estimation of this decision gap $G_i(t)$ applying Taylor expansion.

Ideally, we would like to design θ_i such that at the triggering times t_b, $b \in \mathbb{N}$, $G_i(t_b) = G_j(t_b)$, $\forall i, j \in \{1, 2, \cdots, n\}$. In that case, no conservatism would be introduced with respect to the centralized ETC from [95]: $\varepsilon^2(t_k) - \sigma \xi^2(t_k) > 0$. However, we do not know in advance the triggering instant t_b and obtaining an exact expression of $\varepsilon(t_b)$ and $\xi(t_b)$ is in general not possible. The mechanism in (4.9) aims, through approximating, G_i (by $\hat{G}_i$) and t_{b+1} (by t_e), to equalize $G_i(t_{b+1}) = G_j(t_{b+1})$, $\forall i, j \in \{1, 2, \cdots, n\}$. By doing so, one hopes to reduce the conservatism introduced by decentralization of the triggering, and thus produce inter-sampling times close to those from a centralized triggering implementation.

The mapping $t_e : \mathbb{N} \to \mathbb{R}^+$ can be set to either $t_e(b) = h$ or $t_e(b) = t_b - t_{b-1}$. Thus, with the current $\theta_i(b)$ being calculated and transmitted from the controller to each sensor

node, the sensor node can locally determine the occurrence of the local events. When there is an event, the corresponding sensor node notifies the controller, and then the controller requests fresh measurements from all sensors to compute and update the control input.

Now we present the main problem to be solved in this chapter.

Problem 4.2.1. *For system (4.1-4.6), (4.8), and (4.9), find feasible conditions such that the system is UGES with a decay rate ρ.*

4.3. MAIN RESULT

The system (4.1-4.7) can be re-written as an impulsive system of the form:

$$\begin{bmatrix} \dot{\xi}_d(t) \\ \dot{\tau}(t) \end{bmatrix} = \begin{bmatrix} \bar{A}\xi_d(t) \\ 1 \end{bmatrix}, \text{ when } \tau(t) \in [0, h[,$$
$$\begin{bmatrix} \xi_d(t_k^+) \\ \tau(t_k^+) \end{bmatrix} = \begin{cases} \begin{bmatrix} J_1\xi_d(t_k) \\ 0 \end{bmatrix}, \text{ if there is an event and } \tau(t) = h, \\ \begin{bmatrix} J_2\xi_d(t_k) \\ 0 \end{bmatrix}, \text{ if there is no event and } \tau(t) = h. \end{cases} \tag{4.10}$$

where $\xi_d(t) = \begin{bmatrix} \xi^{\mathrm{T}}(t) & \hat{\xi}^{\mathrm{T}}(t) \end{bmatrix}^{\mathrm{T}}$, and

$$\bar{A} := \begin{bmatrix} A & BK \\ 0 & 0 \end{bmatrix}, J_1 := \begin{bmatrix} I & 0 \\ I & 0 \end{bmatrix}, J_2 := \begin{bmatrix} I & 0 \\ 0 & I \end{bmatrix},$$

I is an identity matrix of proper dimension. Now we present the main result of this chapter.

Proposition 4.3.1. *For system (4.1-4.6), (4.8), and (4.9), given a decay rate $\rho > 0$, if there exist a matrix $P \succ 0$ and scalars $\mu_1, \mu_2, \mu_3 \geq 0$, such that*

$$\begin{cases} \begin{bmatrix} e^{-2\rho h}P - \mu_1 Q & J_1^{\mathrm{T}} e^{\bar{A}^{\mathrm{T}}h} P \\ \star & P \end{bmatrix} \succ 0 \\ \begin{bmatrix} e^{-2\rho h}P + \mu_2 Q & J_2^{\mathrm{T}} e^{\bar{A}^{\mathrm{T}}h} P \\ \star & P \end{bmatrix} \succ 0 \\ \begin{bmatrix} e^{-2\rho h}P + \mu_3 Q & J_1^{\mathrm{T}} e^{\bar{A}^{\mathrm{T}}h} P \\ \star & P \end{bmatrix} \succ 0, \end{cases} \tag{4.11}$$

hold, then the system is UGES with a decay rate ρ.

Proof. Consider a Lyapunov function candidate for the impulsive system (4.10) of the form:

$$W(x, r) = x^{\mathrm{T}} P(r) x, \tag{4.12}$$

where $x \in \mathbb{R}^{2n}$, $r \in [0, h]$, with $P : [0, h] \to \mathbb{R}^{2n \times 2n}$ satisfying the Riccati differential equation:

$$\frac{d}{dr} P = -\bar{A}^{\mathrm{T}} P - P\bar{A} - 2\rho P. \tag{4.13}$$

By (4.12) and (4.13), it is easy to see that the convergence rate can be guaranteed during flows. Now we only need to prove that, $W(\xi_d(t),\tau(t))$ does not increase during jumps.

(4.13) results in:

$$P(0) = e^{2\rho h} e^{\bar{A}^{\mathrm{T}} h} P(h) e^{\bar{A} h}. \tag{4.14}$$

As noted in [72], $\forall i : \varepsilon_i^2(t) - \sigma\xi_i^2(t) \leq \theta_i$ implies $\varepsilon^{\mathrm{T}}(t)\varepsilon(t) \leq \sigma\xi^{\mathrm{T}}(t)\xi(t)$, which is equivalent to $\xi_d^{\mathrm{T}}(t_b)Q\xi_d(t_b) \leq 0$ with $Q := \begin{bmatrix} (1-\sigma)I & -I \\ -I & I \end{bmatrix}$. However, $\exists i : \varepsilon_i^2(t) - \sigma\xi_i^2(t) > \theta_i$ may indicate either $\xi_d^{\mathrm{T}}(t_b)Q\xi_d(t_b) > 0$ or $\xi_d^{\mathrm{T}}(t_b)Q\xi_d(t_b) \leq 0$. Therefore, if all the hypothesis in Proposition 4.3.1 hold, by applying the S-procedure (see e.g. [15]), one obtains

$$\begin{aligned} &\text{if } x^{\mathrm{T}}Qx > 0 \text{ holds, then } W(J_1 x, 0) \leq W(x,h), \\ &\text{if } x^{\mathrm{T}}Qx \leq 0 \text{ holds, then } W(J_2 x, 0) \leq W(x,h), \\ &\text{if } x^{\mathrm{T}}Qx \leq 0 \text{ holds, then } W(J_1 x, 0) \leq W(x,h), \end{aligned}$$

which indicates $W(\xi_d(t),\tau(t))$ does not increase during jumps. Therefore, the system (4.10) is UGES with a decay rate ρ. □

4.4. NUMERICAL EXAMPLE

In this section, we illustrate the presented ETM with a batch reactor system from [106]:

$$A = \begin{bmatrix} 1.38 & -0.20 & 6.71 & -5.67 \\ -0.58 & -4.29 & 0 & 0.67 \\ 1.06 & 4.27 & -6.65 & 5.89 \\ 0.04 & 4.27 & 1.34 & -2.10 \end{bmatrix}, \; B = \begin{bmatrix} 0 & 0 \\ 5.67 & 0 \\ 1.13 & -3.14 \\ 1.13 & 0 \end{bmatrix},$$

$$K = \begin{bmatrix} 0.1006 & -0.2469 & -0.0952 & -0.2447 \\ 1.4099 & -0.1966 & 0.0139 & 0.0823 \end{bmatrix}.$$

The convergence rate is given by $\rho = 0.01$, the sampling period is given by $h = 0.1s$, given the performance parameter $\sigma = 0.3$, by checking the LMIs presented in Proposition 4.3.1, there exist feasible solutions. Therefore, the pre-designed UGES can be guaranteed. The system initial state is given by $\xi(0) = \begin{bmatrix} 12 & 2 & 15 & 3 \end{bmatrix}$. $\theta(0) = \begin{bmatrix} 0 & 0 & 0 & 0 \end{bmatrix}$, and we employ $t_e = h$. A simulation result is shown in Figure 4.1. One can find that the system state exponentially converges to the equilibrium point, the adaptation parameter can rearrange the event conditions, and the communication reduction is 19.8% within $10s$. There are 80 sampling updates in total, while ξ_1 contributes 73 events, ξ_2 contributes 54 events, ξ_3 donates 13 events, and ξ_4 produces 59 events. The experimental comparison of SDPETC with some other triggering mechanisms in terms of stability and performance can be found in Chapter 6.

4.5. CONCLUSIONS

A type of ETC, named SDPETC is presented in this chapter. This SDPETC is a combination of SDETC and periodic sampling. In this ETM, the sensors are required to measure the plant outputs periodically instead of continuously, which allows to reduce the sensor working time. Meanwhile, the centralized event condition is distributed to each sensor

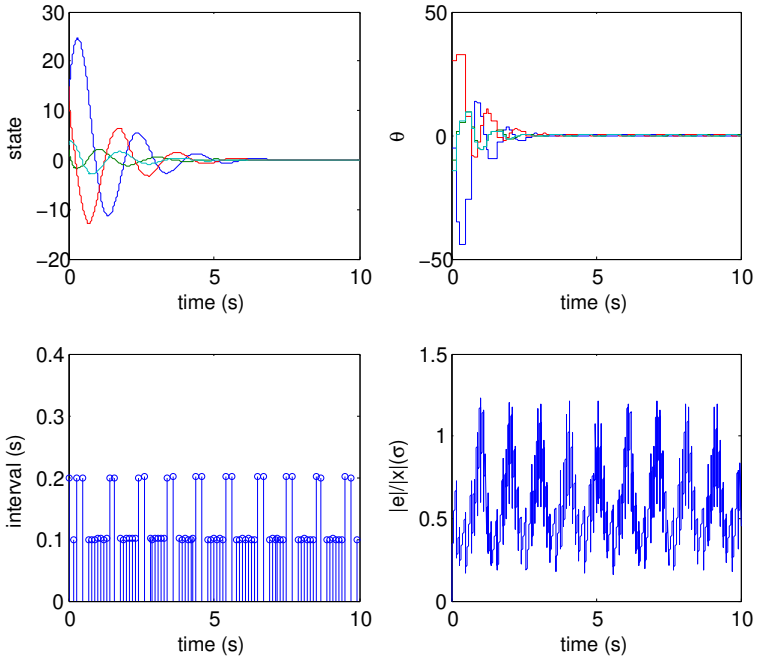

Figure 4.1: Simulation result: system state, adaptation parameter θ, event intervals, and triggering condition.

node with the help of an adaptation parameter. Therefore the event can be generated based on local information. As a result, both the energy consumption and the transmissions can be reduced.

5

TRAFFIC MODELS OF PERIODIC EVENT-TRIGGERED CONTROL SYSTEMS

PETC [48] is a version of ETC that only requires to measure the plant output periodically instead of continuously. In this work, we present a construction of timing models for these PETC implementations to capture the dynamics of the traffic they generate. In the construction, we employ a two-step approach. We first partition the state space into a finite number of regions. Then in each region, the event-triggering behaviour is analysed with the help of LMIs. The state transitions among different regions result from computing the reachable state set starting from each region within the computed event time intervals.

5.1. INTRODUCTION

As we have discussed in Chapter 1, to further reduce the resource consumption and to fully extract the potential gain from PETC, a possible solution is to apply scheduling approaches. We have in mind scheduling of both listening time of wireless communications and medium access time. Efficient scheduling of the resources, the efficiency of energy consumption and bandwidth occupation in a WNCS can be increased. To enable such scheduling, a model for the communication's traffic generated by PETC is required. This constructed model can be used for automatic scheduling design.

This chapter presents how to construct models for the traffic generated by PETC implementations. There are two steps of the construction. We first partition the state-space into a finite number of regions. Then we generate some LMIs to compute the output map of the abstracted system. Both the upper and lower bounds for the inter-event intervals are computed. Transition relations among different regions are derived by computing the reachable state regions starting from each region. In this way, the timing behaviours

Sections 5.2-5.5 and appendix of this chapter are extracted from [40].

of a PETC system can be captured by a finite model. According to [63], the models constructed by employing the proposed approach in this chapter is semantically equivalent to timed automata. Scheduling through timed automata can be done by existing tools, e.g. UPPAAL-Tiga [18].

The most related works are [38] and [64]. Compared with them, we do not require the disturbance to vanish as the state converges. Instead, we only assume the disturbance signal to be $\mathscr{L}_2$ and $\mathscr{L}_\infty$.

This chapter is organized as follows. The problem to be solved is defined in Section 5.2. Section 5.3 shows all the details to construct a power quotient system to model the traffic of a centralized PETC implementation. A numerical example is shown in Section 5.4. Section 5.5 summarize the contributions of this chapter.

5.2. PROBLEM DEFINITION

Consider a continuous LTI plant of the form:

$$\begin{cases} \dot{\xi}_p(t) = A_p\xi_p(t) + B_p\hat{v}(t) + Ew(t) \\ y(t) = C_p\xi_p(t), \end{cases} \tag{5.1}$$

where $\xi_p(t) \in \mathbb{R}^{n_p}$ denotes the state vector of the plant, $y(t) \in \mathbb{R}^{n_y}$ denotes the plant output vector, $\hat{v}(t) \in \mathbb{R}^{n_v}$ denotes the input applied to the plant, $w(t) \in \mathbb{R}^{n_w}$ denotes the perturbation. The plant is controlled by a discrete-time controller, given by:

$$\begin{cases} \xi_c(t_{k+1}) = A_c\xi_c(t_k) + B_c\hat{y}(t_k) \\ v(t_k) = C_c\xi_c(t_k) + D_c\hat{y}(t_k), \end{cases} \tag{5.2}$$

where $\xi_c(t_k) \in \mathbb{R}^{n_c}$ denotes the state vector of the controller, $v(t_k) \in \mathbb{R}^{n_v}$ denotes the controller output vector, and $\hat{y}(t_k) \in \mathbb{R}^{n_y}$ denotes the input applied to the controller. A periodic sampling sequence is given by:

$$\mathscr{T}_s := \{t_k | t_k := kh, k \in \mathbb{N}\}, \tag{5.3}$$

where $h > 0$ is the sampling interval. Define two vectors:

$$\begin{aligned} u(t) &:= \begin{bmatrix} y^{\mathrm{T}}(t) & v^{\mathrm{T}}(t) \end{bmatrix}^{\mathrm{T}} \in \mathbb{R}^{n_u} \\ \hat{u}(t_k) &:= \begin{bmatrix} \hat{y}^{\mathrm{T}}(t_k) & \hat{v}^{\mathrm{T}}(t_k) \end{bmatrix}^{\mathrm{T}} \in \mathbb{R}^{n_u}, \end{aligned} \tag{5.4}$$

with $n_u := n_y + n_v$. $u(t)$ is the output of the implementation, $\hat{u}(t)$ is the input of the implementation. A zero-order hold mechanism is applied between samplings to the input, i.e. $\hat{u}(t) = \hat{u}(t_k)$, $\forall t \in [t_k, t_{k+1}[$. At each sampling time t_k, the input applied to the implementation $\hat{u}(t_k)$ is updated $\forall t_k \in \mathscr{T}_s$:

$$\hat{u}(t_k) = \begin{cases} u(t_k), & \text{if } \|u(t_k) - \hat{u}(t_k)\| > \sigma\|u(t_k)\| \\ \hat{u}(t_{k-1}), & \text{if } \|u(t_k) - \hat{u}(t_k)\| \leq \sigma\|u(t_k)\|, \end{cases} \tag{5.5}$$

where $\sigma > 0$ is a given constant. Reformulating the event condition as a quadratic form, the event sequence can be defined by:

$$\mathscr{T}_e := \left\{t_b | b \in \mathbb{N}, t_b \in \mathscr{T}_s, \xi^{\mathrm{T}}(t_b)Q\xi(t_b) > 0\right\}. \tag{5.6}$$

where $\xi(t) := \begin{bmatrix} \xi_p^{\mathrm{T}}(t) & \xi_c^{\mathrm{T}}(t) & \hat{y}^{\mathrm{T}}(t) & \hat{v}^{\mathrm{T}}(t) \end{bmatrix}^{\mathrm{T}} \in \mathbb{R}^{n_\xi}$, with $n_\xi := n_p + n_c + n_y + n_v$. And:

$$Q = \begin{bmatrix} Q_1 & Q_2 \\ Q_2^{\mathrm{T}} & Q_4 \end{bmatrix}$$

in which:

$$\begin{cases} Q_1 = \begin{bmatrix} (1-\sigma)C_p^{\mathrm{T}}C_p & \mathbf{0} \\ \mathbf{0} & (1-\sigma)C_c^{\mathrm{T}}C_c \end{bmatrix} \\ Q_2 = \begin{bmatrix} -C_p^{\mathrm{T}} & \mathbf{0} \\ (1-\sigma)C_c^{\mathrm{T}}D_c & -C_c^{\mathrm{T}} \end{bmatrix} \\ Q_4 = \begin{bmatrix} I + (1-\sigma)D_c^{\mathrm{T}}D_c & -D_c^{\mathrm{T}} \\ -D_c & I \end{bmatrix} \end{cases}$$

$\mathbf{0}$ is a zero matrix with proper dimension, I is an identity matrix with appropriate dimension.

It is obvious that $\mathscr{T}_e \subseteq \mathscr{T}_s$. The system (5.1-5.6) is UGES and has $\mathscr{L}_2$-gain from w to z smaller than or equal to γ, where $z(t) := g(\xi(t), w(t))$, if all the hypotheses in Theorem V.2 of [48] are satisfied.

To model the timing behaviour of a PETC system, we aim at constructing a power quotient system for this implementation.

Remark 5.2.1. *Because of the uncertainty brought by the perturbation, it may happen that the perturbation compensates the effect of sampling, helping the state of the implementation to converge. Therefore the event condition in (5.6) may not be satisfied along the timeline. As a result, there may not be an upper bound for the event intervals. However an upper bound is necessary for constructing a useful power quotient system.*

Remark 5.2.2. *To apply scheduling approaches, an online scheduler is required. The model we are going to construct is non-deterministic, meaning that after an event the system may end up in several possible regions, but those regions are defined in terms of ξ_p, which means that from a measurement is not always clear in which region the system is. That means this online scheduler cannot figure out where the system is from simple output measurements. Therefore, the online scheduler should be able to access in which region the system is.*

Assumption 5.2.3. *The current state region at each event-triggered time t_b can be obtained in real time.*

Because of the observation in Remark 5.2.1, we use instead the following event condition:

$$t_{b+1} = \inf\left\{ t_k \,\middle|\, t_k \in \mathscr{T}_s, t_k > t_b, \xi^{\mathrm{T}}(t_k)Q\xi(t_k) > 0 \bigvee t_k \geq t_b + \bar{\tau}_{\mathscr{R}(\xi(t_b))} \right\}, \tag{5.7}$$

where $\mathscr{R}(\xi(t_b))$ is the state region on state-space $\mathbb{R}^{n_\xi}$ at last sampling time t_b, $\bar{\tau}_{\mathscr{R}(\xi(t_b))}$ is a regional Maximum Allowable Event Interval (MAEI), which is dependent on $\mathscr{R}(\xi(t_b))$. According to Assumption 5.2.3, $\mathscr{R}(\xi(t_b))$ is obtainable. If this value is not possible to be accessed by the triggering mechanisms, one can always employ a global upper bound $\bar{\tau} :\geq \bar{\tau}_{\mathscr{R}(\xi(t_b))}$. We will discuss the computation of $\bar{\tau}_{\mathscr{R}(t_b)}$ in later sections. Note that, if the

PETC implementation employing (5.6) can guarantee some pre-designed stability and performance, then the PETC implementation employing (5.7) can guarantee the same stability and performance.

Consider a period:

$$\tau(x) := t_{b+1} - t_b = k_x h. \tag{5.8}$$

By definition $\hat{u}(t)$ is constant $\forall\, t \in [t_b, t_{b+1}[$ and dependent on $\xi_p(t_b)$ and $\xi_c(t_b)$. The input $\hat{u}(t)$ can be expressed as:

$$\hat{u}(t) = C_E x,\ C_E := \begin{bmatrix} C_p & \mathbf{0} \\ D_c C_p & C_c \end{bmatrix},$$

where

$$x := \begin{bmatrix} \xi_p^{\mathrm{T}}(t_b) & \xi_c^{\mathrm{T}}(t_b) \end{bmatrix}^{\mathrm{T}}.$$

Let

$$\xi_x(k) := \begin{bmatrix} \xi_p^{\mathrm{T}}(t_b + kh) & \xi_c^{\mathrm{T}}(t_b + kh) \end{bmatrix}^{\mathrm{T}}$$

be the state evolution with initial state

$$x = \begin{bmatrix} \xi_p^{\mathrm{T}}(t_b) & \xi_c^{\mathrm{T}}(t_b) \end{bmatrix}^{\mathrm{T}}$$

and $k \in \mathbb{N}$. Now $\xi_x(k)$ can be computed as:

$$\xi_x(k) = M(k)x + \Theta(k), \tag{5.9}$$

where

$$M(k) := \begin{bmatrix} M_1(k) \\ M_2(k) \end{bmatrix},\ \Theta(k) := \begin{bmatrix} \Theta_1(k) \\ \mathbf{0} \end{bmatrix},$$

$$\begin{cases} M_1(k) := \begin{bmatrix} I & \mathbf{0} \end{bmatrix} + \displaystyle\int_0^{kh} e^{A_p s} ds \left(A_p \begin{bmatrix} I & \mathbf{0} \end{bmatrix} + B_p \begin{bmatrix} D_c C_p & C_c \end{bmatrix} \right), \\ M_2(k) := A_c^k \begin{bmatrix} \mathbf{0} & I \end{bmatrix} + \displaystyle\sum_{i=0}^{k-1} A_c^{k-1-i} B_c \begin{bmatrix} C_p & \mathbf{0} \end{bmatrix}, \\ \Theta_1(k) := \displaystyle\int_0^{kh} e^{A_p(kh-s)} E w(s) ds. \end{cases}$$

Thus from the event condition in (5.7), k_x in (5.8) can be computed by:

$$k_x = \min \left\{ \underline{k}_x, \overline{k}_x \right\}, \tag{5.10}$$

where $\overline{k}_x := \frac{\bar{\tau}_{\mathscr{R}(x)}}{h}$ and

$$\underline{k}_x := \inf \left\{ k \in \mathbb{N}^+ \,\middle|\, \begin{bmatrix} M(k)x + \Theta(k) \\ C_E x \end{bmatrix}^{\mathrm{T}} Q \begin{bmatrix} M(k)x + \Theta(k) \\ C_E x \end{bmatrix} > 0 \right\}. \tag{5.11}$$

Now we present the main problem to be solved in this chapter. Consider the system:

$$\mathscr{S} = (X, X_0, U, \longrightarrow, Y, H), \tag{5.12}$$

where

- $X = \mathbb{R}^{n_x}$, $n_x = n_p + n_c$;
- $X_0 \subseteq \mathbb{R}^{n_x}$;
- $U = \emptyset$;
- $\longrightarrow \subseteq X \times U \times X$ such that $\forall x, x' \in X : (x, x') \in \longrightarrow$ iff $\xi_x(H(x)) = x'$;
- $Y \subset \mathbb{N}^+$;
- $H : \mathbb{R}^{n_x} \to \mathbb{N}^+$ where $H(x) = k_x$.

$\mathscr{S}$ is an infinite-state system. The output set Y of system $\mathscr{S}$ contains all the possible amount of sampling steps $\frac{t_{b+1}-t_b}{h} \in \mathbb{N}$, $b \in \mathbb{N}$ that the system (5.1-5.5), and (5.7) may exhibit. Once the sampling time h is chosen, the event interval then can be computed by $k_x h$.

Problem 5.2.4. *Construct a finite abstraction of system $\mathscr{S}$ capturing enough information for scheduling.*

Inspired by [62], we solve this problem by constructing a power quotient system $\mathscr{S}_{/P}$ based on an adequately designed equivalence relation P defined over the state set X of $\mathscr{S}$. The constructed systems $\mathscr{S}_{/P}$ are semantically equivalent to timed automata, which can be used for automatic scheduler design [63].

In particular, the system $\mathscr{S}_{/P}$ to be constructed is as follows:

$$\mathscr{S}_{/P} = \left(X_{/P}, X_{/P,0}, U_{/P}, \underset{/P}{\longrightarrow}, Y_{/P}, H_{/P}\right), \tag{5.13}$$

- $X_{/P} = \mathbb{R}^{n_x}_{/P} := \{\mathscr{R}_1, \cdots, \mathscr{R}_q\}$;
- $X_{/P,0} = \mathbb{R}^{n_x}_{/P}$;
- $\left(x_{/P}, x'_{/P}\right) \in \underset{/P}{\longrightarrow}$ if $\exists x \in x_{/P}, \exists x' \in x'_{/P}$ such that $\xi_x(H(x)) = x'$;
- $Y_{/P} \subset 2^Y \subset \mathbb{N}^+$;
- $H_{/P}(x_{/P}) = \left[\min_{x \in x_{/P}} H(x), \max_{x \in x_{/P}} H(x)\right] := \left[\underline{k}_{x_{/P}}, \bar{k}_{x_{/P}}\right]$.

$\mathscr{S}_{/P}$ is a finite state system.

Compared with the power quotient system constructed in [62], a main difference is that since we focus on PETC, there is no timing uncertainty.

5.3. CONSTRUCTION OF THE QUOTIENT SYSTEM

5.3.1. STATE SET

From the results in [37], we remark the following fact:

Remark 5.3.1. *When $w = 0$, excluding the origin, all the states that lie on a line going through the origin have an identical triggering behaviour.*

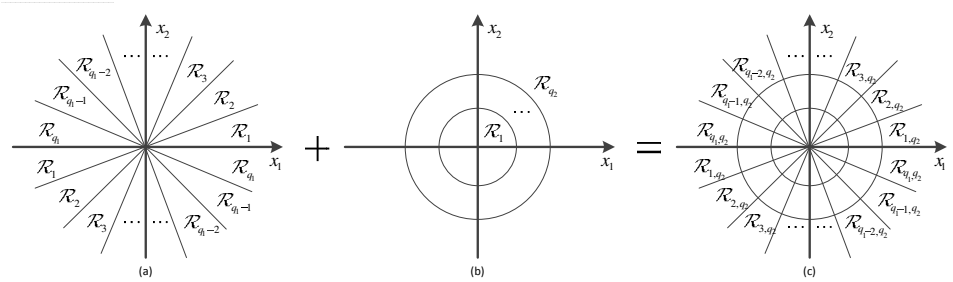

Figure 5.1: An example of the state space partition, into (a) finite number of polyhedral cones, (b) finite number of homocentric spheres, and (c) finite number of regions.

We also call the following assumption:

Assumption 5.3.2. *The perturbation w satisfies $w \in \mathscr{L}_2$ and $w \in \mathscr{L}_\infty$. Besides, assume an upper bound $\mathscr{W} > 0$ for $\|w\|_{\mathscr{L}_\infty}$, i.e. $\|w\|_{\mathscr{L}_\infty} \leq \mathscr{W}$, is known.*

5

Based on Remark 5.3.1 and Assumption 5.3.2, we propose state-space partition as follows:

$$\mathscr{R}_{s_1,s_2} = \left\{ x \in \mathbb{R}^{n_x} \,\middle|\, \bigwedge_{i=1}^{n_x-1} x^{\mathrm{T}} \Xi_{s_1,(i,i+1)} x \geq 0 \bigwedge W_{s_2-1} \leq |x| < W_{s_2} \right\}, \tag{5.14}$$

where $s_1 \in \{1,\cdots,q_1\}$, $s_2 \in \{1,\cdots,q_2\}$, $q_1, q_2 \in \mathbb{N}$ are pre-designed scalars. $\Xi_{s_1,(i,j)}$ is a constructed matrix; $\{W_i | i \in \{0,\cdots,q_2\}\}$ is a sequence of scalars. Note that $W_0 = 0$, $W_{q_2} = +\infty$, and the rest W_{s_2} are bounded and somewhere in between 0 and $+\infty$. It is obvious that $\bigcup_{s_1\in\{1,\cdots,q_1\},s_2\in\{1,\cdots,q_2\}} \mathscr{R}_{s_1,s_2} = \mathbb{R}^{n_x}$.

This state-space partition combines partitioning the state-space into finite number of polyhedral cones (named as *isotropic covering* [37]) and finite number of homocentric spheres. From (5.14), we can see that, the *isotropic covering* describes the relation between entries of the state vector, while the *transverse isotropic covering* is used to capture the relation between the norm of the state vector and the $\mathscr{L}_\infty$ norm of the perturbations, which will be shown later in Theorem 5.3.4. If $w = 0$, the homocentric spheres can be omitted.

Details on the *isotropic covering* can be found in the appendix. Figure 5.1 shows a 2-dimensional example.

5.3.2. OUTPUT MAP

We first free the system dynamics from the uncertainty brought by the perturbation.

Lemma 5.3.3. *Consider the system (5.1-5.5) and (5.7), and that Assumption 5.3.2 holds. If there exist a scalar $\mu \geq 0$ and a symmetric matrix Ψ such that $(Q_1 + \Psi)_1 \preceq \mu I$, then $\underline{k}_x$ generated by (5.11) is lower bounded by:*

$$k'_x := \inf\{k \in \mathbb{N}^+ | \Phi(k) \succ 0\}, \tag{5.15}$$

where

$$Q_1+\Psi=\begin{bmatrix}(Q_1+\Psi)_1 & (Q_1+\Psi)_2\\ (Q_1+\Psi)_3 & (Q_1+\Psi)_4\end{bmatrix}$$
$$(Q_1+\Psi)_1\in\mathbb{R}^{n_p\times n_p},$$
$$\Phi(k):=\begin{bmatrix}\Phi_1(k) & \Phi_2(k) & \mathbf{0}\\ \Phi_2^{\mathrm{T}}(k) & -\Psi & \mathbf{0}\\ \mathbf{0} & \mathbf{0} & \Phi_3(k)\end{bmatrix}, \tag{5.16}$$

$$\begin{cases}\Phi_1(k)=M^{\mathrm{T}}(k)Q_1M(k)+M^{\mathrm{T}}(k)Q_2C_E+C_E^{\mathrm{T}}Q_3M(k)+C_E^{\mathrm{T}}Q_4C_E\\ \Phi_2(k)=M^{\mathrm{T}}(k)Q_1+C_E^{\mathrm{T}}Q_3\\ \Phi_3(k)=kh\mu\lambda_{\max}\left(E^{\mathrm{T}}E\right)d_{A_p}(k),\end{cases} \tag{5.17}$$

and

$$d_{A_p}(k)=\begin{cases}\dfrac{e^{k\lambda_{\max}\left(A_p+A_p^{\mathrm{T}}\right)}-1}{\lambda_{\max}\left(A_p+A_p^{\mathrm{T}}\right)}, & \text{if } \lambda_{\max}\left(A_p+A_p^{\mathrm{T}}\right)\neq 0,\\ kh, & \text{if } \lambda_{\max}\left(A_p+A_p^{\mathrm{T}}\right)=0.\end{cases}$$

Next we construct LMIs that bridge Lemma 5.3.3 and the state-space partition.

Theorem 5.3.4. *(Regional lower bound) Consider a scalar $\underline{k}_{s_1,s_2}\in\mathbb{N}$ and regions with $s_2>1$. If all the hypothesis in Lemma 5.3.3 hold and there exist scalars $\underline{\varepsilon}_{k,(s_1,s_2),(i,i+1)}\geq 0$ where $i\in\{1,\cdots,n_x-1\}$ such that for all $k\in\{0,\cdots,\underline{k}_{s_1,s_2}\}$ the following LMIs hold:*

$$\begin{bmatrix}H & \Phi_2(k)\\ \Phi_2^{\mathrm{T}}(k) & -\Psi\end{bmatrix}\preceq 0, \tag{5.18}$$

where

$$H=\Phi_1(k)+\Phi_3(k)\mathscr{W}^2W_{s_2-1}^{-2}I+\sum_{i\in\{1,\cdots,n_x-1\}}\underline{\varepsilon}_{k,(s_1,s_2),(i,i+1)}\Xi_{s_1,(i,i+1)},$$

with $\Phi_1(k)$, $\Phi_2(k)$, and $\Phi_3(k)$ defined in (5.17), and Ψ from Lemma 5.3.3, then the inter event times (5.7) for system (5.1-5.5) are regionally bounded from below by $(\underline{k}_{s_1,s_2}+1)h$. For the regions with $s_2=1$, the regional lower bound is h.

Remark 5.3.5. *In Theorem 5.3.4, we discuss the situations when $s_2>1$ and $s_2=1$, since for all regions with $s_2>1$, it holds that $W_{s_2-1}\neq 0$; while for all regions with $s_2=1$, $W_{s_2-1}=0$ holds. When $W_{s_2-1}\neq 0$, one can easily validate the feasibility of the LMI (5.18); while when $W_{s_2-1}=0$, H will be diagonal infinity, making the LMI (5.18) infeasible when $k>0$. However, according to the property of PETC, i.e. $t_{b+1}\in\mathcal{T}_s$ and $t_{b+1}>t_b$, the regional lower bound exists and is equal to h.*

Following similar ideas of Theorem 5.3.4, we present next lower and upper bounds starting from each state partition when $w=0$. Consider the following event condition:

$$k_x=\inf\left\{k\in\mathbb{N}^+\,\middle|\,\begin{bmatrix}M(k)x\\ C_Ex\end{bmatrix}^{\mathrm{T}}Q\begin{bmatrix}M(k)x\\ C_Ex\end{bmatrix}>0\right\}. \tag{5.19}$$

Remark 5.3.6. *Since (5.19) does not consider perturbations, when computing the lower and upper bound for each region, according to Remark 5.3.1, only applying* isotropic covering *is enough.*

We define $\mathscr{R}_{s_1,\bullet}$ to represent $\mathscr{R}_{s_1,s_2}$, $\forall s_2 \in \{1,\cdots,q_2\}$.

Corollary 5.3.7. *(Regional lower bound when $w=0$) Consider a scalar $\underline{k}_{s_1,\bullet} \in \mathbb{N}$. If there exist scalars $\underline{\varepsilon}_{k,s_1,(i,i+1)} \geq 0$ where $i \in \{1,\cdots,n_x-1\}$ such that for all $k \in \{0,\cdots,\underline{k}_{s_1,\bullet}\}$ the following LMIs hold:*

$$\Phi_1(k) + \sum_{i\in\{1,\cdots,n_x-1\}} \underline{\varepsilon}_{k,s_1,(i,i+1)} \Xi_{s_1,(i,i+1)} \preceq 0, \tag{5.20}$$

with $\Phi_1(k)$ defined in (5.17), then the inter event times (5.6) of the system (5.1-5.5) with $w=0$ are regionally bounded from below by $(\underline{k}_{s_1,\bullet}+1)h$.

Corollary 5.3.8. *(Regional upper bound when $w=0$) Let $\bar{l} \in \mathbb{N}$ be a large enough scalar. Consider a scalar $\bar{k}_{s_1,\bullet} \in \left\{\underline{k}_{s_1,\bullet},\cdots,\bar{l}\right\}$. If there exist scalars $\bar{\varepsilon}_{k,s_1,(i,i+1)} \geq 0$ where $i \in \{1,\cdots,n_x-1\}$ such that for all $k \in \left\{\bar{k}_{s_1,\bullet},\cdots,\bar{l}\right\}$ the following LMIs hold:*

$$\Phi_1(k) - \sum_{i\in\{1,\cdots,n_x-1\}} \bar{\varepsilon}_{k,s_1,(i,i+1)} \Xi_{s_1,(i,i+1)} \succ 0, \tag{5.21}$$

with $\Phi_1(k)$ defined in (5.17), then the inter event times (5.6) of the system (5.1-5.5) with $w=0$ are regionally bounded from above by $\bar{k}_{s_1,\bullet}h$.

Remark 5.3.9. *For the choice of $\bar{l}$, we follow Remark 2 in [62], and apply a line search approach: increasing $\bar{l}$ until $\Phi_1(\bar{l}) \succ 0$. This results in $\bar{l}$ being a global upper bound for the inter event time (5.6) of the system (5.1-5.5) with $w=0$.*

It is obvious that $\bar{l} \geq \bar{k}_{s_1,\bullet} > \underline{k}_{s_1,\bullet} \geq \underline{k}_{s_1,s_2}$, $\forall s_2$. We can now set the regional MAEI $\bar{\tau}_{\mathscr{R}(\xi(t_b))}$ in (5.7) as: $\bar{\tau}_{\mathscr{R}(\xi(t_b))} := \bar{k}_{s_1,\bullet}h$, $\forall x \in \mathscr{R}_{s_1,\bullet}$.

5.3.3. TRANSITION RELATION

In this subsection, we discuss the construction of the transition relation and the reachable state set. Denote the initial state set as $X_{0,(s_1,s_2)}$, after k-th samplings without an update, the reachable state set is denoted as $X_{k,(s_1,s_2)}$. According to (5.9), a relation can be obtained as:

$$X_{k,(s_1,s_2)} = M(k)X_{0,(s_1,s_2)} + \Theta(k). \tag{5.22}$$

It is obvious that, $X_{k,(s_1,s_2)}$ cannot be computed directly, because the perturbation is uncertain and the state region may not be convex. Therefore, we aim to find sets $\hat{X}_{k,(s_1,s_2)}$ such that:

$$X_{k,(s_1,s_2)} \subseteq \hat{X}_{k,(s_1,s_2)}.$$

To compute $\hat{X}_{k,(s_1,s_2)}$, we take the following steps:

PARTITION THE DYNAMICS

According to (5.22), $\hat{X}_{k,(s_1,s_2)}$ can be computed by:

$$\hat{X}_{k,(s_1,s_2)} = \hat{X}^1_{k,(s_1,s_2)} \oplus \hat{X}^2_{k,(s_1,s_2)},$$

where $\oplus$ is the Minkowski addition, $\hat{X}^1_{k,(s_1,s_2)}$ and $\hat{X}^2_{k,(s_1,s_2)}$ are sets to be computed.

COMPUTE $\hat{X}^1_{k,(s_1,s_2)}$

One can compute $\hat{X}^1_{k,(s_1,s_2)}$ by:

$$\hat{X}^1_{k,(s_1,s_2)} = M(k)\hat{X}_{0,(s_1,s_2)},$$

where $\hat{X}_{0,(s_1,s_2)}$ is a polytope that over approximates $X_{0,(s_1,s_2)}$, i.e. $X_{0,(s_1,s_2)} \subseteq \hat{X}_{0,(s_1,s_2)}$. $\hat{X}_{0,(s_1,s_2)}$ can be computed as in the optimization problem (1) in [22], i.e. choose a $C_{0,(s_1,s_2)}$, compute a $d_{0,(s_1,s_2)}$ such that

$$\min_{d_{0,(s_1,s_2)}} \text{volume}\left[\left\{x|C_{0,(s_1,s_2)}x \le d_{0,(s_1,s_2)}\right\}\right]$$
$$X_{0,(s_1,s_2)} \subseteq \left\{x|C_{0,(s_1,s_2)}x \le d_{0,(s_1,s_2)}\right\}.$$

And now let $\hat{X}_{0,(s_1,s_2)} = \left\{x|C_{0,(s_1,s_2)}x \le d_{0,(s_1,s_2)}\right\}$.

COMPUTE $\hat{X}^2_{k,(s_1,s_2)}$

For the computation of $\hat{X}^2_{k,(s_1,s_2)}$, it follows that:

$$\hat{X}^2_{k,(s_1,s_2)} = \{x \in \mathbb{R}^{n_x} || x| \le |\Theta(k)|\},$$

where

$$\begin{aligned}
|\Theta(k)| &= \left| \int_0^{kh} e^{A_p(kh-s)} E w(s) ds \right| \\
&\le \int_0^{kh} \left| e^{A_p(kh-s)} E w(s) \right| ds \\
&\le \int_0^{kh} \left| e^{A_p(kh-s)} \right| ds |E| \| w \|_{\mathscr{L}_\infty} \\
&\le \int_0^{kh} e^{\lambda_{\max}\left(\frac{A_p^{\mathrm{T}}+A_p}{2}\right)(kh-s)} ds |E| \mathscr{W}.
\end{aligned}$$

In which the last inequation holds according to (2.2) in [104].

Thus the reachable set $X_{\left\{\underline{k}_{s_1,s_2},\overline{k}_{s_1,\bullet}\right\},(s_1,s_2)}$ of the system (5.1-5.5), and (5.7) starting from $X_{0,(s_1,s_2)}$ can be computed by:

$$\begin{aligned}
X_{\left\{\underline{k}_{s_1,s_2},\overline{k}_{s_1,\bullet}\right\},(s_1,s_2)} &\subseteq \hat{X}_{\left\{\underline{k}_{s_1,s_2},\overline{k}_{s_1,\bullet}\right\},(s_1,s_2)} \\
&= \bigcup_{k \in \left\{\underline{k}_{s_1,s_2},\cdots,\overline{k}_{s_1,\bullet}\right\}} \hat{X}_{k,(s_1,s_2)}.
\end{aligned}$$

To compute the transitions in $\mathscr{S}_{/P}$, one can check the intersection between the over approximation of reachable state set and all the state regions $\mathscr{R}_{s_1',s_2'}$, $\forall s_1' \in \{1,\cdots,q_1\}, s_2' \in \{1,\cdots,q_2\}$. More specifically, one can check if the following feasibility problem for each state region holds:

$$\mathscr{R}_{s_1',s_2'} \cap \hat{X}_{\left\{\underline{k}_{s_1,s_2},\overline{k}_{s_1,\bullet}\right\},(s_1,s_2)} \neq \emptyset,$$

in which case

$$\left(\mathscr{R}_{s_1,s_2}, \mathscr{R}_{s_1',s_2'}\right) \in \xrightarrow[/P]{}.$$

5

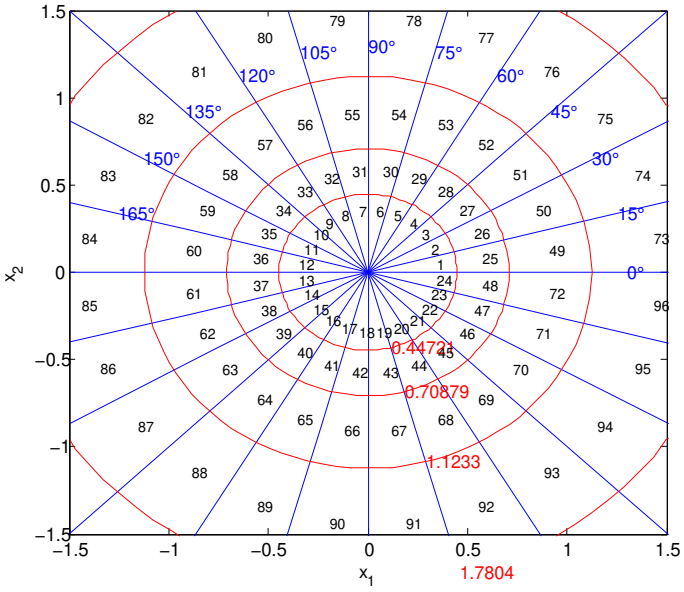

Figure 5.2: State-space partition and the labelling of each region.

5.3.4. MAIN RESULT

Now we summarize the main result of the chapter in the following theorem.

Theorem 5.3.10. *The metric system* $\mathscr{S}_{/P} = \left(X_{/P}, X_{/P,0}, U_{/P}, \underrightarrow{\ }_{/P}, Y_{/P}, H_{/P}\right)$, ϵ*-approximately simulates* $\mathscr{S}$, *where* $\epsilon = \max d_H\left(y, y'\right)$, $y = H(x) \in Y$, $y' = H_{/P}\left(x'\right) \in Y_{/P}$, $\forall \left(x, x'\right) \in P$, *and* $d_H(\cdot,\cdot)$ *is the Hausdorff distance.*

5.4. NUMERICAL EXAMPLE

In this section, we consider a system employed in [48] and [95]. The plant is given by:

$$\dot{\xi}(t) = \begin{bmatrix} 0 & 1 \\ -2 & 3 \end{bmatrix} \xi(t) + \begin{bmatrix} 0 \\ 1 \end{bmatrix} v(t) + \begin{bmatrix} 1 \\ 0 \end{bmatrix} w(t),$$

and the control gain is given by:

$$K = \begin{bmatrix} 1 & -4 \end{bmatrix}.$$

This plant is chosen since it is easy to show the feasibility of the presented theory in 2-dimensional plots. The state-space partition is presented in Figure 5.2.

We set $\mathscr{W} = 2$, the convergence rate $\rho = 0.01$, $\mathscr{L}_2$ gain $\gamma = 2$, sampling time $h = 0.005s$, event condition $\sigma = 0.1$. By checking the LMI presented in [48], we can see that there exists a feasible solution, thus the stability and performance can be guaranteed. The result of the computed lower bound by Theorem 5.3.4 is shown in Figure 5.3. Figure 5.4

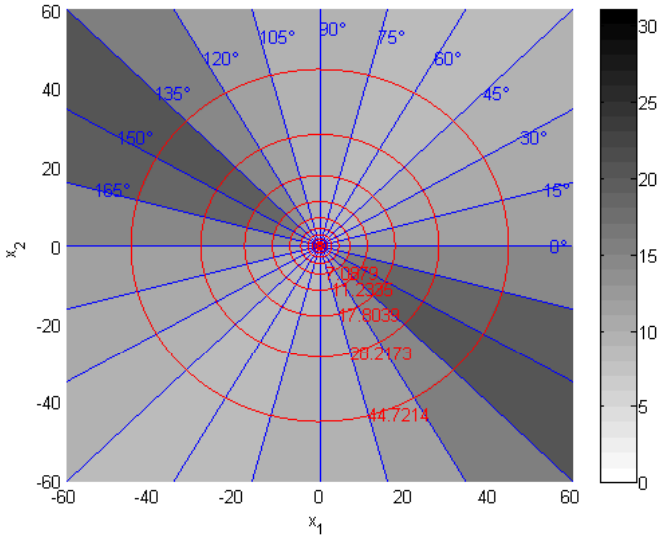

Figure 5.3: Computed result of the regional lower bound with $\mathscr{W} = 2$.

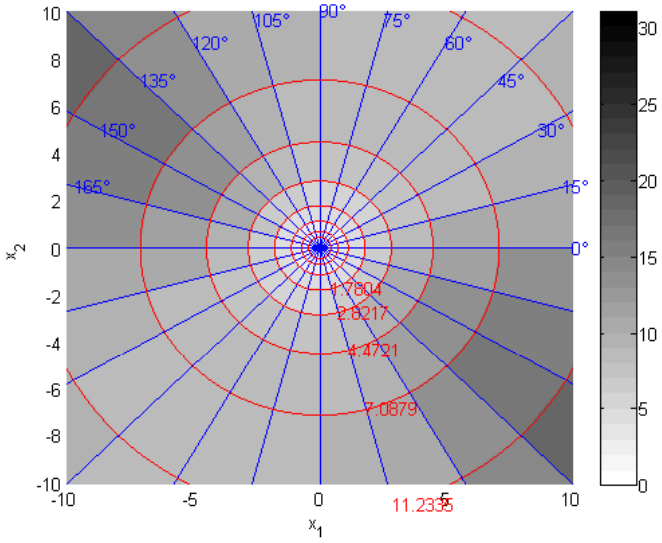

Figure 5.4: Zoomed-in result of the regional lower bound with $\mathscr{W} = 2$.

shows a zoomed-in version. The computed upper bound by Corollary 5.3.8 is shown in Figure 5.5. The resulting abstraction precision is $\epsilon = 0.15s$.

The simulation results of the system evolution and event intervals with perturbations

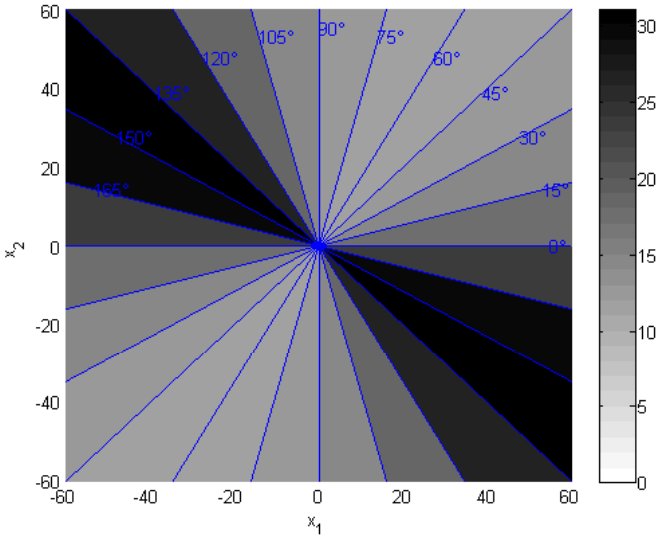

Figure 5.5: Computed result of the regional upper bound with $w = 0$.

are shown in Figure 5.6. The upper bound triggered 6 events during the $10s$ simulation. Note that, increasing the number of subdivisions can lead to less conserved lower and upper bounds of the inter event time. The conservativeness can also be reduced by decreasing $\mathcal{W}$.

The reachable state regions starting from each region is shown in Figure 5.7. As an example, the reachable state region of the initial region $(s_1, s_2) = (4, 6)$ is shown in Figure 5.8.

We also present a simulation when $w = 0$. The lower bound is shown in Figure 5.9. The evolution of the system is shown in Figure 5.10, which shows that, the inter event intervals are within the computed bounds. The reachable state regions starting from each region are shown in Figure 5.11.

5.5. CONCLUSIONS

In this chapter, we present a construction of a power quotient system for the traffic model of the PETC implementations from [48]. The constructed models can be used to estimate the next event time and the state set when the next event occurs. These models allow to design scheduling to improve listening time of wireless communications and medium access time to increase the energy consumption and bandwidth occupation efficiency.

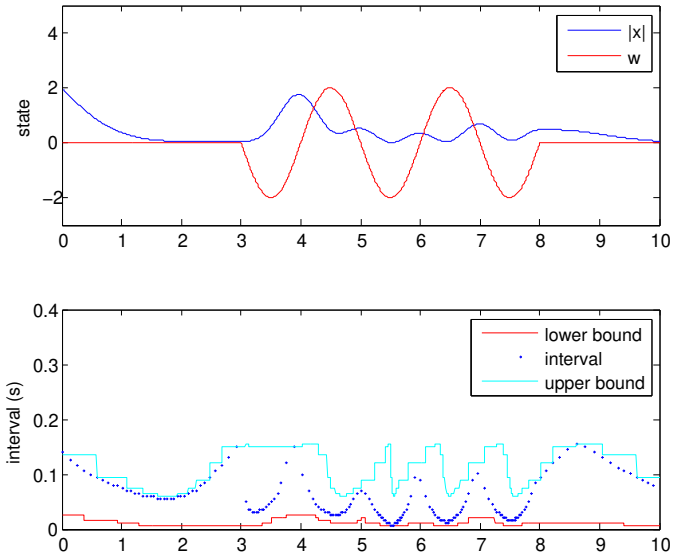

Figure 5.6: System evolution and event intervals when $w = 2\sin(\pi t), t \in [3,8]$: state evaluation and perturbance, event intervals with the bounds.

APPENDIX

Isotropic covering Consider $x = \begin{bmatrix} x_1 & x_2 & \cdots & x_n \end{bmatrix}^{\mathrm{T}} \in \mathbb{R}^n$. We first present a case when $x \in \mathbb{R}^2$. Let $\Theta = [-\frac{\pi}{2}, \frac{\pi}{2}[$ be an interval. Splitting this interval into q sub-intervals and $\Theta_s = [\underline{\theta}_s, \overline{\theta}_s[$ be the s-th sub-interval. Then for each sub-interval, one can construct a cone pointing at the origin:

$$\mathscr{R}_s = \left\{ x \in \mathbb{R}^2 | x^{\mathrm{T}} \tilde{\Xi}_s x \geq 0 \right\},$$

where

$$\tilde{\Xi}_s = \begin{bmatrix} -\sin\underline{\theta}_s \sin\overline{\theta}_s & \frac{1}{2}\sin(\underline{\theta}_s + \overline{\theta}_s) \\ \frac{1}{2}\sin(\underline{\theta}_s + \overline{\theta}_s) & -\cos\underline{\theta}_s \cos\overline{\theta}_s \end{bmatrix}.$$

Remark 5.3.1 shows that x and $-x$ have the same behaviours; therefore it is sufficient to only consider half of the state-space.

Now we derive the case when $x \in \mathbb{R}^n$, $n > 2$. Define $(x)_{i,j} = (x_i, x_j)$ as the projection of this point on its $i-j$ coordinate plane. Now a polyhedral cone $\mathscr{R}_s$ can be defined as:

$$\mathscr{R}_s = \left\{ x \in \mathbb{R}^n \middle| \bigwedge_{i=1}^{n-1} (x)_{(i,i+1)}^{\mathrm{T}} \tilde{\Xi}_{s,(i,i+1)} (x)_{(i,i+1)} \geq 0 \right\},$$

where $\tilde{\Xi}_{s,(i,i+1)}$ is a constructed matrix. A relation between $\tilde{\Xi}_{s,(i,i+1)}$ and $\Xi_{s,(i,i+1)}$ from

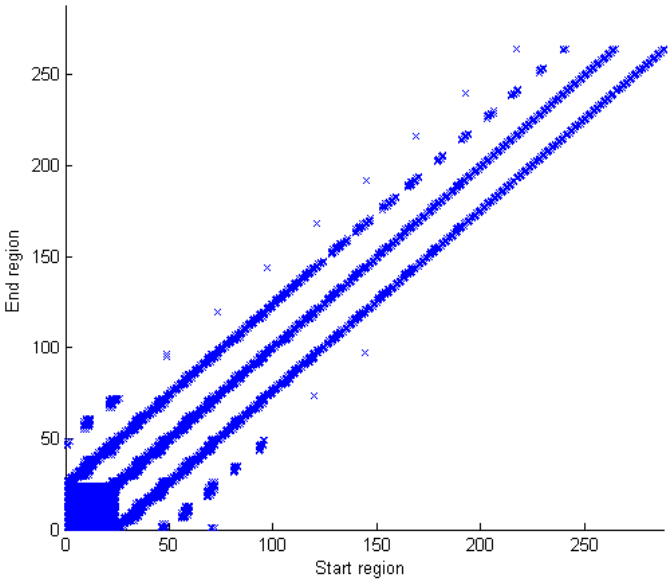

Figure 5.7: Reachable regions starting from each state region, with labelling from Figure 5.2.

(5.14) is given by:

$$\begin{cases} [\Xi_{s,(i,i+1)}]_{(i,i)} & =[\tilde{\Xi}_{s,(i,i+1)}]_{(1,1)} \\ [\Xi_{s,(i,i+1)}]_{(i,i+1)} & =[\tilde{\Xi}_{s,(i,i+1)}]_{(1,2)} \\ [\Xi_{s,(i,i+1)}]_{(i+1,i)} & =[\tilde{\Xi}_{s,(i,i+1)}]_{(2,1)} \\ [\Xi_{s,(i,i+1)}]_{(i+1,i+1)} & =[\tilde{\Xi}_{s,(i,i+1)}]_{(2,2)} \\ [\Xi_{s,(i,i+1)}]_{(k,l)} & =0, \end{cases}$$

where $[M]_{(i,j)}$ is the i-th row, j-th column entry of the matrix M, k and l satisfy $(k,l) \neq (i,i+1)$. □

Proof of Lemma 5.3.3 We decouple the ETM in (5.11) first:

$$\begin{aligned} &\begin{bmatrix} M(k)x+\Theta(k) \\ C_E x \end{bmatrix}^{\mathrm{T}} Q \begin{bmatrix} M(k)x+\Theta(k) \\ C_E x \end{bmatrix} \\ =&x^{\mathrm{T}}\Phi_1(k)x + x^{\mathrm{T}}\Phi_2(k)\Theta(k) + \Theta^{\mathrm{T}}(k)\Phi_2^{\mathrm{T}}(k)x + \Theta^{\mathrm{T}}(k)Q_1\Theta(k) \\ \leq&x^{\mathrm{T}}(\Phi_1(k)+\Phi_2(k)\Psi^{-1}\Phi_2^{\mathrm{T}}(k))x + \Theta^{\mathrm{T}}(k)(Q_1+\Psi)\Theta(k), \end{aligned} \tag{5.23}$$

where the last inequality comes from Lemma 6.2 in [47]. Now for the uncertainty part,

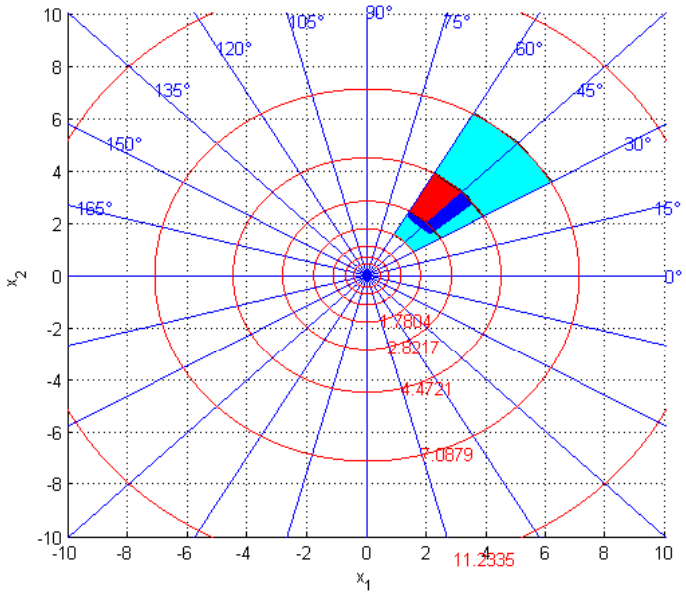

Figure 5.8: Flow pipe of $(s_1, s_2) = (4, 6)$: indicating initial state set (red), reachable state set (blue), and reachable regions (cyan).

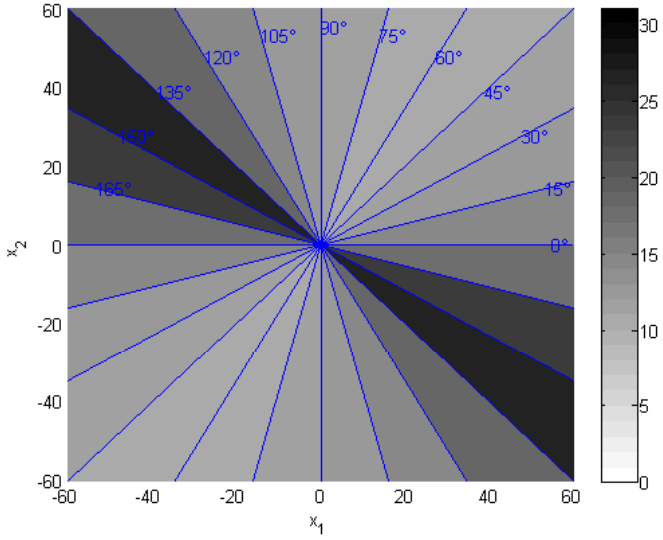

Figure 5.9: Computed result of the regional lower bound with $w = 0$.

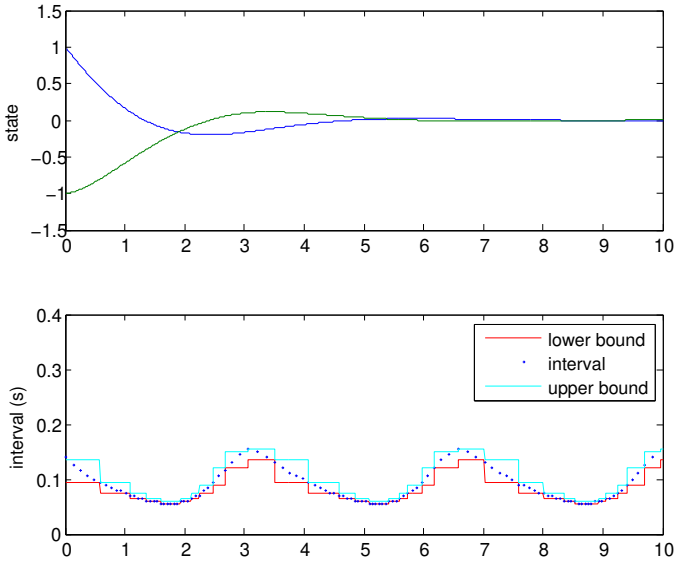

Figure 5.10: System evolution and event intervals when $w = 0$: state evaluation and event intervals vs computed bounds.

we have:

$$\begin{aligned}
&\Theta^{\mathrm{T}}(k)(Q_1+\Psi)\Theta(k)\\
=&\begin{bmatrix}\Theta_1(k)\\ \mathbf{0}\end{bmatrix}^{\mathrm{T}}\begin{bmatrix}(Q_1+\Psi)_1 & (Q_1+\Psi)_2\\ (Q_1+\Psi)_3 & (Q_1+\Psi)_4\end{bmatrix}\begin{bmatrix}\Theta_1(k)\\ \mathbf{0}\end{bmatrix}\\
=&\Theta_1^{\mathrm{T}}(k)(Q_1+\Psi)_1\Theta_1(k).
\end{aligned}$$

From the hypothesis of the theorem that there exists μ such that $(Q_1+\Psi)_1 \preceq \mu I$, together with Jensen's inequality [47], inequality (2.2) in [104], and Assumption 5.3.2, i.e. $w \in \mathscr{L}_\infty$,

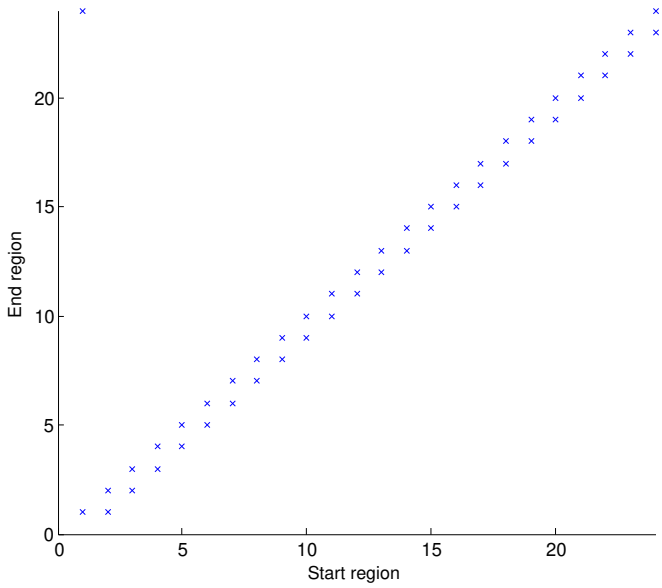

Figure 5.11: Reachable regions starting from each conic region, with labeling from Figure 5.2.

$\Theta^{\mathrm{T}}(k)(Q_1+\Psi)\Theta(k)$ can be bounded from above by:

$$
\begin{aligned}
&\Theta^{\mathrm{T}}(k)(Q_1+\Psi)\Theta(k)\\
=&\Theta_1^{\mathrm{T}}(k)(Q_1+\Psi)_1\Theta_1(k)\\
\leq&\mu\left(\int_0^{kh} e^{A_p(kh-s)}Ew(s)ds\right)^{\mathrm{T}}\left(\int_0^{kh} e^{A_p(kh-s)}Ew(s)ds\right)\left(\text{by } (Q_1+\Psi)\preceq\mu I\right)\\
\leq&kh\mu\int_0^{kh}\left(e^{A_p(kh-s)}Ew(s)\right)^{\mathrm{T}}\left(e^{A_p(kh-s)}Ew(s)\right)ds\,(\text{by Jensen's equality})\\
\leq&kh\mu\int_0^{kh} e^{(kh-s)\lambda_{\max}\left(A_p+A_p^{\mathrm{T}}\right)}w^{\mathrm{T}}(s)E^{\mathrm{T}}Ew(s)ds\,(\text{by (2.2) in [104]})\\
\leq&kh\mu\lambda_{\max}\left(E^{\mathrm{T}}E\right)\int_0^{kh} e^{(kh-s)\lambda_{\max}\left(A_p+A_p^{\mathrm{T}}\right)}ds\|w\|^2_{\mathscr{L}_\infty}\,(\text{by } w\in\mathscr{L}_\infty)\\
=&kh\mu\lambda_{\max}\left(E^{\mathrm{T}}E\right)d_{A_p}(k)\|w\|^2_{\mathscr{L}_\infty}.
\end{aligned}
\tag{5.24}
$$

With (5.24), (5.23) can be further bounded as:

$$
\begin{aligned}
&\begin{bmatrix}M(k)x+\Theta(k)\\ C_Ex\end{bmatrix}^{\mathrm{T}}Q\begin{bmatrix}M(k)x+\Theta(k)\\ C_Ex\end{bmatrix}\\
\leq&x^{\mathrm{T}}\left(\Phi_1(k)+\Phi_2(k)\Psi^{-1}\Phi_2^{\mathrm{T}}(k)\right)x+\Phi_3(k)\|w\|^2_{\mathscr{L}_\infty}.
\end{aligned}
\tag{5.25}
$$

From the hypothesis of the theorem, if $\Phi(k)\preceq 0$ holds, then by applying the Schur com-

plement to (5.16), the following inequality holds:

$$x^{\mathrm{T}}\left(\Phi_1(k)+\Phi_2(k)\Psi^{-1}\Phi_2^{\mathrm{T}}(k)\right)x+\Phi_3(k)\|w\|^2_{\mathscr{L}_\infty}\leq 0,$$

which indicates:

$$\begin{bmatrix} M(k)x+\Theta(k) \\ C_E x \end{bmatrix}^{\mathrm{T}} Q \begin{bmatrix} M(k)x+\Theta(k) \\ C_E x \end{bmatrix} \leq 0. \tag{5.26}$$

Therefore, $\underline{k}_x$ generated by (5.11) is lower bounded by k'_x generated by (5.15). This ends the proof. □

Proof of Theorem 5.3.4 We first consider the regions with $s_2 > 1$. If all the hypotheses of the theorem hold, by applying the Schur complement to (5.18), one has:

$$x^{\mathrm{T}}\left(H+\Phi_2(k)\Psi^{-1}\Phi_2^{\mathrm{T}}(k)\right)x\leq 0. \tag{5.27}$$

From (5.14), and applying the S-procedure, it holds that:

$$x^{\mathrm{T}}\left(\Phi_1(k)+\Phi_3(k)\mathscr{W}^2W_{s_2-1}^{-2}I+\Phi_2(k)\Psi^{-1}\Phi_2^{\mathrm{T}}(k)\right)x\leq 0. \tag{5.28}$$

From (5.14) we also have:

$$x^{\mathrm{T}}x\geq W_{s_2-1}^2. \tag{5.29}$$

Since $\Phi_3(k)$, $\mathscr{W}$, and W_{s_2-1} are non-negative scalars and $W_{s_2-1}>0$, we have the following inequality:

$$\begin{aligned} x^{\mathrm{T}}\Phi_3(k)\mathscr{W}^2W_{s_2-1}^{-2}Ix=&\Phi_3(k)\mathscr{W}^2W_{s_2-1}^{-2}x^{\mathrm{T}}x\\ \geq&\Phi_3(k)\mathscr{W}^2W_{s_2-1}^{-2}W_{s_2-1}^2\\ =&\Phi_3(k)\mathscr{W}^2\\ \geq&\Phi_3(k)\|w\|^2_{\mathscr{L}_\infty}, \end{aligned} \tag{5.30}$$

in which the last inequality comes form the definition of $\mathscr{W}$. Now inserting (5.30) into (5.28) results in:

$$x^{\mathrm{T}}\left(\Phi_1(k)+\Phi_2(k)\Psi^{-1}\Phi_2^{\mathrm{T}}(k)\right)x+\Phi_3(k)\|w\|^2_{\mathscr{L}_\infty}\leq 0,$$

which together with applying the Schur complement to (5.16) provides the regional lower bound.

When $s_2=1$, $k>0$, the diagonal elements of H will be infinity. Thus one cannot find a feasible solution to the LMI (5.18). According to the event-triggered condition (5.7), which indicates that $t_{b+1}\in\mathscr{T}_s$ and $t_{b+1}>t_b$, the regional lower bound for those regions with $s_2=1$ is h. This finishes the proof. □

Proof of Corollary 5.3.7 The result can be easily obtained from Theorem 5.3.4 considering $E=\mathbf{0}$. □

Proof of Corollary 5.3.8 The result can be easily obtained analogously to Theorem 5.3.4 considering $E=\mathbf{0}$: if all the hypotheses of this corollary hold, then according to (5.21), $\Phi_1(k)\succ 0$, $k\in\{\bar{k}_{s_1,\bullet},\cdots,\bar{l}\}$. According to the definition of $\Phi_1(k)$ in (5.17), for all $k\geq\bar{k}_{s_1,\bullet}$, it holds that:

$$\begin{bmatrix} M(k)x \\ C_E x \end{bmatrix}^{\mathrm{T}} Q \begin{bmatrix} M(k)x \\ C_E x \end{bmatrix} > 0,$$

which together with event condition (5.19) provides the regional upper bound. □

Proof of Theorem 5.3.10 The result follows from Lemma 2.3.9 and the construction described in Section 5.3. □

6

COMMUNICATION SCHEMES FOR CENTRALIZED AND DECENTRALIZED EVENT-TRIGGERED CONTROL SYSTEMS

Energy constrained long-range wireless sensor/actuator based solutions are theoretically the perfect choice to support the next generation of city-scale CPSs. Traditional systems adopt periodic control which increases network congestion and actuations while burdening the energy consumption. Recent control theory studies overcome these problems by introducing aperiodic strategies, such as ETC. In spite of the potential savings, these strategies assume actuators continuously listening while ignoring the sensing energy costs. In this work, we fill this gap, by enabling sensing and actuator listening duty-cycling and by proposing two innovative MAC protocols for three decentralized ETC approaches. A laboratory experimental testbed, which emulates a smart water network, was modelled and extended to evaluate the impact of system parameters and the performance of each approach. Experimental results reveal the predominance of the decentralized ETC against the classic periodic control either in terms of communication or actuation by promising significant system lifetime extension.

Sections 6.2-6.6 of this chapter are extracted from [59].

6.1. INTRODUCTION

In this chapter, we apply and compare the triggering approaches proposed in Chapter 2, 3, and 4 to a real physical plant, WaterBox.

WaterBox is a scaled smart water distribution system [57]. It employs a wireless network to connect its physically distributed components. We equip the WaterBox with a controller in order to guarantee stability and performance, so that a pre-designed Quality of Service (QoS) can be guaranteed. The WaterBox is a good candidate plant to test and compare different triggering mechanisms designed for WNCS, since it has many physically distributed components that communicate via a wireless network. In this chapter, we present the work we have performed on the WaterBox. We first identify the system model, based on which we design a controller to render the system stable. Then we choose several triggering mechanisms for the implementation. After designing customized TDMA based communication protocols and corresponding triggering condition parameters to guarantee UGES with the same convergence rate, we apply these triggering mechanisms to the implementation. Following which we complete more than four hundreds experiments, collect, and analyze the data to make comparisons within the selected triggering mechanisms.

For the WaterBox, we choose to compare TTC, centralized PETC, and decentralized PETC with synchronous and asynchronous communication. For the sake of brevity and to specify each ETM, in this chapter we use PETC as a shorthand for centralized PETC. Note that all the triggering mechanisms have a fine static quantizer due to the analogue to digital conversion at the sensors. In practice, for the ADPETC, according to (3.7), the $\text{sign}(\hat{\xi}_i(t_{k-1})-\xi_i(t_k))$ and $m_i(t_k)$ have to be transmitted from the sensor to the controller. Therefore, an additional coarse dynamic quantizer can be applied with maximum quantization error $\sqrt{\eta_i(t_k)}$ for each sensor. We thus call the ADPETC with this relative value transmission by ADPETCrel, where the increment and sign represent the relative value. We also implement the ADPETC with absolute value transmission, i.e. $\hat{\xi}_i(t_k) = \xi_i(t_k)$, which is named as ADPETCabs. However, since the fine static quantizers we install in our experimental setting have a quantization error negligible compared to the noise; only ADPETCrel can be considered to introduce some noticeable output quantization error.

For the ETM selection, basically we take two considerations. First, they must be discrete-time triggering mechanisms. Because of the sensor limitations, the plant output cannot be continuously monitored by the sensors and ETMs. Therefore, ETMs with discrete-time event condition validation are required. There are two ways to compensate the delay caused by this condition validation: designing a more conservative event condition or modifying the Lyapunov function, as we have discussed in Chapter 1. Because of the special dynamics of the WaterBox, which will be presented in Section 6.4, only the latter method can be used. Second, there must exist feasible parameters for each mechanism. Also because of the dynamics, we cannot find a feasible solution to the inequalities (50) in [48], therefore we did not apply the decentralized PETC therein to the WaterBox.

A network requires a protocol to schedule the packet transmissions from different nodes to avoid collisions. There are several candidates, as we have discussed in Chapter 1. However, to guarantee an upper bound on the transmission delays, in this work the

MAC protocols we designed for the different triggering mechanisms are TDMA based.

For these 4 triggering mechanisms, we are interested in the system performance, bandwidth occupation, and energy consumption under different parameters. Therefore, we choose to compare water level overshoot, switching time, sleep time, battery discharge, total number of the changes of the actuation, total valve movements, event condition violations, and total plant output transmissions as measures of performance. Details are presented in Section 6.5.

The rest of this chapter is organized as follows. Section 6.2 presents the designed MAC protocols for the corresponding triggering mechanisms. Following which is a system overview of the WaterBox in Section 6.3. Section 6.4 gives the controller design. The experiment results and analyse are shown in Section 6.5. This chapter is concluded in Section 6.6 with a brief discussion.

6.2. INCORPORATING ETC WITH THE MAC LAYER

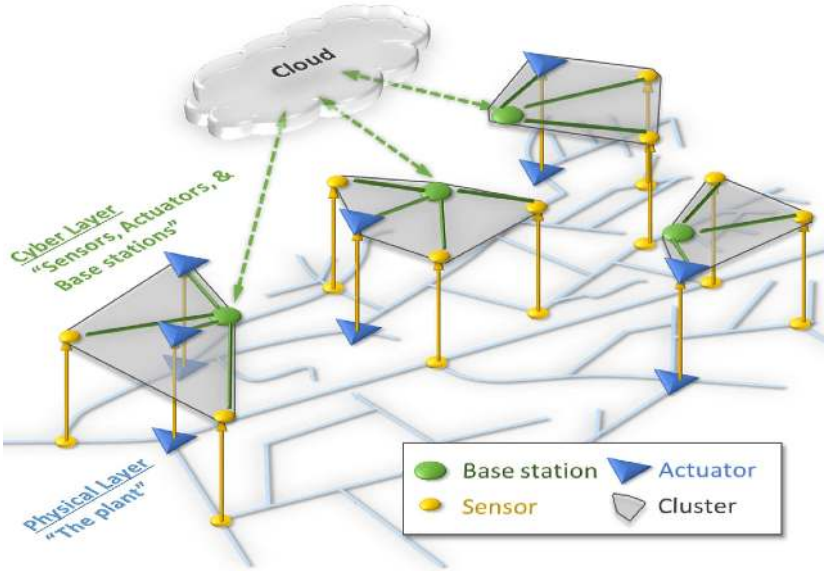

Figure 6.1: Network architecture.

In this section, we present the design and implementation of three innovative TDMA-based MAC protocols which enable the deployment of TTC, PETC, SDPETC, and ADPETC approaches accordingly: Control Time-Division Multiple Access (C-TDMA), Sychnronous Decentrlized Control Time-Division Multiple Access (SDC-TDMA), and Asynchronous Decentralized Control Time-Division Multiple Access (ADC-TDMA). The main benefits of these ETC-specific MAC protocols are: the optimization of communications by fully exploiting the behaviour and needs of ETC; the minimization of actuator node listening through duty cycling; and the off-load of the local controller node by allowing ***only*** one node to communicate with a base station per time.

For the proposed TDMA-based communication schemes, we assume a large scale CPS network infrastructure, such as in Figure 6.1, which represents a smart water network. In this architecture, the sensors and actuators are divided into clusters. Each clusters consists of only the sensors, actuators, and a base station which are involved in the control loop of an application for a specific area. The sensor/actuator nodes communicate in single-hop[1] with a base station and retrieve acknowledgement messages per transmission. Based on this architecture, we assume a star topology in which all the nodes of the same cluster can communicate with the base station (in which the controller is running) of the cluster. Contemporary long-range communication technologies, such as Low-Power Wide-Area (LPWA) [58], are representative examples of embodiments this architecture. Further, the controller which computes the control signals is executed in the base station. In this chapter, the terms controller and base station are used interchangeably. Our communication schemes are applied within each cluster while the the information exchange among different clusters is out of the scope of this work. Note that, despite the single-hop and centralized communication, the triggering of state transmission is distributed for decentralized ETC mechanisms.

6.2.1. SIMPLISTIC TDMA PROTOCOL

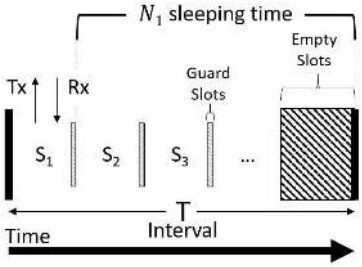

Figure 6.2: Simplistic TDMA MAC protocol.

TDMA is a channel access method for shared medium networks, which allows several users to share the same frequency channel. Specifically, time is divided into intervals T_i with length T, so-called super-frames. Each interval is split into smaller time slots S_j, with $\sum_{j=1}^{N} S_j \leq T$, where N is the number of sensor/actuator nodes which share the same channel[2]. In each time slot, only one predefined sensor/actuator node N_j can transmit (T_x) or receive (R_x) a burst of messages to and from a base station. Outside the timeslot S_j, N_j sleeps or executes other tasks depending on the hardware infrastructure and the provided ability to duty cycle. To avoid time violations of time slot bounds due to N_j possible clock drift, a guard slot forces the termination of communication before the

[1] We selected a single-hop communication because a dynamic multi-hop network infrastructure cannot provide guarantees for time delays; a critical factor for control systems.

[2] A super-frame can be divided into equal time slots that fully utilize the channel or to minimal slots which cover the application requirements and allow the communication to new nodes into the same channel.

end of each S_j. Figure 6.2 illustrates the communication scheme of a simplistic TDMA protocol.

Due to synchronous operation, a TDMA-based protocol (e.g. [46]) can guarantee tight bounds on delays which are critical for network control systems. On the other hand, synchronizing sensor/actuator nodes is considered as the main drawback of TDMA-based systems. However, state of the art solutions, i.e. Global Positioning System (GPS) clock synchronization technologies [92], ensure typical accuracy better than 1 microsecond by consuming ultra low power and without introducing communication overheads. This time synchronization technology has been tested widely, in term of robustness and performance, in real city-scale deployments, such as the smart water network in [51].

6.2.2. C-TDMA AND TTC & PETC

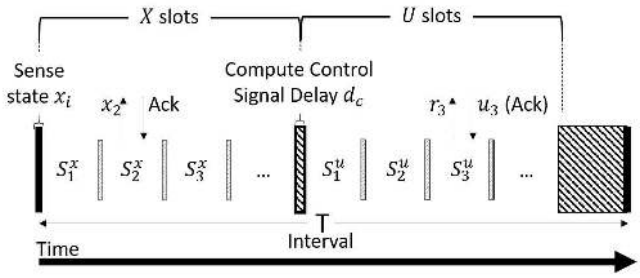

Figure 6.3: C-TDMA protocol.

C-TDMA is designed to enable TTC and PETC approaches (see Figure 6.3). In order to ensure the simultaneous state sampling, in the beginning of every interval T_i at time t_i, every node N_j has to retrieve a state measurement x_j from the available sensors. Then, the channel bandwidth is divided into two sets of time slots which are separated by a time delay:

MEASUREMENT SLOTS S_j^x (X-SLOTS)

Every sensor/actuator node N_j transmits x_j within the time slot S_j^x to the controller. Within each time slot only one successful message is required. Thus, the size selection of S_j^x is application specific and depends on the size of x_j (e.g. 2 Bytes per sensor) and the number of re-transmissions to achieve high reliability based on the selected hardware.

DELAY d_c

After receiving the complete sampled state by receiving $x_j, \forall j \in N$, a time delay is required to allow the computation of appropriate control signals u_j for every sensor/actuator node N_j. The length of this delay depends on the controller infrastructure and the complexity of the control model.

ACTUATION SLOTS S_j^u (U-SLOTS)

The last set of time slots is related to the control message retrieval by the sensor/ actuator nodes N_j. In each time slot S_j^u, node N_j transmits a request r_j for a control signal u_j

to the controller. Then, the u_j is piggybacked to the acknowledgement message. The benefit of the r_j request is two-fold: (a) off-loads the controller side and (b) reduces N_j listening time. Otherwise, the controller has to transmit or broadcast u_j continuously by blocking other tasks, while N_j has to be active in receive mode during the full length of the S_j^u slot until a successful control message retrieval. Further, this approach causes more energy savings for nodes with communication modules that consume the same amount of energy for transmission and listening, i.e. [101]. The length of S_j^u depends on the size of u_j signals.

Based on the above, the minimum interval size T_{min} can be defined by the length of X-slots, U-slots and delay d_c, and the number of the nodes. Further, the T_{min} can be considered as the maximum time delay of the system.

TTC and PETC are centralised approaches and are executed in the controller. In both cases, the system requires the transmission of the current state to the controller at every T_i during the X-slots. Then, in the TTC technique, the controller replies back in the U-slots of every interval T_i with a new u_j control signal. On the other hand, in PETC, the controller evaluates the event condition, as has been described in equation (2.14), and transmits the new u_j only if there is a violation. This behaviour allows PETC to save energy due to actuation reduction. Note that the base-station has only as extra overhead the evaluation of the event-triggered condition in equation (2.14). Therefore, the introduced computational complexity is minor compared to that of TTC systems.

6

6.2.3. SDC-TDMA AND SDPETC

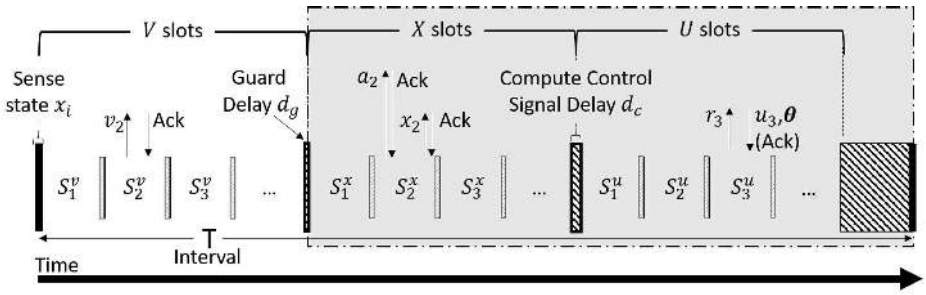

Figure 6.4: SDC-TDMA protocol for SDPETC approach.

SDPETC is a distributed technique and each sensor node is responsible for the state transmission decision in every T_i. The computation of control signals u_j and θ_j parameters require the **complete** knowledge of the system's state for the interval T_i in which a threshold violation has happened. For example, consider a system with three nodes, $\{N_1, N_2, N_3\}$, in which only two of the nodes, i.e. $\{N_2, N_3\}$, observe threshold violations. The controller requires the state from all the three nodes to compute the control signals. Using the same example, in a TDMA-based communication scheme in which each node is assigned to a pre-defined time slot S_j, node N_1 is precluded from transmitting its state by being unable to be informed about the threshold violations of N_2 and N_3. To overcome these limitations, SDC-TDMA introduces a new set of time slots S_j^v, the V-slots

(see Figure 6.4).

VIOLATIONS SLOTS S_j^v (V-SLOTS)
In the beginning of every T_i, each node retrieves a measurement and evaluates equation (4.8). Then, the result of each threshold v_j is transmitted by the corresponding node N_j to the controller at time slot S_j^v.

MEASUREMENT SLOTS S_j^x (X-SLOTS)
In the beginning of every S_j^x in X-slots, each node N_j asks the controller, by sending an a_j request, whether a threshold violation was observed in the V-slots. If no threshold violation occurred, the sensor node sleeps immediately until the next interval T_{i+1} (gray box in Figure 6.4). Otherwise, each node transmits each state x_j to controller, wait for the delay d_c and actuation slots, U-slots, follow.

DELAY d_c & ACTUATION SLOTS S_j^u (U-SLOTS)
Similar to the C-TDMA approach, after a delay d_c, each node requests the new control signal u_j from the controller. The u_j and the new threshold parameters θ_j, which is being calculated based on equation (4.8), are being piggybacked into the acknowledgement messages of U-slots.

Based on the above, SDC-TDMA sacrifices channel availability and increases the minimum interval length, T_{min} and consequently the system's maximum delay, by adapting V-slots into the TDMA scheme. However, in the case of threshold violation absence, the communication is being minimized significantly by avoiding the transmission of state x_j and the entire execution of U-slots.

6.2.4. ADC-TDMA AND ADPETC

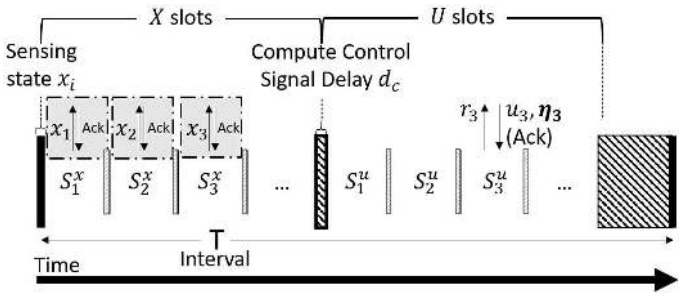

Figure 6.5: ADC-TDMA protocol for ADPETC approach.

Similar to SDPETC, the ADPETC approach transfers the communication decision making from the controller down to the sensor/actuator nodes. Additionally, due to its asynchronous feature, this approach increases the communication savings by avoiding the state transmission x_j from every node N_j in every interval T_i. The only overhead in the communication is the η_j update based on equation (3.15) and transmission to N_j. The value of η_j is being piggybacked with the control signal u_j in the acknowledgement message.

Specifically, the architecture of ADC-TDMA is similar to C-TDMA and consists of sensing task, X-slots, d_c delay, and U-slot (see Figure 6.5). In a S_j^x slot, the node N_j evaluates the threshold of equation (3.9). In the case of no threshold violation, the node N_j skips the communication and returns to sleep mode until S_j^u. For example, the communication in gray boxes of Figure 6.5 can be avoided completely or partially depending on the violations. Otherwise, N_j transmits to the controller: x_j in ADPETCabs or the increment m_j in ADPETCrel. Then, the controller computes the appropriate control signals and updates the local and global η based on equation (3.15) by using **only** the available x_j states.

In the U-slots, every node has to send a r_j request message to the controller, in order to be notified about a possible threshold violation from another node. Therefore, the violation of at least one threshold causes the update of u_j and η_j to be sent to every actuator node. The values of u_j and η_j are piggybacked to the acknowledgement message.

6.3. EVALUATION PLATFORM: WATERBOX

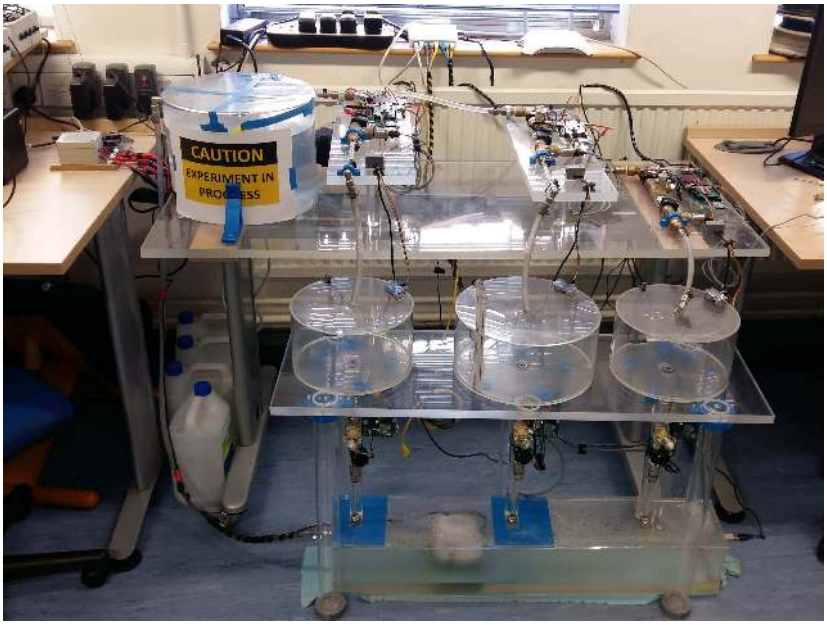

Figure 6.6: WaterBox testbed.

Smart water networks have been used as a proof of concept for our proposed framework. The WaterBox platform (see Figure 6.6) is a scaled version of such a water network [57] and developed to demonstrate real time monitoring and control by adapting innovative communication theories and control methodologies.

In this chapter, our aim is to demonstrate the event-triggered techniques on possible practical relative setups. Therefore, WaterBox was used as evaluation platform for our

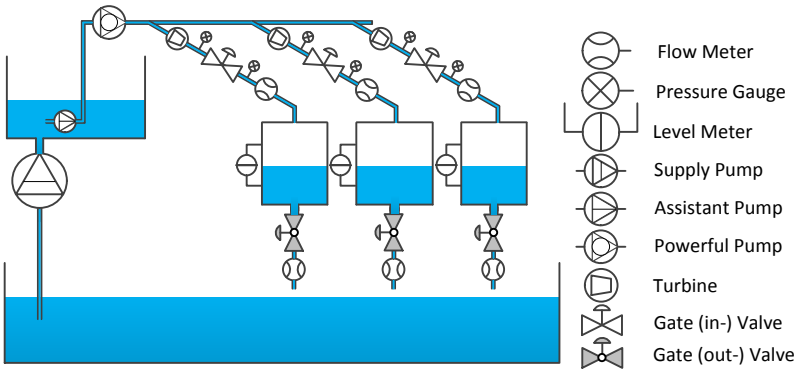

Figure 6.7: WaterBox schematic structure.

proposed ETC techniques and communication schemes. In the future, the same infrastructure will allow us to evaluate nonlinear ETMs.

6.3.1. WATERBOX INFRASTRUCTURE

A Water supply network structure consists of three individual layers: (a) storage and pumping, (b) water supply zones and District Meter Area (DMA), and (c) end users (water demand). While valves control flows and pressures at fixed points in the water network, pumps pressurise water to overcome gravity and frictional losses along supply zones, which are divided into smaller fixed network topologies (in average 1500 customer connections) with permanent boundaries, DMAs. The DMAs are continuously monitored with the aim to enable proactive leakage management, simplistic pressure management, and efficient network maintenance. WaterBox was designed to support this architecture as follows:

WATER STORAGE AND PUMPING

The structure of the WaterBox is shown as Figure 6.7. The WaterBox has a lower tank (i.e. ground, soil), an upper tank (i.e. reservoir, lake) and three small tanks (i.e. DMAs). The lower tank collects water from small tanks, and supplies water to the upper tank by an underwater bilge supply pump. This supply pump can supply enough water as the system requires. An assistant bilge pump and a new powerful pump are installed in series inside and after the upper tank respectively, and supply water to the small tanks. When the small tanks require more water supply, the assistant pump and powerful pump work together. When the small tanks require less water supply, only the assistant weak pump works. This behaviour emulates the day and night pumping operation of a water network in which the demand changes dramatically.

WATER SUPPLY & SENSOR/ACTUATOR NODE

The water from the powerful pump flows into three small “DMA" tanks via a pipe network. For the inlet each tank, a sensor/actuator node (see Figure 6.8), based on the Intel

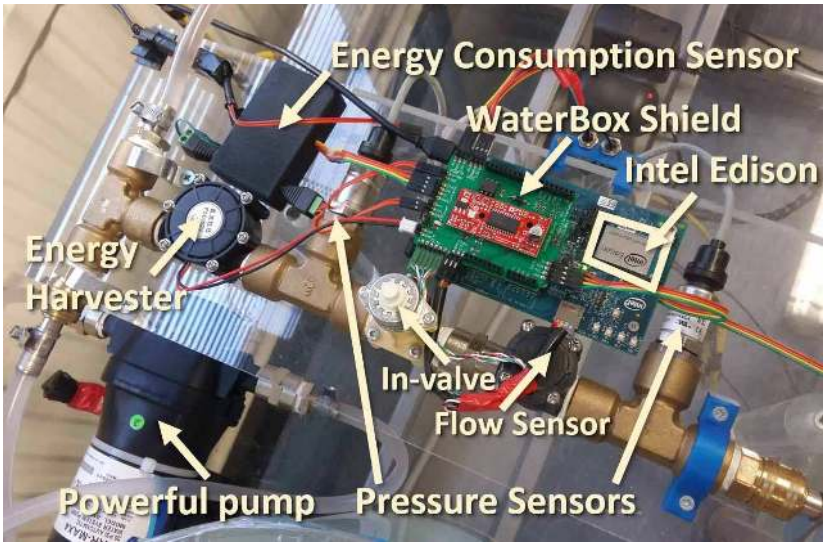

Figure 6.8: WaterBox sensor/actuator node.

Edison development board [55], controls the water flow though a motorized gate valve, so-called in-valve, and monitors the water flow, pressure (before and after in-valve) and the in-tank water level. Further, a turbine (flow-based energy harvester) is installed before each in-valve to harvest energy. To capture the total energy consumption of each sensor/actuator node, a custom made sensor module was created.

Remark 6.3.1. *In the WaterBox infrastructure, the sensors and actuator of each inlet are connected to the same node. However, our proposed communication schemes can be applied to non-collocated infrastructures.*

WATER DEMAND EMULATION

At the bottom of each small tank, there is an opening which enables the emulation of water consumption. A gate valve, so-called out-valve, is installed after each opening and can be controlled by a sensor/actuator node. The control of out-valves changes the outlet flow rate and facilitates the emulation of user's random water consumptions (i.e. external disturbance).

BASE STATION (CONTROLLER)

Every sensor node is connected to a local isolated WiFi network [3]. A laptop is used as a controller or base station and hosts a visualization application (see Figure 6.9) which presents in real time the current state of the system, allows the manual control of actuators, logs the retrieved messages, and enables our proposed communication schemes

[3] The isolation was achieved by disabling SSID operation (broadcast of WiFi availability to new users) from the router and selecting the low occupied communication channel for the nodes based on spectrometer experiments

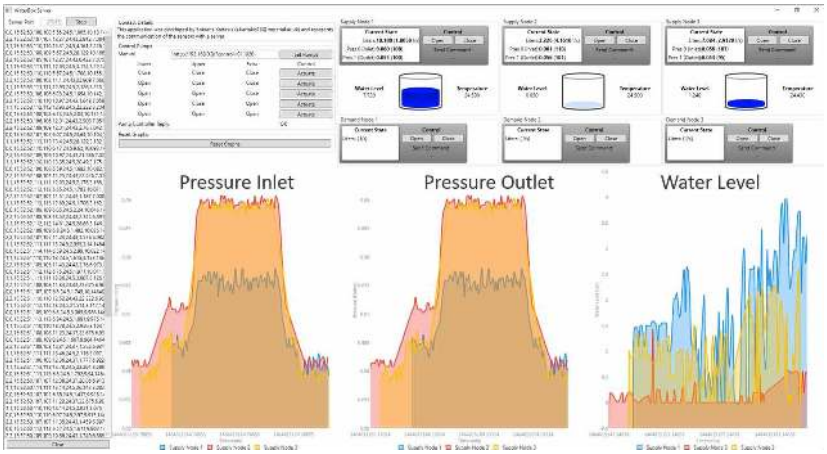

Figure 6.9: Local controller visualization application.

and ETC scenarios per experiment. Additionally, due to lack of an indoor GPS time synchronization, a Network Time Protocol (NTP) server is running in the local controller and ensures less than millisecond time synchronization accuracy among the nodes. To avoid the communication overhead of the NTP approach, each node executes the synchronization process only at the beginning of each experiment.

6.3.2. SYSTEM IDENTIFICATION & MODELLING

We apply Grey-Box identification [69] to generate the system model and to find the uncertain parameters. A first principles model is obtained following [108]. We identify independently models under both mode 1: only the assistant pump works and mode 2: both pumps work. Using the Matlab cftool, we generate fitting curves for the gate valve coefficient of each in-valve, the turbine efficiency, and the pump efficiency. These curves are used to compute the first principles model. Since our aim is to stabilize the water level of each tank $j \in \{1,2,3\}$ at the desired height h'_j, the model is linearised around this height. In this process, in order to simplify the simulation of the user water consumption, we keep the out-valves open, thus, constant out flow rates can be assumed.

6.4. HYBRID CONTROLLER DESIGN

To evaluate the proposed ETC-based communication schemes, the following **control scenario** was used: *"Control in-valves to stabilize the water level of the small 'DMA' tanks to a certain level ensuring pressure and flow bounds. Enable mode 2 (weak and powerful pump) only if the system is away from the target levels. Switch to mode 1 (weak pump) only when the system is close to the reference state to guarantee efficient low pressure and flow operation."*

In the design of the controller, the following limitations need to be considered:

1. *Saturation of the actuators:* The maximum open level of one in-valve is 360°, while the minimum is 0°.

2. *Actuator quantization:* Due to the limitation of the valve's control components, their open levels can only be changed in steps of 10°. Therefore, small disturbances may result in dramatic changes of actuations due to this actuator quantization.

3. *Over-pressure protection:* Due to mechanical limitations of the pipe network, there is a maximum allowable pressure for the pipe network.

Since the height of the water levels have a direct effect on the QoS, the closed-loop system requires a fast response; however, since the size of the small tanks are limited, the overshoot should simultaneously be constrained. Experiments show that, in mode 2, the pipe network may be over pressured, when the open level of the in-valves, defined by α_j^{in}, cannot satisfy:

$$\sum_{j=1}^{3} \alpha_j^{in} \geq 180^\circ. \tag{6.1}$$

Overshoot and disturbances could make condition (6.1) be violated. While in mode 1, there is no such constrain, that is, even all three in-valves are totally closed, the pipe network will not be over pressured. Therefore, filling the small tanks in mode 2 and switching to mode 1 when (6.1) is violated is required. Also experimentally, we observe that, when the system is in mode 1, the pump may not provide enough water supply to the small tanks even at the maximum open level, i.e. $\alpha_j^{in} = 360^\circ,\ \forall j \in \{1,2,3\}$. Therefore, switching back to mode 2 when the water in the tanks reaches some pre-defined low levels is necessary. To support this mode switching, we define $\underline{h} := \begin{bmatrix}\underline{h}_1 & \underline{h}_2 & \underline{h}_3\end{bmatrix}^{\mathrm{T}}$, $\underline{h}_j < h'_j$, $j \in \{1,2,3\}$, as the lower water levels. If $\exists j \in \{1,2,3\}$ such that $h_j(t) \leq \underline{h}_j$, the system switches from mode 1 to mode 2. With carefully chosen $\underline{h}_j$ and properly designed controllers, this violation can only happen in mode 1. Further analysis shows that, (6.1) can only be violated when $h_j(t) > h'_j$, which together with the fact that $\underline{h}_j < h'_j$ precludes Zeno behaviour.

Let $\vartheta \in \{1,2\}$ represents the corresponding system mode. The linearised switched model and switched controller of WaterBox are described by:

$$\dot{\xi}(t) = A \times (\xi(t) + h') + B_\vartheta v(t),\ \vartheta = \{1,2\}, \tag{6.2}$$

$$v(t) = S(-K_\vartheta \xi(t) + \bar{\alpha}_\vartheta^{in}),\ \vartheta = \{1,2\}, \tag{6.3}$$

where $\xi(t) = \begin{bmatrix}\xi_1(t) & \xi_2(t) & \xi_3(t)\end{bmatrix}^{\mathrm{T}}$, $\xi_j(t) := h_j(t) - h'_j$, $j = 1,2,3$ are the system states, $h_j(t) \in \mathbb{R}$ are the water levels, and $h'_j \in \mathbb{R}$ are the reference water levels with

$$h' = \begin{bmatrix}h'_1 & h'_2 & h'_3\end{bmatrix}^{\mathrm{T}},\ v(t) = \begin{bmatrix}v_1(t) & v_2(t) & v_3(t)\end{bmatrix}^{\mathrm{T}},$$

$v_j(t) := \alpha_j^{in}$, $j = 1,2,3$ are the system control inputs and $\bar{\alpha}_\vartheta^{in}$ are the equilibrium open levels of the in-valves per operation mode ϑ; S is a map $\mathbb{R}^m \to \mathbb{R}^m$ representing actuator saturation and quantization, that is

$$S(s_j) := \max\left\{\min\left\{10\left\lfloor 10^{-1} s_j \right\rfloor, 360^\circ\right\}, 0^\circ\right\}.$$

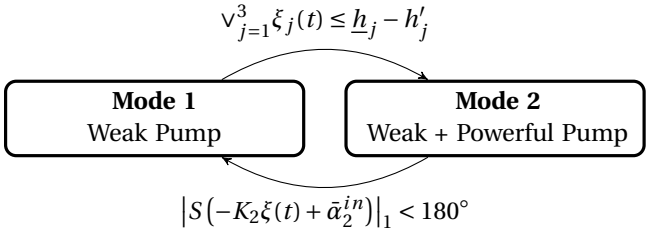

Figure 6.10: Hybrid controller state automaton.

Then, the WaterBox hybrid controller state automaton is illustrated in Figure 6.10.

From the Grey-Box identification procedure, the system parameters are defined as follows. Due to the physical structure of the tanks and the low sensitivity of the flow meters, the flow rates are identified as constants, i.e:

$$A \times (\xi(t) + h') = -10^{-4} \times \begin{bmatrix} 5.809 & 3.554 & 5.102 \end{bmatrix}^{\mathrm{T}}.$$

And

$$B_1 = 10^{-5} \times \begin{bmatrix} 0.1436 & -0.0170 & -0.0164 \\ -0.0098 & 0.1060 & -0.0100 \\ -0.0139 & -0.0139 & 0.1492 \end{bmatrix},$$

$$B_2 = 10^{-5} \times \begin{bmatrix} 0.7666 & -0.0493 & -0.0457 \\ -0.0274 & 0.5848 & -0.0279 \\ -0.0393 & -0.0432 & 0.7865 \end{bmatrix}.$$

Given $h'_j = 0.06$ and $\underline{h}_j = 0.03$, $\forall j \in \{1,2,3\}$. Assume that there is no actuator saturation and quantization, thus $\bar{\alpha}_1^{in}$ and $\bar{\alpha}_2^{in}$ are computed by solving $A \times (\xi(t) + h') + B_\vartheta \bar{\alpha}_\vartheta^{in} = 0$:

$$\bar{\alpha}_1^{in} = \begin{bmatrix} 503.5950 \\ 422.4378 \\ 428.5839 \end{bmatrix}, \bar{\alpha}_2^{in} = \begin{bmatrix} 84.5099 \\ 68.2069 \\ 72.8442 \end{bmatrix}.$$

Since $A \times (\xi(t) + h')$ is compensated by $B_\vartheta \bar{\alpha}_\vartheta^{in}$, the A in (2.7) can be treated as a zero 3×3 matrix. The controllers designed are given by:

$$K_1 = \begin{bmatrix} 99950 & 3029 & 872 \\ -3014 & 99940 & -1679 \\ -922 & 1652 & 99982 \end{bmatrix},$$

$$K_2 = \begin{bmatrix} 9998.5 & 167.1 & 41.0 \\ -166.6 & 9997.9 & -116.0 \\ -43.0 & 115.3 & 9999.2 \end{bmatrix}.$$

The designed controller is stable in both mode 1 and 2 because $-B_1K_1$ and $-B_2K_2$ are Hurwitz matrices. Further, due to the long dwell time of the system, the closed loop retains stable.

For the presented ETMs, once the inequalities shown in (2.15), (3.17), and (4.11) are feasible, the system is stable either if $A = 0$ or $A \neq 0$. However, the specific dynamics may not result in a large difference regarding the effects of ETC on communications. In our future work, further analysis and tests will be conducted with different system dynamics for more conclusive results. Note that, since the linearised model, switching condition, and input quantization are the same for all the ETMs, the comparison is fair.

6.5. EVALUATION

This section summarizes the experimental results of more than 40 cases conducted in WaterBox, with each case being repeated 10 times to evaluate our proposed communication schemes for the different ETC strategies. Each experiment executes the same control scenario (as described in Section 6.4) and the total process lasts between 7 and 10 minutes, including the water state initialization, the execution of experiment, and data logging from sensor/ actuator nodes and local controller.

6.5.1. EVALUATION SETUP

Table 6.1: Communication parameter evaluation setup.

	Parameter	Value	Description
Packet Size	x_j	36 Bytes	Node ID Timestamp (in msec) Inlet pressure Outlet pressure Flow rate Total water volume Distance from surface Energy consumption Energy harvesting
	$Ack \mid r_j, a_j$	1 Byte	0 or 1 | Node ID
	u_j, η_j, θ_j	2 Bytes	Control signal and DETC parameters
	m_j	4 Bytes	State delta
Time Duration	S_j^x	80 msec	X slot size
	S_j^u, S_j^v	50 msec	U and V slot size
	d_c	10 msec	Control decision delay
	d_g	5 msec	Threshold violation decision delay
	Guard slot	1 msec	Forced task termination time

The proposed communication protocols of Section 6.2 were deployed to the WaterBox sensor/actuator nodes by wrapping the functionality of the Intel Edison WiFi module. Table 6.1 presents the configuration of the communication parameters. Based on the predefined packet sizes of the specific hardware infrastructure, a set of experiments

was conducted to determine reliable time slot and guard delay sizes.

Table 6.2: Parameters of triggering strategies.

Method	T (sec)	Parameter	Value
TTC	**0.5**, 1, **2**	-	-
PETC	**0.5**, 1, **2**	σ	0.05, 0.1, **0.2**
SDPETC	1, **2**		
ADPETC (abs & rel)	**0.5**, 1, **2**	μ	0.75, **0.95**
		ϱ	**85**, 120

Based on the Table 6.1 timing parameters and the Section 6.2 time slot analysis, the minimum interval size T_{min} for C-TDMA and ADC-TDMA has to be more than 406 msec while for SDC-TDMA more than 564 msec (because of the V-slots). Thus, we evaluate TTC, PETC, and ADPETC (with absolute or reference value) with interval size $T = 0.5, 1, 2$ and $T = 1, 2$ sec for SDPETC. The selected interval sizes and the rest parameters of the ETC strategies are listed in Table 6.2. The σ and ρ ETC parameters are chosen by finding feasible solutions of the corresponding algorithms (2.15) and (3.17), while μ is tuned experimentally. Note that, Assumption 3.3.1 holds for all those T listed in Table 6.2.

In the first set of experiments, we examine the impact of the ETC parameters (σ, μ, and ϱ) to the performance of the system. A fixed interval size $T = 1$ was used with all the different combinations of ETC parameter values of Table 6.2. Another set of experiments was conducted to explore the effect of T in the behaviour of the system. Keeping $\sigma = 0.2$, $\mu = 0.95$, and $\varrho = 85$ constant, all the experiments were re-executed with $T = 0.5$ and $T = 2$ (Table 6.2 bold text). To ensure the validity of the evaluation results, each experiment was repeated 10 times[4] for each different combination of ETC parameters and T. Mean values are used to illustrate the evaluation results. The data was captured from the nodes and controller for the period of time between the beginning of each experiment ($t_0 = 0$) until a fixed end time ($t_{end} = 110s$), which guarantees the system turns to mode 1 and converges to steady state, denoted T_{exp}.

6.5.2. EXPERIMENTAL RESULTS

In this section we compare TTC, PETC, SDPETC, ADPETCabs and ADPETCrel experimental results, in terms of:

- *Water Level Overshoot:* the maximum water level during the experiment. This parameter indicates the system's maximum state overshoot which is critical for water network asset safe operation.

- *Switching Time (t_{sm}):* the duration between experiment start time t_0 and first switch mode time t_{sm}, as described in condition (6.1). The time to mode switching is employed as an estimate of the system settling time (due to its ease of detection in our setup).

[4]The number of experiment repetitions was selected experimentally by analysing the variance of the results (i.e. under 2% of mean).

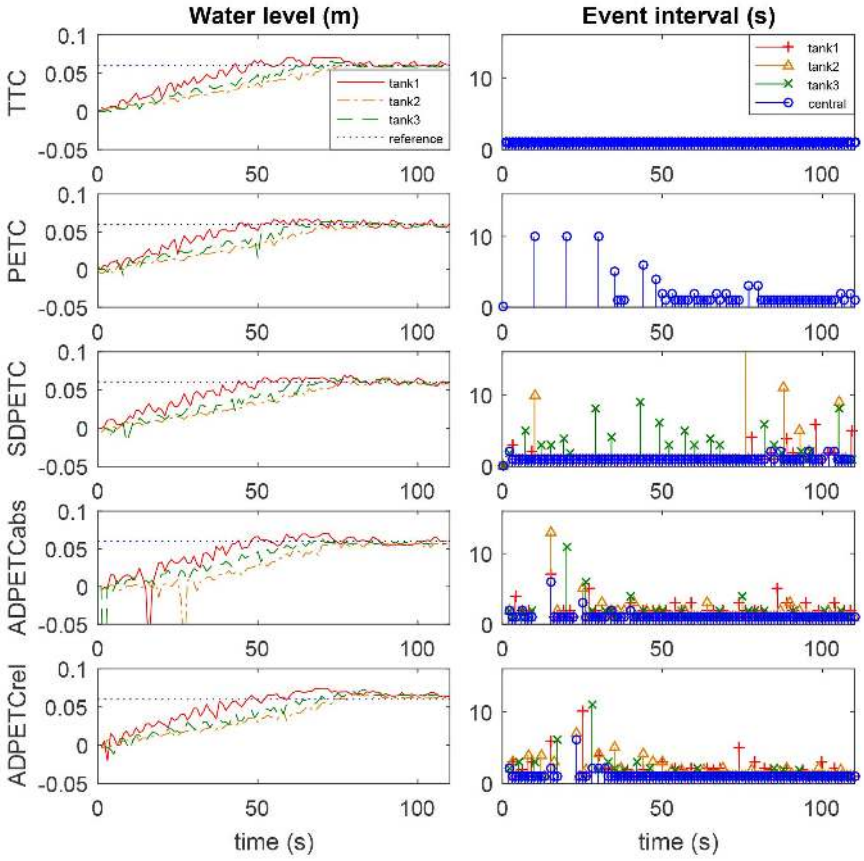

Figure 6.11: Experimental results. Note that, for SDPETC, the maximum event-interval of small tank 2 is 66 sec.

- *Sleep Time:* the total sleep time of all the nodes. This parameter evaluates the use of the bandwidth and CPU in the sensor/actuator node.

- *Discharge (Energy Consumption):* our custom made sensor module retrieves current measurements c_n in mA at a fixed frequency of 10kHz. The energy consumption of a specific time period Δt in seconds and with average current measurements over this period $\langle C \rangle_{\Delta t}$ can derived from $E(\Delta t) = \langle C \rangle_{\Delta t} \cdot \frac{\Delta t}{3600}$. We used a hardware average to ensure the continuity of the current measurements and validated our instrument against a calibrated reference [60]. The energy consumption includes the consumption because of the communication, sensing, actuation, and idle mode. We present two discharge values, i.e. the whole discharge and discharge without sleep time. Based on these parameters, the battery lifetime of different hardware infrastructures can be implied.

- *Actuations:* the number of valves' changes, i.e. $\sum_{\forall t_k \in [t_0, t_{end}]} \sum_{j=1}^{3} \mathscr{Y}_j(t_k)$, where:

$$\mathscr{Y}_j(t_k) = \begin{cases} 1, \text{ if } \alpha_j^{in}(t_k) \neq \alpha_j^{in}(t_{k-1}) \\ 0, \text{ otherwise.} \end{cases}$$

  where t_k is defined in (2.12). The amount of actuations indicates the lifetime of actuators which is vital for industrial deployments. For example, in water networks, an increase to the valve actuations implies fatigue enhancement of mechanical parts and frequent expensive maintenance.

- *Valve Movement:* the total number of valves' movements in degrees between two consecutive changes, i.e. $\sum_{\forall t_k \in [t_0, t_{end}]} \sum_{j=1}^{3} |\alpha_j^{in}(t_k) - \alpha_j^{in}(t_{k-1})|$. Combined with the number of actuations, the valve movement can be used to estimate physical system lifetime.

- *Violations:* the total number of event condition violations. For each violation the local controller transmits a control signal u_j to each node i.e. three times. Therefore, the total transmitted control signal are equal to 3 times the violations. This metric indicates the communication requirements of actuators. Violations and actuations are different values because the local controller can produce the same consecutive control signal.

- *State Transmissions:* the total number of state x_j transmissions to local controller. This metric indicates the communication requirements of sensors. Both violations and state transmissions represents the total communication requirements of the system.

Figure 6.11 shows an example of raw data as captured from the nodes and the controller. Next, we analyse the energy consumption trends compared to sleep time for different hardware infrastructures, the effect of ETC parameter setup and interval length T to the performance of the system, and we aggregate the savings of ETC approaches against the vanilla scenario of TTC.

ENERGY CONSUMPTION AND SLEEP TIME

The hardware infrastructure of a WaterBox node consumes more energy in sleep mode compared to work mode. During sleep mode, our process yields priority to the background tasks of the operating system which are more energy hungry. In order to generalize the results to different hardware infrastructures which support lower energy consumption during sleep mode (i.e. deep sleep), we provide the upper and a lower bound of energy consumption. The upper bound presents the real experimental results based on our node while the lower bound represents an estimation of energy consumption of a node which supports deep sleep[5]. The need of energy consumption range can be clearly seen in Figure 6.12c and 6.12d, Figure 6.13c and 6.13d. In spite of the sleep time increase in all cases, the upper bound of energy consumption increases proportionally

[5] We calculated the lower energy consumption by subtracting the energy consumption during sleep mode from the total

(the opposite holds for the lower bound). Additionally, SDPETC is expected to consume more energy than the others because of the V-slots. However, Figure 6.12c and 6.12d illustrate the opposite trend for the upper bound (opposite for lower bound) due to the energy hungry sleep mode. Overall, ADPETCabs and ADPETCrel consume the least energy compared to the other approaches. In spite of the uses of the same communication scheme, PETC performs slightly better than TTC of actuation reduction (quantitative results will presented later on).

EFFECT OF ETC PARAMETERS

Figure 6.12 presents the effect of different parameters, e.g. σ, ρ, μ with the same interval length $T = 1$.The experiment results follow the trends shown in the theory. In PETC and SDPETC, a smaller σ forces the system to be more conservative and leads to more event condition violations (Figure 6.12g) and consequently to more actuation (Figure 6.12e) and energy consumption (Figure 6.12d). For the same reason, in the decentralized SDPETC, the state transmission reduces with bigger σ (Figure 6.12h).

Table 6.3: Savings compared to TTC (%) total experiment time, i.e. $[0, t_{end}]$, with $\sigma = 0.2, \rho = 85$, and $\mu = 0.95$

Approach	PETC	SDPETC	ADPETCabs	ADPETCref
Water level overshoot	3.18	1.24	2.44	-19.72
Switching time	-0.69	-0.55	3.47	-20.53
Discharge	0.97	11.03	4.74	3.28
Discharge include deep sleep	1.1	-57.6	6.9	13.2
Actuation	18.6	8.2	27.2	9.7
Aggr. valve movement	-1.7	1.5	7.5	30.5
Violation	42.8	21.5	44.8	51.8
State transmission	0	21.5	51.6	56.0

Table 6.4: Savings compared to TTC (%) until mode switching time, i.e. $[0, t_{sm}]$, with $\sigma = 0.2, \rho = 85$, and $\mu = 0.95$

Approach	PETC	SDPETC	ADPETCabs	ADPETCref
Water level overshoot	3.15	1.67	3.02	-19.72
Switching time	-0.69	-0.55	3.47	-20.53
Discharge	1.34	10.97	9.22	-15.23
Discharge include deep sleep	2.4	-66.9	11.9	-4.5
Actuation	30.3	10.4	34.7	14.4
Aggr. valve movement	17.3	8.3	24.1	22.6
Violation	55.2	14.6	57.0	49.1
State transmission	-0.7	14.6	63.9	54.5

In ADPETC, a bigger ϱ has similar effect as a smaller σ in PETC. This can be clearly seen in Figure 6.12e and 6.12g, in which bigger ϱ causes more actuations and violations respectively. A bigger μ can result in more frequent threshold updates, but maintains the threshold less conservative, and thus, the sampling errors can be enlarged. Additionally, Figure 6.12g shows that μ has greater impact on violations than σ and ϱ parameters.

IMPACT OF INTERVAL LENGTH SELECTION

Figure 6.13 illustrates the impact of different interval lengths, in which the same pre-designed Lyapunov converge rate can be guaranteed, for the same set of rest of the parameters, e.g. σ, ρ, μ. It can be clearly seen in Figure 6.13 that smaller interval T results in better performance but worse energy consumption. The water level overshoots are almost the same because of the actuator quantization. Larger sampling times always result in longer convergence times and longer sleeping times. Similarly, the upper bound discharge indicates this trend; longer sleep time leads to higher energy consumption due to the energy hungry operating system background tasks. Oppositely, the lower bound of discharge shows that hardware infrastructures with deep sleep consume significant lower energy for larger interval T due to long sleeping time.

SAVINGS COMPARED TO TTC

Table 6.3 and 6.4 show the total savings of different ETC techniques against TTC for the time period $period_1 = [0, t_{end}]$ (total experiment time) and $period_2 = [0, t_{sm}]$ (time until switching mode) respectively. We provide this data separately due to the existence of the switched controller and the different behaviour of the two modes.

In $period_1$ PETC performs similarly to TTC with the difference of reduced actuations and violations by 18.6% and 42.8% respectively. In spite the saving, PETC causes more valve movements than TTC. The SDPETC is more conservative than the centralized PETC, with a result, the lower savings in terms of violations. However, SDPETC reduces the valve movements and the state transmissions due to the decentralized architecture. ADPETCabs outperforms all the other approaches because of the asynchronous behaviour, reducing significantly the violations, state transmissions and actuations by achieving 44.8%, 51.6%, and 27.2% savings respectively. ADPETCrel occurs similar actuation and communication saving with ADPETCrel but with the trade-off of lower performance in terms of water level overshoots and switching time. As has been described in Chapter 3, this happens because the ADPETC with reference value updates introduces an extra error, known as maximum dynamic quantization error. However, this extra error allows this triggering mechanism to be more robust against noise than any of the other mechanisms with pre-designed maximum dynamic error.

In $period_2$, some ETC approaches deviate compared to the total savings. For example, in PETC approach, $period_2$ reveals higher actuation savings than $period_1$. The reason is that in mode 1, the weak pump is unable to supply the tanks with enough water and the system deviates from steady state continuously. Thus, event condition violations are being increased and often large valve movements are required. SDPETC and ADPETCabs have a smaller overshoot than the other ETC approaches. Again ADPETCabs outperforms the other ETC approaches achieving outstanding violation (57%) and actuation (35%) savings.

6.6. CONCLUSIONS

In this chapter, we have proposed duty-cycling of the sensing and actuator listening activities and enabled decentralized ETC techniques introducing innovative communication schemes. Specifically, we designed and implemented three new MAC layers, which enable the application of four different periodic centralized and decentralized event-

triggered control approaches. By implementing our proposed communication schemes in the WaterBox testbed [57], we provided experimental results from more than 400 experiments.

Based on the experimental results, ETC approaches can introduce considerable benefits into industrial deployments. Due to the outstanding decrease of actuations either in number (up to 35%) or size (i.e. for valve movement up to 24%), the ETC techniques can increase the robustness, resilience, and lifetime of physical plants and actuators significantly. This increase can lead to significant maintenance cost reduction by postponing expensive replacements of plant assets.

WaterBox consists of energy hungry sensor/ actuator nodes to allow computational intensive algorithm deployments. An optimal hardware infrastructure will reduce the energy consumption even more than the evaluation results. Intuitively, the level of energy reduction will be closer to threshold violations (up to 57%) and state transmission (up to 64%) savings which indicate the actuator and sensors communication requirement respectively.

An additional benefit of applying periodic centralized or decentralized ETC approaches is the reduction of sensing rate. Continuous measurement retrieval from high energy demanding sensors (e.g. the water content sensor [29] which consumes 570 mJ per measurement) may lead to higher energy consumption than the communication process (e.g. low power wide area communication modules in [58] which consumes 1.5 to 42 J per 10 bytes). Further, based on our experimental results, higher sensing rates do not guarantee higher control performance.

The experiment results have clearly shown that, reducing listening time for the applied ETC is desirable to further reduce energy consumption. Applying efficient scheduling of the model's listening to the channel, based on properly constructed communication's traffic models, see e.g. Chapter 5, this can be achieved.

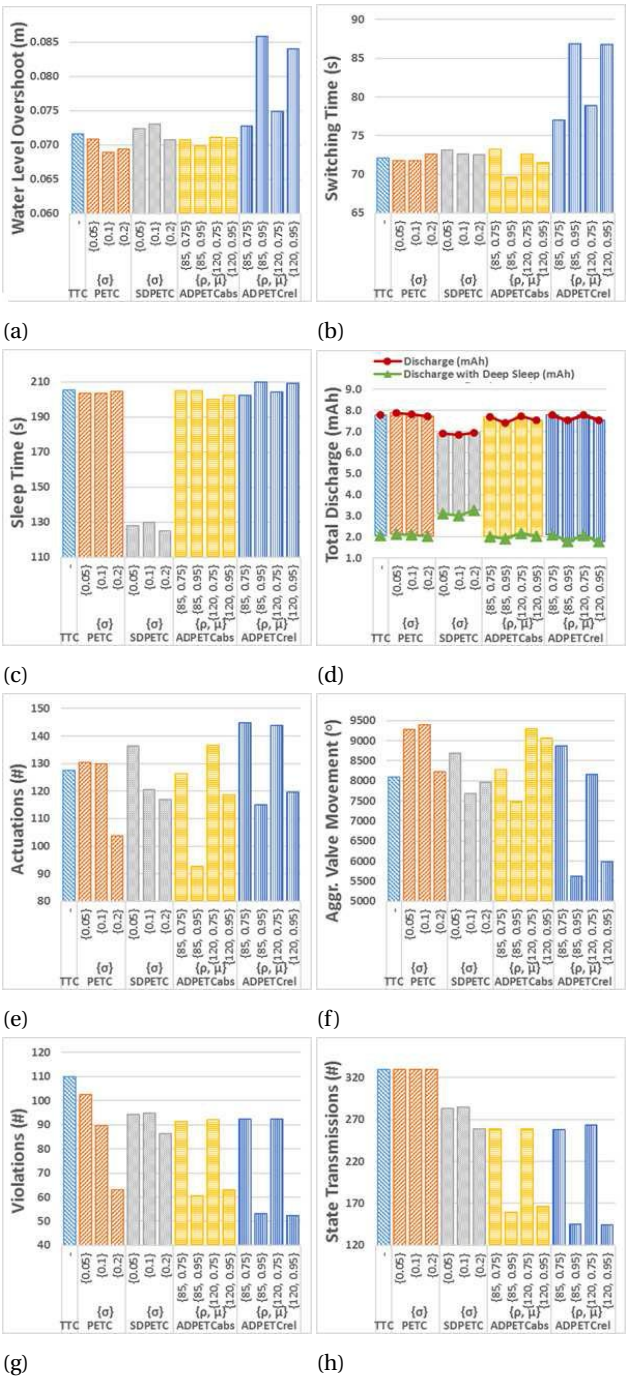

Figure 6.12: Impact of ETC parameters (σ, μ, ρ) in: (a) water level overshoot, (b) switching time, (c) sleep time, (d) discharge, (e) actuations, (f) valve movement, (g) violation, and (h) state transmissions.

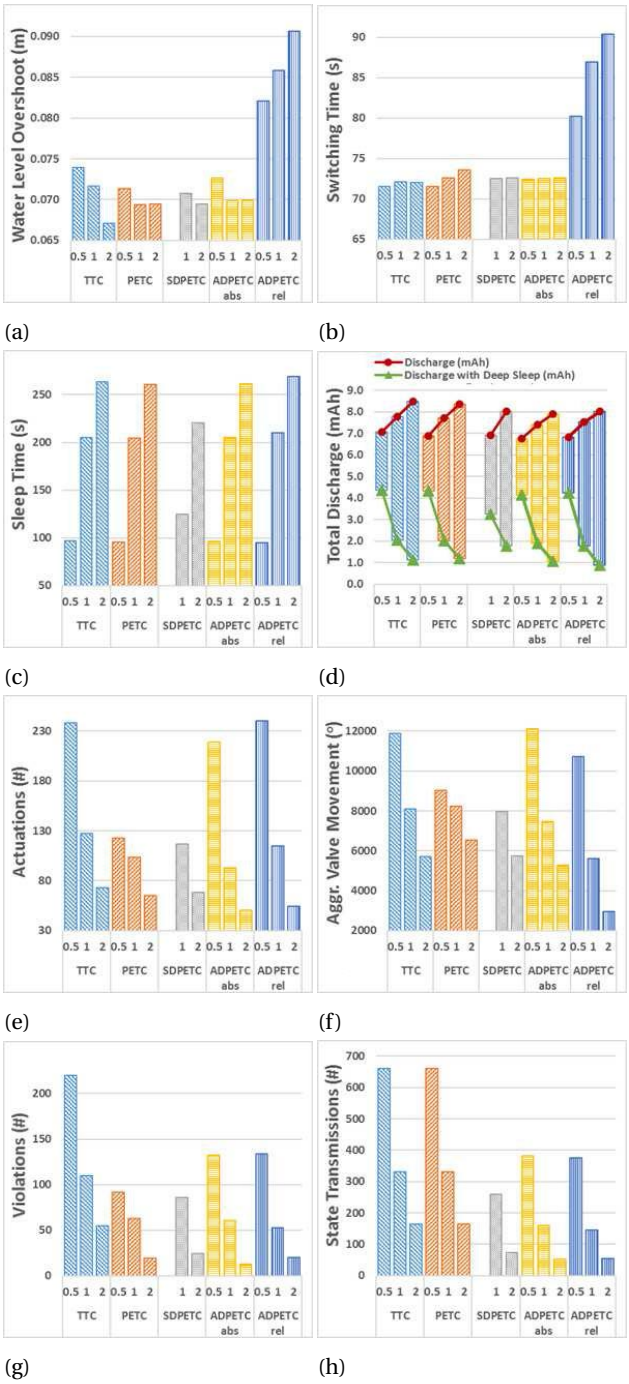

Figure 6.13: Impact of interval length T in: (a) water level overshoot, (b) switching time, (c) sleep time, (d) discharge, (e) actuations, (f) valve movement, (g) violation, and (h) state transmissions.

7

CONCLUSIONS AND FUTURE RESEARCH

This chapter summarizes the thesis and briefly discusses the main contributions presented in the manuscript. We also present open challenges and give recommendations for further research.

7.1. SUMMARY OF CONTRIBUTIONS AND CONCLUSIONS

In this thesis, we have discussed one major problem faced while designing a WNCS: how to guarantee pre-designed stability and performance with bandwidth and energy constraints. To enable a desirable allocation of WNCS, it is meaningful and important to study these control problems. Also we fill an additional gap in the literature by making experimental comparisons between different ETC systems, especially the decentralized ones, in a real physical plant.

In this thesis, we present two ETC mechanisms: ADPETC and SDPETC; an abstraction of PETC to model the communication's traffic it generates (with the goal to facilitate its scheduling); and the work and experimental results on the WaterBox.

We present a detailed summary of each piece of work.

- **ADPETC.** We introduce ADPETC as a version of ETC that combines periodic sampling, decentralized ETC with asynchronous communications, and dynamic quantization. It is designed for output-feedback systems with the transmissions of the controller output also included in the ETM. ADPETC can reduce the number of transmissions from each node, packet length of each transmission, listening time of the nodes, and working time of the sensors, thus providing savings in both bandwidth occupation and energy consumption. The upper bound of each packet is also presented for actual implementation design. Meanwhile, given a set and corresponding performance function, the UGpAS of that set and $\mathscr{L}_2$ performance can be guaranteed.

- **SDPETC.** We introduce SDPETC as another version of ETC. It realizes decentralized and periodic event-triggered condition validation. The local event is thus triggered only based on the local information. However, all the sensors are required to update the samplings synchronously after an event. Besides, this mechanism can only work for state-feedback systems. Without disturbances, the system state is shown to converge to the origin exponentially. This proposed mechanism can also reduce both bandwidth occupation and energy consumption.

- **Abstraction of PETC traffic.** A detailed construction of the power quotient system for the communication's traffic model of the original PETC implementation is also presented. With this traffic model, the upper and lower bounds of the event intervals and the reachable set from each state region can be computed. These results can be used to schedule the actions of a PETC implementation to further reduce the bandwidth occupation and energy consumption, under the mild practical requirement that the disturbances are both $\mathscr{L}_2$ and $\mathscr{L}_\infty$.

- **WaterBox.** We extend the WaterBox by adding a controller to it, making it a testbed for different controller triggering mechanisms. We identify the plant, and design a hybrid controller to stabilize the water levels at pre-designed heights. We apply four triggering mechanisms to this implementation, and correspondingly we design four customized TDMA based communication protocols for each triggering mechanisms. Experimental results have shown ETC's advantages on industrial deployments compared with TTC on bandwidth occupation and energy consumption measurements. Further analysis has shown that different ETC mechanisms have their own most suitable cases. For example, PETC has the most similar behaviors compared to TTC, but with considerable battery discharge savings considering deep sleep; SDPETC has the most battery discharge reductions; ADPETC has the least wireless bandwidth occupation, and obvious battery discharge savings. Additionally, ADPETC with dynamic quantization has the least valve movements, therefore it is the most machine-friendly triggering mechanism compared with all the others. Moreover, if we could customize the transmitted packet, i.e. with various length, ADPETC with dynamic quantization should perform even better.

7.2. RECOMMENDATIONS FOR FUTURE RESEARCH

As a result of the investigations presented in this thesis, we have identified a number of future challenges worth further investigation. These are summarized in the following items:

- **Security constraints.** Besides the addressed challenges of improving the resource consumption efficiency for WNCS with respect to bandwidth and energy constraints, anther main challenge a NCS may face is the security challenge. Because of the introduction of the wireless channel, WNCSs face more severe security problems due to easily disrupted communication [102]. Two main types of attacks for CPSs are often considered: deception attacks and Denial of Service (DoS) attacks. Deception attacks, as the name indicates, attempt to deceive the system to manipulate the behaviours of the CPS to satisfy the attackers' aims. DoS attacks

aim at completely disrupting the operation of the attacked system. In a feedback closed-loop system, both attacks can pollute the feedback channel to prevent the system from being stable. Some pieces of work have been done on analysing the influence of DoS attacks and designing anti-attack strategies, see e.g. [3], [9], [13], [26], [27], [28], [36], [68], [75], [78], [82], [84], [86], [89], [93], [97], [98], [112], [114], and [115]. However, the analysis of the effect of the deception attacks mostly concentrate on SCADA systems, e.g. [13], [26], [36], [68], [75], [78], [82], [89], and [97]. When looking at ETC implementations, since the transmission happens only when necessary, lack of enough information redundancy poses a challenge to make the system robust enough against these attacks. Therefore, an interesting challenge for research is to reduce the transmission and energy consumption while still guaranteeing some level of security.

- **The extension of the WaterBox.** We encourage the WNCS community to construct similar testbeds in order to investigate and validate other theoretical approaches. Besides validating different triggering approaches, there are three challenges in extending the WaterBox. (1) In the WaterBox, the control objective is to guarantee the water levels at some pre-designed heights aiming at guaranteeing a required QoS. However, in a real water distribution system, to guarantee QoS, stabilizing the water levels is not enough. Additional considerations should be included, as e.g. the pressure in the water pipe system, to make the system more realistic. Therefore, another relevant challenge is how to construct and analyse a complex model including all these considerations. (2) Moreover, the water consumption in practice is dependent on time, which currently is only considered as constant. Including the water consumption estimation into the control strategy to supervise the controller is also an interesting extension. (3) In the current testbed, the wireless network is built based on WiFi. However, this may not be a suitable choice for plants with very large physical scales. Therefore, it would be helpful to validate results over these protocols for wireless networks, e.g. LoRaWAN [91].

- **Abstraction of PETC traffic.** Following the conclusions of Chapter 6, we believe it is meaningful to enrich the construction approaches of communication's traffic models for different ETC. Currently, our communication's traffic model only considers an isolated system. It is a great challenge to reduce the transmission and energy consumption of all the systems sharing the same wireless network. For WNCSs employing decentralized ETC, it is also a challenge to construct the traffic model for each sensor node to capture the local timing behaviour, by either global information or even only local information. Moreover, it would be interesting to construct traffic models generated by an ETC implementation under various attacks.

- **Observers for ETC systems.** There are already large amounts of studies on designing observers for continuous and periodic sampling systems. However, the studies are scarce when the systems have aperiodic samplings. This problem is of a great challenge since the information available in the controller is limited. If the exact system states cannot be observed in real time, the desired observers should at least be able to tell the controllers and schedulers, if there are any, in which state-space

region the current system state falls when a sampling happens. These observers are important, at least for communication scheduling of PETC implementations, due to Assumption 5.2.3 in Chapter 5.

- **Toolbox for ETC design.** There are many different versions of ETC, as we have shown in Chapter 1. It is a desirable and challenging quest to collect all of the proposed ETC strategies and design a specialized MATLAB/Simulink Toolbox that integrates the ETC condition parameter design.

- **Exploration of ETC application.** Applying ETC in a closed-loop control system can bring many advantages as indicated throughout this thesis, e.g. save required communications. However, the experimental results about applying ETC to real physical systems are not as varied compared to those applying TTC, since ETC is not that developed compared to TTC. Therefore, it is very interesting to show how different physical systems perform with ETC strategies, to establish under which typical practical scenarios are (TTC or ETC) strategy is advantageous over the other.

BIBLIOGRAPHY

[1] Norman Abramson. The aloha system: another alternative for computer communications. In *Proc. ACM Joint Computer Conference*, pages 281–285, 1970.

[2] Faisal Altaf, José Araújo, Aitor Hernandez, Henrik Sandberg, and Karl Henrik Johansson. Wireless event-triggered controller for a 3d tower crane lab process. In *Proc. IEEE MED*, pages 994–1001, 2011.

[3] Saurabh Amin, Alvaro A Cárdenas, and S Shankar Sastry. Safe and secure networked control systems under denial-of-service attacks. In *Hybrid Systems: Computation and Control*, pages 31–45. Springer, 2009.

[4] Tom M Apostol. *Calculus, vol 1: one-variable calculus, with an introduction to linear algebra*. 1967.

[5] José Araújo, Manuel Mazo Jr., Adolfo Anta, Paulo Tabuada, and Karl H Johansson. System architectures, protocols and algorithms for aperiodic wireless control systems. *IEEE Trans. Ind. Informat.*, 10(1):175–184, 2014.

[6] Eugene Asarin, Thao Dang, and Antoine Girard. Reachability analysis of nonlinear systems using conservative approximation. In *HSCC*, volume 2623, pages 20–35. Springer, 2003.

[7] Eugene Asarin, Thao Dang, and Antoine Girard. Hybridization methods for the analysis of nonlinear systems. *Acta Informatica*, 43(7):451–476, 2007.

[8] Karl Johan Åström and Bo Bernhardsson. Comparison of riemann and lebesque sampling for first order stochastic systems. In *Proceedings of the 41st IEEE Conference on Decision and Control, 2002*, volume 2, pages 2011–2016. IEEE, 2002.

[9] Emrah Bayraktaroglu, Christopher King, Xin Liu, Guevara Noubir, Rajmohan Rajaraman, and Bishal Thapa. Performance of ieee 802.11 under jamming. *Mobile Networks and Applications*, 18(5):678–696, 2013.

[10] Octavian Beldiman, Gregory C Walsh, and Linda Bushnell. Predictors for networked control systems. In *American Control Conference, 2000. Proceedings of the 2000*, volume 4, pages 2347–2351. IEEE, 2000.

[11] Rainer Blind and Frank Allgöwer. Analysis of networked event-based control with a shared communication medium: Part i–pure aloha. *Proc. IFAC*, 44(1):10092–10097, 2011.

[12] Rainer Blind and Frank Allgöwer. On time-triggered and event-based control of integrator systems over a shared communication system. *Mathematics of Control, Signals, and Systems*, 25(4):517–557, 2013.

[13] Rakesh B Bobba, Katherine M Rogers, Qiyan Wang, Himanshu Khurana, Klara Nahrstedt, and Thomas J Overbye. Detecting false data injection attacks on dc state estimation. In *Preprints of the First Workshop on Secure Control Systems, CPSWEEK*, volume 2010, 2010.

[14] DP Borgers. *Event-triggered control with robust communication and guaranteed performance*. PhD thesis, Eindhoven University of Technology, 2017.

[15] Stephen P Boyd, Laurent El Ghaoui, Eric Feron, and Venkataramanan Balakrishnan. *Linear matrix inequalities in system and control theory*, volume 15. SIAM, 1994.

[16] Francesco Bullo and Andrew D Lewis. *Geometric control of mechanical systems: modeling, analysis, and design for simple mechanical control systems*, volume 49. Springer Science & Business Media, 2004.

[17] Federico Calì, Marco Conti, and Enrico Gregori. Dynamic ieee 802.11: design, modeling and performance evaluation. In *International Conference on Research in Networking*, pages 786–798. Springer, 2000.

[18] Franck Cassez, Alexandre David, Emmanuel Fleury, Kim G Larsen, and Didier Lime. Efficient on-the-fly algorithms for the analysis of timed games. In *CONCUR*, volume 5, pages 66–80. Springer, 2005.

[19] Anton Cervin and Toivo Henningsson. Scheduling of event-triggered controllers on a shared network. In *Decision and Control, 2008. CDC 2008. 47th IEEE Conference on*, pages 3601–3606. IEEE, 2008.

[20] Jinglei Chen, Jian Sun, and Jie Chen. Event-triggered networked predictive control for linear systems via output feedback. In *Proc. IEEE ICCA*, pages 749–754, 2016.

[21] Alongkrit Chutinan and Bruce H Krogh. Computing polyhedral approximations to flow pipes for dynamic systems. In *Decision and Control, 1998. Proceedings of the 37th IEEE Conference on*, volume 2, pages 2089–2094. IEEE, 1998.

[22] Alongkrit Chutinan and Bruce H Krogh. Computational techniques for hybrid system verification. *IEEE Transactions on Automatic Control*, 48(1):64–75, 2003.

[23] Marieke BG Cloosterman, Laurentiu Hetel, Nathan Van de Wouw, WPMH Heemels, Jamal Daafouz, and Henk Nijmeijer. Controller synthesis for networked control systems. *Automatica*, 46(10):1584–1594, 2010.

[24] Marieke BG Cloosterman, Nathan Van de Wouw, WPMH Heemels, and Hendrik Nijmeijer. Stability of networked control systems with uncertain time-varying delays. *IEEE Transactions on Automatic Control*, 54(7):1575–1580, 2009.

[25] Daniel F Coutinho, Minyue Fu, and Carlos E de Souza. Input and output quantized feedback linear systems. *IEEE Transactions on Automatic Control*, 55(3):761–766, 2010.

[26] György Dán and Henrik Sandberg. Stealth attacks and protection schemes for state estimators in power systems. In *Smart Grid Communications (SmartGridComm), 2010 First IEEE International Conference on*, pages 214–219. IEEE, 2010.

[27] Claudio De Persis and Pietro Tesi. Input-to-state stabilizing control under denial-of-service. *IEEE Transactions on Automatic Control*, 60(11):2930–2944, 2015.

[28] Bruce DeBruhl and Patrick Tague. Digital filter design for jamming mitigation in 802.15. 4 communication. In *Computer Communications and Networks (ICCCN), 2011 Proceedings of 20th International Conference on*, pages 1–6. IEEE, 2011.

[29] Delta-T Devices. WET-2 Sensor. `https://www.delta-t.co.uk/product/wet-2/`, 2016. [Online; accessed 23-October-2017].

[30] Burak Demirel, Vijay Gupta, Daniel E Quevedo, and Mikael Johansson. On the trade-off between communication and control cost in event-triggered dead-beat control. *IEEE Transactions on Automatic Control*, 62(6):2973–2980, 2017.

[31] Dimos V Dimarogonas, Emilio Frazzoli, and Karl H Johansson. Distributed event-triggered control for multi-agent systems. *IEEE Transactions on Automatic Control*, 57(5):1291–1297, 2012.

[32] MCF Donkers and WPMH Heemels. Output-based event-triggered control with guaranteed $\mathscr{L}_\infty$-gain and improved and decentralized event-triggering. *IEEE Transactions on Automatic Control*, 57(6):1362–1376, 2012.

[33] MCF Donkers, WPMH Heemels, Nathan Van de Wouw, and Laurentiu Hetel. Stability analysis of networked control systems using a switched linear systems approach. *IEEE Transactions on Automatic control*, 56(9):2101–2115, 2011.

[34] Nicola Elia and Sanjoy K Mitter. Stabilization of linear systems with limited information. *IEEE Transactions on Automatic Control*, 46(9):1384–1400, 2001.

[35] Günter Ewald. *Combinatorial convexity and algebraic geometry*, volume 168. Springer Science & Business Media, 2012.

[36] Hamza Fawzi, Paulo Tabuada, and Suhas Diggavi. Secure state-estimation for dynamical systems under active adversaries. In *Communication, Control, and Computing (Allerton), 2011 49th Annual Allerton Conference on*, pages 337–344. IEEE, 2011.

[37] Christophe Fiter, Laurentiu Hetel, Wilfrid Perruquetti, and Jean-Pierre Richard. A state dependent sampling for linear state feedback. *Automatica*, 48(8):1860–1867, 2012.

[38] Christophe Fiter, Laurentiu Hetel, Wilfrid Perruquetti, and Jean-Pierre Richard. A robust stability framework for lti systems with time-varying sampling. *Automatica*, 54:56–64, 2015.

[39] A. Fu and M. Mazo, Jr. Decentralized periodic event-triggered control with quantization and asynchronous communication. *ArXiv e-prints*, March 2017.

[40] A. Fu and M. Mazo, Jr. Traffic models of periodic event-triggered control systems. *ArXiv e-prints*, November 2017.

[41] Anqi Fu and Manuel Mazo Jr. Periodic asynchronous event-triggered control. In *Decision and Control (CDC), 2016 IEEE 55th Conference on*, pages 1370–1375. IEEE, 2016.

[42] Minyue Fu and Lihua Xie. The sector bound approach to quantized feedback control. *IEEE Transactions on Automatic Control*, 50(11):1698–1711, 2005.

[43] Rob H Gielen, Sorin Olaru, Mircea Lazar, WPMH Heemels, Nathan van de Wouw, and S-I Niculescu. On polytopic inclusions as a modeling framework for systems with time-varying delays. *Automatica*, 46(3):615–619, 2010.

[44] Rafal Goebel, Ricardo G Sanfelice, and Andrew Teel. Hybrid dynamical systems. *Control Systems, IEEE*, 29(2):28–93, 2009.

[45] Rafal Goebel, Ricardo G Sanfelice, and Andrew R Teel. *Hybrid Dynamical Systems: modeling, stability, and robustness*. Princeton University Press, 2012.

[46] FieldComm Group. WirelessHART. `https://fieldcommgroup.org/`, 2017. [Online; accessed 23-October-2017].

[47] Keqin Gu, Jie Chen, and Vladimir L Kharitonov. *Stability of time-delay systems*. Springer Science & Business Media, 2003.

[48] WPMH Heemels, MCF Donkers, and Andrew R Teel. Periodic event-triggered control for linear systems. *IEEE Transactions on Automatic Control*, 58(4):847–861, 2013.

[49] WPMH Heemels, Andrew R Teel, Nathan Van de Wouw, and Dragan Nešić. Networked control systems with communication constraints: Tradeoffs between transmission intervals, delays and performance. *IEEE Transactions on Automatic Control*, 55(8):1781–1796, 2010.

[50] Laurentiu Hetel, Jamal Daafouz, and Claude Iung. Stabilization of arbitrary switched linear systems with unknown time-varying delays. *IEEE Transactions on Automatic Control*, 51(10):1668–1674, 2006.

[51] A Hoskins and I Stoianov. Infrasense: A distributed system for the continuous analysis of hydraulic transients. *Procedia Engineering*, 70:823–832, 2014.

[52] IEEE. IEEE 802.15.4 Standard: Wireless Medium Access Control (MAC) and Physical Layer (PHY) Specifications for Low-Rate Wireless Personal Area Networks (WPANs). http://www.ieee802.org/15/pub/TG4.html, 2006. [Online; accessed 23-October-2017].

[53] IEEE. IEEE Standard for Information Technology - Telecommunications and Information Exchange Between Systems - Local and Metropolitan Area Networks - Specific Requirements - Part 11: Wireless LAN Medium Access Control (MAC) and Physical Layer (PHY) Specifications. http://www.ieee802.org/11/, 2007. [Online; accessed 23-October-2017].

[54] IEEE. IEEE Standard for Ethernet. http://www.ieee802.org/3/, 2015. [Online; accessed 23-October-2017].

[55] Intel. Intel Edison board. https://software.intel.com/en-us/get-started-edison-windows, 2017. [Online; accessed 23-October-2017].

[56] Sokratis Kartakis, Edo Abraham, and Julie A McCann. Waterbox: A testbed for monitoring and controlling smart water networks. In *Proceedings of the 1st ACM International Workshop on Cyber-Physical Systems for Smart Water Networks*, page 8. ACM, 2015.

[57] Sokratis Kartakis, Edo Abraham, and Julie A McCann. Waterbox: A testbed for monitoring and controlling smart water networks. In *Proc. ACM CysWater*, page 8, 2015.

[58] Sokratis Kartakis, Babu D. Choudhary, Alexander D. Gluhak, Lambros Lambrinos, and Julie A. McCann. Demystifying low-power wide-area communications for city iot applications. In *Proc. ACM WiNTECH '16*, pages 2–8, 2016.

[59] Sokratis Kartakis, Anqi Fu, Manuel Mazo Jr., and Julie A McCann. Communication schemes for centralized and decentralized event-triggered control systems. *IEEE Transactions on Control Systems Technology*, 2017.

[60] Keysight Technologies. N6705B DC Power Analyzer. http://www.keysight.com/en/pd-1842303-pn-N6705B/dc-power-analyzer-modular-600-w-4-slots?cc=NL&lc=dut, 2016. [Online; accessed 23-October-2017].

[61] Hassan K Khalil. *Noninear Systems*. Prentice-Hall, New Jersey, 1996.

[62] Arman Kolarijani and Manuel Mazo Jr. A formal traffic characterization of lti event-triggered control systems. *IEEE Transactions on Control of Network Systems*, 2016.

[63] Arman Sharifi Kolarijani, Dieky Adzkiya, and Manuel Mazo Jr. Symbolic abstractions for the scheduling of event-triggered control systems. In *Decision and Control (CDC), 2015 IEEE 54th Annual Conference on*, pages 6153–6158. IEEE, 2015.

[64] Arman Sharifi Kolarijani, Manuel Mazo Jr., and Tamás Keviczky. Timing abstraction of perturbed lti systems with l2-based event-triggering mechanism. In *Decision and Control (CDC), 2016 IEEE 55th Conference on*, pages 1364–1369. IEEE, 2016.

[65] D Lehmann and J Lunze. Extension and experimental evaluation of an event-based state-feedback approach. *Control Engineering Practice*, 19(2):101–112, 2011.

[66] Daniel Liberzon. Hybrid feedback stabilization of systems with quantized signals. *Automatica*, 39(9):1543–1554, 2003.

[67] Daniel Liberzon and Dragan Nešić. Input-to-state stabilization of linear systems with quantized state measurements. *IEEE Transactions on Automatic Control*, 52(5):767–781, 2007.

[68] Yao Liu, Peng Ning, and Michael K Reiter. False data injection attacks against state estimation in electric power grids. *ACM Transactions on Information and System Security (TISSEC)*, 14(1):13, 2011.

[69] L. Ljung. *System Identification: Theory for the User*. Prentice Hall information and system sciences series. 1999.

[70] Manuel Mazo Jr. and Ming Cao. Asynchronous decentralized event-triggered control. *Automatica*, 50(12):3197–3203, 2014.

[71] Manuel Mazo Jr. and Anqi Fu. Decentralized event-triggered controller implementations. In *Event-Based Control and Signal Processing*, pages 119–148. CRC Press, 2015.

[72] Manuel Mazo Jr. and Paulo Tabuada. Decentralized event-triggered control over wireless sensor/actuator networks. *IEEE Transactions on Automatic Control*, 56(10):2456–2461, 2011.

[73] Guowang Miao, Jens Zander, Ki Won Sung, and Slimane Ben Slimane. *Fundamentals of Mobile Data Networks*. Cambridge University Press, 2016.

[74] Marek Miskowicz and Jan Lunze. Event-based control: Introduction and survey. In *Event-Based Control and Signal Processing*, pages 3–20. CRC Press, 2015.

[75] Yilin Mo and Bruno Sinopoli. Secure control against replay attacks. In *Communication, Control, and Computing, 2009. Allerton 2009. 47th Annual Allerton Conference on*, pages 911–918. IEEE, 2009.

[76] Dragan Nesic and Andrew R Teel. Input-output stability properties of networked control systems. *IEEE Transactions on Automatic Control*, 49(10):1650–1667, 2004.

[77] Roman Obermaisser and Walter Lang. Event-triggered versus time-triggered real-time systems: A comparative study. *Event-Based Control and Signal Processing*, page 59, 2015.

[78] Fabio Pasqualetti, Florian Dorfler, and Francesco Bullo. Attack detection and identification in cyber-physical systems. *IEEE Transactions on Automatic Controln*, 58(11):2715–2729, 2013.

[79] Chen Peng, Dong Yue, and Min-Rui Fei. A higher energy-efficient sampling scheme for networked control systems over ieee 802.15. 4 wireless networks. *IEEE Transactions on Industrial Informatics*, 12(5):1766–1774, 2016.

[80] Chithrupa Ramesh, Henrik Sandberg, and Karl H Johansson. Performance analysis of a network of event-based systems. *IEEE Transactions on Automatic Control*, 61(11):3568–3573, 2016.

[81] Chithrupa Ramesh, Henrik Sandberg, and Karl Henrik Johansson. Steady state performance analysis of multiple state-based schedulers with csma. In *Proc. IEEE CDC-ECC*, pages 4729–4734, 2011.

[82] Henrik Sandberg, André Teixeira, and Karl H Johansson. On security indices for state estimators in power networks. In *First Workshop on Secure Control Systems (SCS), Stockholm, 2010*, 2010.

[83] Rolf Schneider. *Convex bodies: the Brunn–Minkowski theory*. Number 151. Cambridge university press, 2014.

[84] Danial Senejohnny, Pietro Tesi, and Claudio De Persis. Self-triggered coordination over a shared network under denial-of-service. In *Decision and Control (CDC), 2015 IEEE 54th Annual Conference on*, pages 3469–3474. IEEE, 2015.

[85] Yoav Sharon and Daniel Liberzon. Input to state stabilizing controller for systems with coarse quantization. *IEEE Transactions on Automatic Control*, 57(4):830–844, 2012.

[86] H. Shisheh-Foroursh and S. Martínez. On event-triggered control of linear systems under periodic dos attacks. In *Proc. of the 51st IEEE International Conference on Decision and Control*, pages 2551–2556, Maui, HI, December 2012.

[87] Manuela Sigurani, Christian Stöcker, Lars Grüne, and Jan Lunze. Experimental evaluation of two complementary decentralized event-based control methods. *Control Engineering Practice*, 35:22–34, 2015.

[88] Joëlle Skaf and Stephen Boyd. Analysis and synthesis of state-feedback controllers with timing jitter. *IEEE Transactions on Automatic Control*, 54(3):652–657, 2009.

[89] Roy S Smith. A decoupled feedback structure for covertly appropriating networked control systems. *Network*, 6:6, 2011.

[90] Eduardo D Sontag. Input to state stability: Basic concepts and results. In *Nonlinear and optimal control theory*, pages 163–220. Springer, 2008.

[91] N. Sornin, M. Luis, T. Eirich, T. Kramp, and O. Hersent. Lorawan specification. `https://www.lora-alliance.org/lorawan-for-developers`, 2017. [Online; accessed 23-October-2017].

[92] Spectracom. GPS Clock Synchronization. http://spectracom.com/resources/essential-education/gps-clock-synchronization, 2008. [Online; accessed 23-October-2017].

[93] Nadeem Sufyan, Nazar Abbass Saqib, and Muhammad Zia. Detection of jamming attacks in 802.11 b wireless networks. *EURASIP Journal on Wireless Communications and Networking*, 2013(1):1–18, 2013.

[94] Young Soo Suh. Stability and stabilization of nonuniform sampling systems. *Automatica*, 44(12):3222–3226, 2008.

[95] Paulo Tabuada. Event-triggered real-time scheduling of stabilizing control tasks. *IEEE Transactions on Automatic Control*, 52(9):1680–1685, 2007.

[96] Paulo Tabuada. *Verification and control of hybrid systems: a symbolic approach*. Springer Science & Business Media, 2009.

[97] André Teixeira, Saurabh Amin, Henrik Sandberg, Karl H Johansson, and Shankar S Sastry. Cyber security analysis of state estimators in electric power systems. In *Decision and Control (CDC), 2010 49th IEEE Conference on*, pages 5991–5998. IEEE, 2010.

[98] David Thuente and Mithun Acharya. Intelligent jamming in wireless networks with applications to 802.11 b and other networks. In *Proc. of MILCOM*, volume 6, 2006.

[99] TI. CC2420 RF Transceiver. http://www.ti.com/product/CC2420, 2014. [Online; accessed 23-October-2017].

[100] TI. CC2530 RF Transceiver. http://www.ti.com/product/CC2530, 2014. [Online; accessed 23-October-2017].

[101] TI. CC430F5137 Communication Module. http://www.ti.com/product/CC430F5137, 2016. [Online; accessed 23-October-2017].

[102] Ivana Tomić and Julie A McCann. A survey of potential security issues in existing wireless sensor network protocols. *IEEE Internet of Things Journal*, 2017.

[103] Rosario Toscano. Signal and system norms. In *Structured Controllers for Uncertain Systems*, pages 25–44. Springer, 2013.

[104] Charles Van Loan. The sensitivity of the matrix exponential. *SIAM Journal on Numerical Analysis*, 14(6):971–981, 1977.

[105] Mikhail Vilgelm, Mohammadhossein H Mamduhi, Wolfgang Kellerer, and Sandra Hirche. Adaptive decentralized mac for event-triggered networked control systems. In *Proc. ACM HSCC*, pages 165–174, 2016.

[106] Gregory C Walsh and Hong Ye. Scheduling of networked control systems. *Control Systems, IEEE*, 21(1):57–65, 2001.

[107] Gregory C Walsh, Hong Ye, and Linda G Bushnell. Stability analysis of networked control systems. *IEEE Transactions on Control Systems Technology*, 10(3):438–446, 2002.

[108] Thomas M Walski, Donald V Chase, Dragan A Savic, Walter Grayman, Stephen Beckwith, and Edmundo Koelle. Advanced water distribution modeling and management. 2003.

[109] Di Wang, Jian Sun, and Jie Chen. Event-triggered networked predictive controller design for linear systems with communication delay. In *Proc. IEEE CCC*, pages 5785–5790, 2014.

[110] Xiaofeng Wang and Michael D Lemmon. Event-triggering in distributed networked control systems. *IEEE Transactions on Automatic Control*, 56(3):586–601, 2011.

[111] Xiaofeng Wang and Michael D Lemmon. On event design in event-triggered feedback systems. *Automatica*, 47(10):2319–2322, 2011.

[112] Wenyuan Xu, Wade Trappe, Yanyong Zhang, and Timothy Wood. The feasibility of launching and detecting jamming attacks in wireless networks. In *Proceedings of the 6th ACM international symposium on Mobile ad hoc networking and computing*, pages 46–57. ACM, 2005.

[113] Majid Zamani, Manuel Mazo Jr, Mahmoud Khaled, and Alessandro Abate. Symbolic abstractions of networked control systems. *IEEE Transactions on Control of Network Systems*, PP(99), 2017.

[114] Heng Zhang, Peng Cheng, Ling Shi, and Jiming Chen. Optimal dos attack scheduling in wireless networked control system. *IEEE Transactions on Control Systems Technology*, 24(3):843–852, 2016.

[115] Minghui Zhu and Sonia Martinez. Stackelberg-game analysis of correlated attacks in cyber-physical systems. In *American Control Conference (ACC), 2011*, pages 4063–4068. IEEE, 2011.

NOMENCLATURE

2^S the set of all subsets of S, i.e. the power set of S.

$M \prec 0$ negative definite symmetric matrix.

$M \preceq 0$ negative semi-definite symmetric matrix.

$M \succ 0$ positive definite symmetric matrix.

$M \succeq 0$ positive semi-definite symmetric matrix.

$Q \subseteq Z \times Z$ an equivalence relation on a set Z.

Z/Q the set of all equivalence classes of Z by Q.

$[z]$ the equivalence class of $z \in Z$.

$\lambda_{\max}(P)$ the maximum eigenvalue of a symmetric matrix P.

$\lambda_{\min}(P)$ the minimum eigenvalue of a symmetric matrix P.

$\lceil s \rceil$ the nearest integer from above of a scalar s.

$\lfloor s \rfloor$ the nearest integer from below of a scalar s.

$\mathbb{IN}^+$ the set of all closed intervals $[a, b]$ such that $a, b \in \mathbb{N}^+$ and $a \leq b$.

$\mathbb{N}$ natural numbers including zero.

$\mathbb{N}^+$ natural numbers.

$\mathbb{R}^+$ positive real numbers.

$\mathbb{R}_0^+$ positive real numbers and zero.

$\mathbb{R}^n$ n-dimensional real valued vector.

$\mathscr{L}_2$ the space of all locally integrable signals with a finite $\mathscr{L}_2$ norm.

$\mathscr{L}_\infty$ the space of all locally integrable signals with a finite $\mathscr{L}_\infty$ norm.

$\mathscr{M}_n$ the set of all $n \times n$ real-valued symmetric matrices.

$\mathscr{M}_{m \times n}$ the set of all $m \times n$ real valued matrices.

$|\cdot|$ Euclidean norm in the appropriate vector space for vectors; l_2 induced matrix norm for matrices; cardinality for sets.

$|x|_{\mathscr{A}}$ The distance of vector x to closed set $\mathscr{A}$.

ABBREVIATIONS

ACK Acknowledgment.

ADC-TDMA Asynchronous Decentralized Control Time-Division Multiple Access.

ADETC Asynchronous Decentralized Event-Triggered Control.

ADPETC Asynchronous Decentralized Periodic Event-Triggered Control.

BMI Bilinear Matrix Inequality.

C-TDMA Control Time-Division Multiple Access.

CPS Cyber-Physical System.

CPU Central Processing Unit.

CSMA Carrier-Sense Multiple Access.

CSMA/CA Carrier-Sense Multiple Access with Collision Avoidance.

CSMA/CD Carrier-Sense Multiple Access with Collision Detection.

DMA District Meter Area.

DoS Denial of Service.

ETC Event-Triggered Control.

ETM Event-Triggered Mechanism.

GPS Global Positioning System.

ISS Input-to-State Stablility.

LMI Linear Matrix Inequality.

LPWA Low-Power Wide-Area.

LQR Linear–Quadratic Regulator.

LTI Linear Time-Invariant.

MAC Media Access Control.

MAEI Maximum Allowable Event Interval.

MEF Maximum-Error First.

NCS Networked Control System.

NTP Network Time Protocol.

PETC Periodic Event-Triggered Control.

QoS Quality of Service.

RR Round-Robin.

SDC-TDMA Sychnronous Decentrlized Control Time-Division Multiple Access.

SDETC Synchronous Decentralized Event-Triggered Control.

SDPETC Synchronous Decentralized Periodic Event-Triggered Control.

TDMA Time-Division Multiple Access.

TOD Try-Once-Discard.

TTC Time-Triggered Control.

UDP Unified Datagram Protocol.

UGAS Uniformly Global Asymptotical Stable.

UGES Uniformly Global Exponential Stable.

UGpAS Uniformly Global pre-Asymptotical Stable.

WNCS Wireless Networked Control System.

CURRICULUM VITÆ

Anqi Fu was born on January 15th, 1988 in Qinhuangdao, Hebei province, P.R.China. He received his B.Sc. degree in Measurement and Control Technology and Instrumentation from Beijing Jiaotong University (BJTU), Beijing, P.R.China in 2010 and his M.Sc. degree in Instrumentation Science and Technology from Beihang University (BUAA), Beijing, P.R.China in 2013. After his M.Sc. graduation, he got a scholarship from China Scholarship Council (CSC) and became a PhD candidate in the Delft Center for Systems and Control (DCSC), Delft University of Technology, Delft, The Netherlands. During his PhD studies, he was a visiting researcher at the Adaptive Emergent Systems Engineering (AESE) Group, Imperial College London, London, United Kingdom in July 2016.

His research interests include Cyber-physical systems, hybrid systems, event-triggered control, wireless networked control system security, electric machinery control.

LIST OF PUBLICATIONS

JOURNAL PAPERS

3. A. Fu and M. Mazo Jr., Traffic models of periodic event-triggered control systems, submitted.

2. A. Fu and M. Mazo Jr., Decentralized periodic event-triggered control with quantization and asynchronous communication, submitted.

1. S. Kartakis, A. Fu, M. Mazo Jr. and J. McCann. Communication schemes for centralized and decentralized event-triggered control systems, IEEE Transactions on Control Systems Technology, 2017.

BOOK CHAPTER

1. M. Mazo Jr. and A. Fu, Decentralized event-triggered controller implementations. Event-Based Control and Signal Processing. CRC Press, 2015.

CONFERENCE PAPERS

4. A. Fu and M. Mazo Jr., Asynchronous mix-triggered control. Proceedings of the IEEE International Conference on Control and Automation (ICCA), 2017.

3. A. Fu and M. Mazo Jr., Periodic asynchronous event-triggered control, Proceedings of the IEEE Conference on Decision and Control (CDC), 2016.

2. A. Fu and M. Mazo Jr., Improved asynchronous event-triggered control for linear systems with performance guarantees. Proceedings of European Control Conference (ECC), 2016.

1. A. Fu and M. Mazo Jr., Advances on asynchronous event-triggered control. Proceedings of the International Conference on Event-based Control, Communication, and Signal Processing (EBCCSP), 2015.